NAT.LAB. VERSLAG Nr.3701

D.K. Wickenden
Dr. O. Reifenschweiler

SOME INVESTIGATIONS INTO THE BREMSSTRAHLUNG OF TRITIUM

NAT.LAB.
VERSLAG Nr. 3701
D.K.Wickenden
Dr.O.Reifenschweiler

SOME INVESTIGATIONS INTO THE BREMSSTRAHLUNG OF TRITIUM

Period of work: July - september 1961
Notebooks : None

SUMMARY

The internal and external bremsstrahlung of tritium have been investigated by a new method, using titanium-tritium films. A great discrepancy was found between the experimental results and the theory. The experimental values of the ratio $\frac{I_{EBS}}{I_{IBS}}$ were between four and thirty times lower than the ratio predicted by theory. This discrepancy may be due either to the generation of characteristic x-radiation in the experimental arrangement used or to the fact that the theory is not applicable to tritium on account of its extremely low atomic number and β-ray energy. The wide scatter in the experimental results may likewise be due to the generation of characteristic x-radiation.

INTRODUCTION

When free electrons encounter a nucleus they are decelerated by the nuclear field and so lose energy. This energy appears as an electromagnetic radiation called bremsstrahlung and is divided into two classes. External bremsstrahlung, discovered by Röntgen in 1895, occurs when electrons originating from a β-decay process encounter nuclei in the surrounding matter. Internal bremsstrahlung occurs when an electron encounters the nuclear field of the nucleus from which it has

been emitted. The latter class is independent of the surrounding matter since it is generated by the electron while it is still within the parent atom; hence the description internal. It was discovered for the just time by Aston [1] in the 1920's, when he found a mild inhomogeneous γ-radiation during his γ-radiation measurements of RaE.

Since the discovery of internal bremsstrahlung other isotopes that show β-decay have been tested for the associated bremsstrahlung. Isotopes with little or no contaminating homogeneous γ-radiation were preferred for these tests. Normally the researchers give their results as the proportion of the kinetic energy of the emitted electron that appears as internal bremsstrahlung.

The most important difficulty in measuring internal bremsstrahlung is the effect of the external bremsstrahlung, which is hard to overcome. Langevin-Joliot [2] overcame the external bremsstrahlung by leading the electrons with a magnetic field to a sufficient distance from the detection apparatus.

However, external bremsstrahlung varies linearly with the atomic number of the surrounding matter, and the use of various absorbers and extrapolation to z=o represents a simple method of determining the internal bremsstrahlung effect. Up till now no experimental data of the internal bremsstrahlung of tritium are known.

Practically it will be useful to express the amount of generated external bremsstrahlung in proportion to the amount of internal bremsstrahlung in a certain material due to the constant presence of internal bremsstrahlung. The external bremsstrahlung is approximately proportional to z so that for every material it would be possible to calculate the proportion of external and internal bremsstrahlung. The measured activity being the sum of internal and external bremsstrahlung, is thus a relative measure of the amount of tritium present ceteris paribus.

THEORY *)

When a tritium nucleus decays radio active the products are a helium nucleus, of mass number 3, and a β-electron. The energy spectrum of the emitted β-electron is a continuous one and, as the helium nucleus may possess discrete energy states only, a third particle, the neutrino, also results from the decay. The total disintegration energy is then distributed between the β-electron and neutrino. The neutrino hypothesis is justified when one considers the conservation of angular momentum also. From classical electrodynamic theory one can expect that at the emission of a β-electron a quantum of electro-magnetic radiation is also generated. The β-electron and helium nucleus constitute an electrostatic dipole whose energy suddenly drops when the β-electron is emitted. This loss of energy would appear as an electromagnetic radiation, the internal bremsstrahlung (I.B.S.).

Using the approximation that z=o, Knipp and Uhlenbeck [3], and Bloch [4] calculated theoretically the expected spectra of internal bremsstrahlung for permissible β-transitions, the publication of the two independent works took place at approximately the same time in 1936. Wang Chang and Falkoff [5] extended these calculations to prohibited transitions while Nilsson[6] made corrections for the Z-dependance of the internal bremsstrahlung.

Knipp and Uhlenbeck, using two methods, calculated the probability per β-electron that an I.B.S. quantum is produced. In the first method they calculated the probability for electrons of a given energy and integrated this probability over the energy spectrum of the electrons. Thus the intensity spectrum of I.B.S. was obtained. In the second method they used the Fermi theory on β-decay; i.e. a neutron is spontaneously converted into a proton with the emission of an electron and a neutrino. Quantum mechanical views then introduce the electromagnetic radiation field of the Fermi-theory. Calculations of the probability that an electron, a neutrino and a γ-quantum

*) This theoretical treatment was given earlier by v.d. Vate, Reifenschweiler and v.d. Ligt [13]. For the sake of completeness it will be repeated here.

are acquired, and summing the result over the permissible states of the electron and the neutrino, gave the probability that a radiation quantum of a certain energy would be obtained.

Bloch [4] considered that the β-decay process is built up of two separate steps. In the first step, the nucleus disintegrates with the emission of an electron and a neutrino in states s' and σ respectively. This is followed by the second step in which the electron changes from state s' to state s with the emission of a quantum radiation. Bloch then deduced, by means of the Fermi-theory, the total internal bremsstrahlung intensity

$$I_{LBS.} = \tfrac{1}{2}\, c_1\, (mc^2)^6 \phi(\Delta) \qquad (1)$$

where c_1 a constant and $\phi(\Delta)$ is a function of Δ only ($\Delta = 1 + \varepsilon$ where ε is the maximum kinetic energy of the emitted electrons expressed in units of mc^2).

According to the Fermi theory the average kinetic energy of the β-electrons is given by

$$\bar{E}_{kin} = c_1 (mc^2)^6 \left(\frac{hc}{e^2}\right) \psi(\Delta) \qquad (2)$$

where c_1 is the same constant as in (1)
and $\psi(\Delta)$ is a function of Δ only.

The ratio of internal bremsstrahlung to total energy is given by

$$r(\Delta) = \frac{\bar{I}_{IBS}}{\bar{E}_{kin}} = \frac{e^2}{2hc}\,\frac{\phi(\Delta)}{\psi(\Delta)} = 5{,}81 \times 10^{-4}\, \chi(\Delta) \qquad (3)$$

In the case of tritium where $\varepsilon \ll 1$ this becomes

$$r(\Delta) = 5{,}81 \times 10^{-4}\, \frac{32}{33}\, \varepsilon = 5{,}63 \times 10^{-4}\, \varepsilon \qquad (4)$$

If $\Delta \gg 1$

$$\chi(\Delta) = \frac{16}{3}\left(\ln 2\Delta - \frac{11}{5}\right) \qquad (5)$$

This expression is of no importance since $\varepsilon \gg 1$ is never realised in practice.

Using the considerations of Konopinski and Uhlenbeck [7], on β-decay, Bloch obtained another value of $\chi(\Delta)$ in the region for $\varepsilon \ll 1$

$$\chi(\Delta) = \left(\frac{32}{45}\right)\varepsilon$$

so that

$$\nu(\Delta) = 5,81 \times 10^{-4} \frac{32}{45} \varepsilon = 4,13 \times 10^{-4} \varepsilon \qquad (6)$$

Thus, the proportion of energy emitted as I.B.S. is dependent on the maximum kinetic energy of the β-radiation only and is proportional to E when $\varepsilon \ll 1$

Wang Chang and Falkoff [5] say that the proportion of I.B.S. increases with an increasing prohibition rate but however, that the ratio between total I.B.S. intensity and the total β-intensity is independent of the prohibition rate of the β-transitions, and they give as a result

$$\frac{I_\gamma}{I_\beta} = \frac{4\alpha}{3\pi}(\ln 2\Delta - 2,3) \qquad (7)$$

where α is the fine structure constant.

This formula is literally the same as (5), which suggests it applies to all possible types of β-transitions.

Nillson [6] corrected the formulae by taking into account the finite Z and relativistic energies which Knipp and Uhlenbeck, and Bloch disregarded. According to Bloch these approximations may in some cases lead to an error of several tens of percents.

It was indeed shown that there were large discrepancies between theory and practical results, especially when working with low values of $E_{max.}$. However, Michalowicz [8] pointed out that Nillson's corrections did not explain the discrepancies satisfactorily.

The path of the emitted electron, once outside the influence of the nuclear field of the parent nucleus, is governed by the manner in which it loses energy to the surrounding medium. With energies lower than 1 Mev the main loss of energy is caused by photo-electric ionisation. A small part of the energy loss is by E.B.S. when the electrons encounter nuclei and are decelerated. According to Heitler [9] the average loss of energy due to E.B.S. per centimetre is given by

$$\left(\frac{dE}{dx}\right)_{EBS} = N r_0^2 \frac{Z^2}{137} (E + mc^2)\left[4 \ln \frac{2(E+mc^2)}{mc^2} - \frac{4}{3}\right]$$

$$= 3{,}44 \times 10^{-4} (E + mc^2) \frac{Z^2 \varrho}{A} \left[4 \ln \frac{2(E+mc^2)}{mc^2} - \frac{4}{3}\right] \quad (8)$$

Where N = Loschmidt's number = $\frac{L\varrho}{A}$ L = Avagadro's number

ϱ - density

A = Atomic weight

Z = Atomic number

r_0 = Classical electron radius = $2{,}8 \times 10^{-13}$ cm.

For low energies this reduces to

$$\left(\frac{dE}{dx}\right)_{EBS} = 3{,}44 \times 10^{-4} \frac{Z^2 \varrho mc^2}{A} \left[4 \ln 2 - 4/3\right]$$

$$= 0{,}255 \frac{Z^2 \varrho}{A} \quad \text{KeV/cm} \quad (9)$$

$$(dE)_{EBS} = 0{,}255 \frac{Z^2 \varrho}{A} dx \quad \text{KeV}$$

Over the entire energy spectrum of the β-electrons the loss of energy by E.B.S. per electron is

$$\frac{E_{EBS}}{E_{kin}} = 0{,}255 \frac{Z^2 \varrho}{A} \int_0^{E_{max}} \frac{1}{F(E)} dE \quad (10)$$

Where $F(E) = -\frac{dE}{dx}$ and is determined experimentally.

To make an estimation of the E.B.S. effect for a particular isotope it is necessary to integrate this expression over the β-energy spectrum of that isotope.

As F(E) is often a complicated function of E one has to look for a relation from which the loss of energy can be calculated. It has been deduced experimentally [10] that the output of an x ray tube, operating on V kev, is

$$\frac{E_{EBS}}{E_{kin}} = \frac{\text{energy of x-rays}}{\text{energy of cathode rays}} = 1{,}1 \times 10^{-6}\, Z V \qquad (11)$$

This formula holds in the energy range 10-100 keV and can be deduced theoretically [11] for a solid anticathode, except for a multiplication factor of $9{,}2 \times 10^{-7}$.
An electron with an energy E_{kin} thus, emits over its range a quantity of external bremsstrahlung given by:

$$\frac{E_{EBS}}{E_{kin}} = C_2 Z E \qquad \text{where} \quad C_2 = \frac{1{,}1 \times 10^{-6}}{e}$$

(e is the elementary electrical charge, and is unity if the electron volt unit is used for the energy)

$$\text{or} \qquad E_{EBS} = C_2 Z E^2 \qquad (12)$$

To calculate E_{EBS} produced by a β-electron of an isotope, equation (12) must be integrated over the whole continuous energy spectrum of that isotope:

$$E_{EBS} = C_2 Z \int_0^{E_{max}} I(E)\, E^2\, dE \qquad (13)$$

As in Bloch's theory on I.B.S. we express the quantity of EBS produced as compared with the average energy of the β-electrons and obtain

$$\frac{E_{EBS}}{\overline{E}} = \frac{C_2 Z \int_0^{E_{max}} I(E)\, E^2\, dE}{\overline{E}} \qquad (14)$$

Wyard [12] calculated the E.B.S. of β-electrons of energy up to 2 Mev and deduced that the form of the curve $I = I\left(\frac{h\nu}{E_{max}}\right)$ is the same as that for β-electrons of isotopes with an energy spectrum of the same form.

The function $I = I\left(\frac{h\nu}{E_{max}}\right)$ is obtained by the integration of

$$I(h\nu) = E_0 \left[4\left(1 - \frac{h\nu}{E_0}\right) - 3\,\frac{h\nu}{E_0}\,\log\,\frac{E_0}{h\nu} \right] \qquad (15)$$

over the β-electron energy spectrum.

(15) is obtained by integrating I(hv) = $4 - 3\,\frac{h\nu}{E}$ from E_0 to $h\nu$ where E_0 is the initial energy of the electron ($h\nu \leqq E_0 \leqq E_{max}$).

Thus by comparing equations (4) and (14) we obtain an relation between E.B.S. and I.B.S.

$$\frac{E_{EBS}}{E_{IBS}} = \frac{C_2 Z \int_0^{E_{max}} I(E) E^2 dE}{5{,}63 \times 10^{-4} \varepsilon \bar{E}} \qquad (16)$$

To correct for the unit difference (ε is in units of mc^2 and E in KeV) we multiply the denominator by $\frac{1}{mc^2}$ and obtain

$$\frac{E_{EBS}}{E_{IBS}} = \frac{C_2 Z \int_0^{E_{max}} I(E) E^2 dE}{5{,}63 \times 10^{-4} \varepsilon \bar{E} \times \frac{1}{mc^2}} \qquad (17)$$

Thus the ratio of E_{EBS} to E_{IBS} is a linear function of Z only.

C. EXPERIMENTAL METHODS

In the introductory section a method of comparing the external and internal bremsstrahlung of tritium was indicated in which one uses the linear dependence on Z of the ratio I_{EBS}/I_{IBS} as shown in equation 17 of the theory. In this experiment suitable sources of tritium are prepared and the radiation generated by various materials when they are in contact with the source, is measured. From these measurements values of I_{EBS}/I_{IBS} are obtained and can be compared with the results of v.d. Vate, Reifenschweiler and v.d. Ligt [13] who performed a similar experiment in 1960 at the Philips Research Laboratories.

Since tritium is a radio-active gas it is very inconvenient to work with it in a free state but, being an isotope of hydrogen, it is easily absorbed in a metal which has a high affinity for that gas. A good review on the absorbtion of hydrogen by metals was be found in the volume of Smith [14] and this can be used for tritium if one assumes that the absorbtion of the isotopes is the same as of hydrogen itself. According to Smith the most stable exothermic systems are obtained if one absorbs the gas in one of the following metals: Titanium, Zirconium, Thorium, all the alkaline metals and some of the alkaline earth metals. In the work of v.d. Vate et al. a Titanium-tritium powder suspension as prepared by Reifenschweiler [15] was used. This suspension was applied directly to the EBS generators and the radiation generated was measured. In the present experiment a titanium-tritium film is evaporated on a stainless steel foil and untreated bremsstrahlung-generators are placed on the preparation in turn. This is an improved method since exactly the same amount of tritium is used for each generator. Another advantage is that the same generators may be used for different foils, and so any impurities in the materials will be the same for each measurement. A maximum of twenty-eight generators are used for each foil. The perfor-

mance in durability, adhesion and absorbtion of titanium-tritium films on backings of copper, gold, nickel and platinum has been reported by Scott and Owen [16]. In a preliminary experiment the absorbtion of deuterium in titanium films on stainless steel and nickel was studied and stainless steel proved satisfactory. A new method was used for the preparation of the titanium-tritium films. In the conventional procedure the titanium film is formed by evaporation and then the tritium is absorbed by heating the film in a tritium atmosphere. In the present experiments the titanium-tritium film is formed in one step by evaporating the titanium in a titanium atmosphere at a suitable pressure

The construction of the foils (fig.1) is such that the surface is as flat and taut as possible. From figure 1, A is a stainless steel ring with inner and outer diameters 20 and 25 mm respectively and thicknesses at the two edges 12 and 5 mm respectively. A circular foil of stainless steel of thickness 16 μ(c) is placed on the top surface of A and ring B, which is also stainless steel and has an inner diameter the same as the outer diameter of the raised rim, is then pressed down firmly over the rim. The edges of the rim are rounded to prevent the foil from being cut in the process. Rings A and B are then spot-welded together around their periphery. During evaporation the foils are placed in a nickel holder D such that the area presented to the evaporator is the same for each foil. By knowing the distance of the foils from the evaporator one can estimate the amount of titanium deposited. The evaporation of the titanium takes place in a tritium atmosphere of 10^{-3} mm Hg. The vacuum-system (fig.2) shows the arrangement of the foils and covers around a straight evaporating tungsten wire on which is spiralised 1 mg of titanium wire. Six plates are used in each evaporation at distances of 15, 20, 30, 40, 50 and 60 mm from the wire and this gives titanium films of thicknesses from about 800 to 50 Å respectively. The diffusion pump is capable of producing a vacuum of 10^{-7} mm Hg with the pressure being

measured by an ionisation manometer. The replenisher, developed by Reifenschweiler [17] accurately regulates the tritium pressure during the evaporation. It consists of a metal cylinder covered with a fine deposit of titanium "soot" which has been caused to absorb tritium. When this powder is heated the tritium is driven out and the pressure in the vessel increases. Thus by varying the temperature of the powder one can control the pressure in the vessel accurately. To ensure an even titanium-tritium ratio in the film the evaporation takes place in a constant tritium atmosphere of 10^{-3} mm Hg.

The experimental measuring arrangement is shown in figure 3. The Geiger-Müller tube (18507) is connected to:

1. High Voltage Supply and Pre-amplifier (PW4022)
2. Electronic timer (PW4062)
3. Electronic counter (PW4032)

The tube is placed in a cylindrical lead shield to reduce the extraneous background radiation as much as possible. A constant geometry is obtained by having a perspex foil support which can be screwed onto the G.M. tube holder. The foils are placed in a circular recess in the holder so that the distance between foil and G.M. tube window is constant throughout all the experiments. When using gas generators the tube is placed in a spherical glass vessel (fig. 4), because of the longer range of the β-electrons. The range of 18 KeV electrons in hydrogen is approximately 80 mm and therefore the radius of the glass vessel is 100 mm to prevent any electrons from hitting the walls.

Measurements are made with and without the bremsstrahlung-generators on the foil and the ratio $\frac{CR_Z}{CR_o}$ is found as a function of Z. (CR_Z counting rate with generator of atomic number Z, CR_o counting rate without generator).

D. Experiment: Performance and Results

The maximum true counting rate of the apparatus (G.M. tube 18507 and equipment PW 4022, PW 4032 and PW 4062) was found by plotting the measured count rate of a strong Co 60 source as a function of (distance between source and tube window) $^{-2}$. When there are no losses due to dead time of the apparatus the plot is a straight line and so the maximum true count rate of the apparatus was found by noting where the plot began to deviate from the straight line. The maximum true count rate was found to be 48.000 cpm and since the maximum count rate measured in the experiment was 38.000 cpm no corrections were necessary in respect of the dead time of the apparatus.

Two preliminary experiments were performed to test for the adhesion of titanium films on nickel and stainless steel backings and for the absorbtion of deuterium by the films. The films obtained on both types of backing were of good quality but the films on stainless steel had a slightly better appearance. When the apparatus was gradually heated there was a sudden rise in pressure at 350 ^{o}C indicating that the deuterium which had been absorbed by the titanium films had been driven out.

The final choice of backing to be used was decided by its absorption effect. The absorption effect was determined for four possible backings (Nickel of thickness 15 μ, 25 μ and 50 μ and stainless steel of 16 μ) by measuring the counting rate of a tritium-gold source with and without the material between the source and the counter. The tritium gold source was formed as a drive-in target in a sealed-off neutron tube by bombarding a gold plate with a mixture of deuterium and tritium ions of energy 125 KeV [18]. The results can be found in table 1. It was decided to use stainless steel of thickness 16 μ which reduces the measured radiation by a factor of 6.37.

Before the foils were assembled the components were degassed at a temperature of 400°C and after assembly they were cleaned with benzine and distilled water. The holders, which were also degassed, each had a circular aperture of 20 mm diameter so that a film of the same area was formed on each foil. The foils were placed at distances of 15, 20, 30, 40, 50 and 60 mm from the evaporator which was a straight tungsten wire on which 1 mg of titanium wire was spiralized (fig.2a). The completed assembly was placed in a glass vessel, connected to the vacuum system (fig.2) and heated in a furnace to 400°C to degas the glass work and drive out any gas absorbed by the metals parts during assembly. After cooling for two hours and with a vacuum of 2×10^{-6} mm Hg, valve V_1 was closed and breaking seal B_1 opened to allow argon to enter the vessel at a pressure of 1 cm Hg. The flow of argon was controlled by valve V_3 and the pressure measured with the Mac Lead gange. The titanium in the replenisher was evaporated in this atmosphere by passing 220 watts through the heating wire on which the titanium had been spiralised. To prevent the replenisher from getting too hot the evaporation took place in several stages lasting from 6 to 8 seconds each. The argon was pumped off and when the pressure was reduced to 2×10^{-8} mm Hg again valves V_1 and V_2 were closed and tritium was absorbed into the replenisher by breaking breaking-seal B_2. For foils 1-6 100 mc of tritium was used and for foils 11-16 1 c of tritium. The replenisher was then heated and tritium driven out until the pressure, recorded by the ionisation manometer, was 10^{-3} mm Hg. A current was passed through the evaporator until the titanium melted; this was shown by an increase in the current because of the lowering of the resistance of the filament due to the better electrical contact between the titanium and tungsten coils. The titanium was then evaporated slowly while the tritium pressure was held constant at 10^{-3} mm Hg. With 100 mC this was not possible owing to the inadequate amount of

tritium but with 1C the complete evaporation took place with constant pressure. It is important that the pressure during evaporation should not be too high, and the evaporation rate not too great otherwise a fine titanium powder is formed, as described by one of us [15, 17].
The residual tritium was pumped off and valve V_1 closed. Air was slowly introduced into the apparatus by opening and closing valves V_4 and V_5 alternately until atmospheric pressure was reached. The foil and holder assembly was removed and the foils taken from the holders by unscrewing the retaining screws. The amount of tritium in each foil was estimated by measuring the count rate with the Geiger-Müller tube and found to conform with the calculated values.

The external bremsstrahlung generators used in the experiment were:

Hydrogen	z=1	Zinc	z=30
Beryllium	4	Germanium	32
Carbon	6	Selenium	34
Quartz(SiO_2)	10	Zirconium	40
Aluminium	13	Ag-Cu 50-50	40.4
Silicon	14	Molybdenum	42
Sulphur	16	Silver	47
Argon	18	Ag-Au 25-75	53.6
Titanium	22	Ag-Au 50-50	58.1
Chromium	24	Ag-Au 75-25	66.1
Iron	26	Tungsten	74
Nickel	28	Gold	79
Copper	29	Lead	82
		Bismuth	83

The thinnest generator was molybdenum with a thickness of 1.02×10^{-1} gm cm^{-2} and the smallest generator was silicon which overlapped the film by 2.42×10^{-1} gm cm^{-2}. Therefore, no β -electrons passed out of the bremsstrahlung generators since the range of β -electrons with an energy of 18 KeV is

only 7×10^{-4} gm cm^{-2}. Similarly the glass vessel for gas generators had a diameter of 200 mm to prevent any β - electrons from hitting the walls and being absorbed by the glass. All the generators had flat surfaces and except chromium, were finely polished on 000 emergy paper and cleaned with benzene and distilled water. The chromium generator was electro-plated onto a polished copper disc and required no polishing itself. The sulphur generator was cut from a large crystal and ground smooth on emergy paper; the carbon generator was polished by rubbing on a flat piece of paper and the selenum generator was prepared by pouring just molten selenum onto a piece of paper so that the upper surface was flat and lustrous.

The geometry of the measuring arrangement (fig. 3) and the constancy of the measuring equipment were checked throughout the experiment by using a gold standard prepared by the U.K.A.E.A. at Harwell. This standard was set in a polythene cap which could be screwed at fixed distance from the G.M. tube window to give a count rate of 7.200 counts per minute. The external bremsstrahlung generators used for foils 1, 2, 3, 4 and 5 were hydrogen, carbon, aluminium, titanium, chromium, iron, nickel, germanium, zirconium, silver, silver-gold alloy 25-75, tungsten, gold and lead with the experimental procedure for each generator being:

1) Background - counts in 30 seconds
2) Standard - time for 10^4 counts

   1) and 2) repeated twice

3) Foil without EBG - time for 2×10^3 counts
4) Foil with EBG - time for 4×10^3 counts
5) Foil without EBG - time for 2×10^3 counts
6) 1) and 2) repeated twice

Care was taken in placing the generators onto the foils and removing them to prevent any flaking of the film and subsequent loss of tritium. This flaking would become apparent by a significant difference in readings 3) and 5). When hydrogen was used the apparatus was set up as in fig.4, with the gas inlet connected to a high-pressure hydrogen cylinder. The glass vessel was filled with hydrogen and to prevent any air diffusing in during the measurement a constant stream of hydrogen flowed through the vessel. Prior to this experiment it was found that the count rate with air or hydrogen between the foil and the G.M. tube window was the same, so that no corrections were necessary for the different absorption of the x-radiation in this region. The effect of the stainless steel backing was found by using an identical foil without titanium as a generator. The true count rate of the titanium-tritium film plus generators was found by subtracting from each measured count rate the count rate produced by the backing. The results obtained for foils 1, 2, 3, 4 and 5 are tabulated in tables 2, 3, 4, 5 and 6 respectively. They are represented in graphical form as the ratio of the corrected count rate of the generator (CR_z) to the corrected count rate of hydrogen (CR_o) as a function of the atomic number Z in figures 5, 6, 7, 8 and 9 respectively.

For foils 11, 12, 13, 14, 15 and 16 the same method as above was used but with more generators and with the times for the following number of counts being measured:

Foils 1 and 2	5×10^4 counts
Foil 3	4×10^4 counts
Foils 4, 5 and 6	2×10^4 counts.

The pre-set number of counts measured depended on the total time taken for each measurement. The result for foils 11, 12, 13, 14, 15 and 16 are tabulated in tables 7, 8, 9, 10, 11 and 12 respectively and plotted in figures 10, 11, 12, 13, 14 and 15 respectively with the same representation

as for foils 1-5. Argon was used as a generator with foil 11 to estimate the effect of the change in experimental geometry when using gas generators so that the effect of hydrogen could be realised.

To investigate the line structure apparant in figures 5-15 the experiment was repeated using foil 11, which gave the highest count rate, and with various absorbers between the foil and the G.M. tube window. Six absorbers were used: aluminium (50 μ and 100 μ thick), titanium (50 μ), iron (50 μ), nickel (50 μ) and tin (10 μ). They were circular in shape with a diameter of 25 mm so that they completely covered the G.M. tube window and yet did not interfere with the perspex foil support. The results obtained are tabulated in tables 15, 16, 17, 18, 19, 20 and plotted in figures 30, 31, 32, 33, 34 and 35 respectively.

E. Calculations and Discussions

The error in each reading taken during the experiment was equal to the square root of the number of events counted in each reading and varied from 0.45% for 5×10^4 counts to 1.58% for 4×10^3 counts. To obtain values of $\left(\frac{CR_Z}{CR_o}\right)_{corr}$ the following formula is used

$$\left(\frac{CR_z}{CR_o}\right)_{corr} = \frac{CR_z - (CR_B - CR_o)}{CR_o - (CR_B - CR_o)}$$

where CR_Z is the count rate with generator Z

CR_B is the count rate with the backing as generator

CR_o is the count rate with hydrogen.

The numerator is proportional to the effect of the internal bremsstrahlung plus a half of the effect of the external bremsstrahlung because in the bremsstrahlung generator only a half of the β-electrons are decelerated. The denominater is proportional to the effect of the internal bremsstrahlung.

By using the standard propagation of errors formulae the errors in forming this ratio are increased to 2.74% for 5×10^4 counts and to 6.00% for 4×10^3 counts.

The value of $\left(\frac{CR_z}{CR_o}\right)_{corr}$ for argon was 1.04 ± 0.03 (table 7) and by extrapolation the value for z=o would be 0.998 ± 0.002. The range of β-electrons in hydrogen is increased 18 times compared within argon and the change in geometry will probably bring the value for z=o closer to the value for hydrogen and so one is justified in taking hydrogen as z=o when solid generators are used.

From figures 5 to 15 of $\left(\frac{CR_z}{CR_o}\right)_{corr}$ as functions of z it can be seen that there are three departures from the straight line predicted by theory; viz.:

1) The steady departure from the straight line at high Z values
2) The differences in slopes of the graphs
3) The sharp "resonance" peak centered on z=24 (chromium).

If the "resonance" peak is neglected the shape of any individual graph can be explained by the absorption of the bremsstrahlung by the generators. The energy loss per unit length of track of bremsstrahlung is proportional to z^4 and the total path length of β-electrons and therefore of the bremsstrahlung in the generators is inversely proportional to the density and therefore in approximation, inversely proportional to Z. Thus the absorption of bremsstrahlung in the generators is proportional to Z^3. The function $\left(\frac{CR_z}{CR_o}\right)_{corr}$ is therefore represented by the equation

$$\left(\frac{CR_z}{CR_o}\right)_{corr} = 1 + \alpha' z - \beta z^3$$

Now

$$\left(\frac{CR_z}{CR_o}\right)_T = \frac{I_{IBS} + \frac{1}{2}(I_{EBS})}{I_{IBS}} = 1 + \frac{1}{2}\left(\frac{I_{EBS}}{I_{IBS}}\right) \qquad (18)$$

Therefore $\alpha = 2\alpha' = \frac{I_{EBS}}{I_{IBS}}$ per unit atomic number.

$$\Delta CR = \left(\frac{CR_z}{CR_o}\right)_T - \left(\frac{CR_z}{CR_o}\right)_{corr} = \beta Z^3$$

To correct for the absorption effect a rough value of α_{exp} was found by using the fact that $\frac{d}{dz}\left(\frac{CR_z}{CR_o}\right)_{corr} = o$ at z = 74 and graphs were plotted of $\log \Delta CR$ as a function of log Z. By drawing a line of slope 3 through the points on the graph the corrections were found with reference to the rough value. These corrections gave the true experimental values for $\frac{CR_z}{CR_o}$. To obtain the experimental values of I_{EBS}/I_{IBS} equation (18) was used and the resulting graphs can be found in figs. 16-26 with the slopes giving the values of α_{exp} for each foil (table 13). The second term on the right hand side of equation (18) is due to the fact that external bremsstrahlung is generated by half of the electrons only.

From equation (17) in the theory we have

$$\frac{I_{EBS}}{I_{IBS}} = \frac{C_2 Z \int_{\varepsilon}^{E_{max}} I(E) E^2 dE}{5,63 \times 10^{-4} \varepsilon \bar{E} \frac{1}{mc^2}} = \alpha_{th} \times Z \qquad (17)$$

The constants in the equation are

$$C_2 = 1.1 \times 10^{-6}$$

$$\bar{E} = 5.5 \text{ keV}$$

$$\varepsilon = 18 \text{ keV}$$

$$m = 511 \text{ keV}$$

$$\int_o^{E_{max}} I(E)E^2 dE = 46.0$$

The values of $\overline{E}$ and ε are obtained from the β-electron spectrum of tritium (fig.28) and the integral has been calculated by v.d. Vate et al. [13]. Substituting these values in equation (17) we obtain $\alpha_{th} = 0.464$.

Values of α_{exp} obtained were:

Foil	
1	0.0402
2	0.0712
3	0.0902
4	0.1212
5	0.0772
11	0.0538
12	0.0522
13	0.0604
14	0.0498
15	0.0398
16	0.0154

α_{exp} as a function of $\frac{1}{d^2}$ is shown in fig. 27 a) and b) and is shown as a function of $(CR_o)_{corr}$ in fig. 27 c) and d).

In their work with titanium-tritium suspensions v.d. Vate et al. obtained a value $\alpha_{exp} = 0.0264$ which is the same order of magnitude as obtained in this experiment with titanium-tritium films. The low values obtained, compared with theory, mean either that there was too much "internal bremsstrahlung" or too little "external bremsstrahlung" measured with the experimental arrangement used with the former being the most probable. But it is also possible that there is a fault with the theory in this low energy region.

A possible cause of the increased I.B.S. count rate

is the excitation of the extranuclear electrons in the titanium-tritium film by the β-electrons of the tritium. The critical x-ray absorption energies (table 14) are in the same range as the β-electron energy spectrum of tritium. The β-electrons, in passing through the film, may excite the titanium atoms which then return to the ground state with the emission of a characteristic X-ray. The tritium atoms are closely bound to the titanium and this process may have a high probability for occurring. This means that there will be a line spectrum superposed onto the continuous internal bremsstrahlung spectra (fig.29). Because this radiation is independent of the external bremsstrahlung generators, and therefore independent of Z, it decreases the total value of $\frac{I_{EBS}}{I_{IBS}}$ because it appears in the Z-independent denominator only.

The departure of the measured and Z^3-absorption corrected $\frac{I_{EBS}}{I_{IBS}} = f(z)$ can be explained by the excitation of characteristic x-radiation in the external bremsstrahlung generators. With generators outside the resonance region less characteristic radiation will be produced or none at all and therefore the ratio $\frac{I_{EBS}}{I_{IBS}}$ will be on the straight line. With generators inside the resonance region the β-electrons may excite a characteristic x-radiation in the external bremsstrahlung generators in the manner as discussed above for the characteristic x-radiation of the titanium-tritium film. Therefore the measured ratio $\frac{I_{EBS}}{I_{IBS}}$ will be above the straight line because the characteristic x-radiation of the external bremsstrahlung generators appears in the numerator. This would explain the shape of the curves obtained in the experiment.

The experiments with absorbers between the foil and counter were designed to test this hypothesis and do in fact show the presence of some lines. With the aluminium absorbers (figs. 30 and 31) the titanium line was extinguished and the chrome line reduced but the iron line enhanced.

This is explained by the fact that the absorber is more efficient the closer the energy of the line is to the critical absorption limit if all the energies are higher than the limit. For aluminium the k-limit is at 1.559 keV and the titanium, chromium and iron lines are slightly less than 4.966 keV, 5.988 keV and 7.113 keV respectively if one assumes that the outer electrons jump to the K-shell of the excited atoms. The same result is obtained with the nickel and tin absorbers (figs. 34 and 35) as the L-absorption limit of nickel is 1.02 keV and the L_1-absorption limit of tin is 4.445 keV. As the L_1-absorption limit for tin is so close to the lines one would expect that the tin absorber would be the most efficient of the three to reduce the lines. One can see from the figures that this is so. The titanium absorber (fig.32) shows that there is selective transmission of the titanium line and the nickel and chrome lines have been totally absorbed. The low value of α from this experiment can be explained by the selective transmission of the titanium line from the titanium-tritium film through the absorber and hence an increase in the denominator of $\frac{I_{EBS}}{I_{IBS}}$. The iron absorber (fig.33) shows the selective transmission of the iron line and the chromium line much reduced. This shows definitely that there are discrete spectra of at least two of the elements superposed onto the continuous IBS spectra. The complete analysis of the spectrum is necessary to test the theory adequately. This can be done with a proportional counter, for example.

The variation in α_{exp} for the different foils can be explained by the changes in the relative intensities of the lines from the titanium-tritium layer with different foils and the corresponding change in the I.B.S. count rate (z independent denominator).

(CR_o) as a function of d is represented in figures 36 and 37 for foils 1-5 and foils 11-16 respectively. The dotted line represents a $\frac{1}{d^2}$ fall-off which corresponds to a point source of titanium evaporator and the dashed line represents a $\frac{1}{d}$ fall-off which corresponds to an infinitely straight titanium evaporator. It can be seen on inspection that for a short straight evaporator $(CR_o)_{corr}$ as a function of it is between these two theoretical limits.

It would appear that the characteristic x-radiations present in this experiment are unavoible when a tritium-metal system is used for this method. However, to reduce the characteristic x-radiation in intensity and complexity a beryllium foil as backing could be used since the critical absorption limit of beryllium is 0.112 keV only. The tritium layer can be produced by using the beryllium as a drive-in target in a sealed neutron tube.

Eindhoven, november 30th 1961

Philips Research Laboratories
N.V. Philips' Gloeilampenfabrieken

FMS

D. Wickenden.

O. Reifenschneider

REFERENCES

1) G.H.Aston - Proc.Cam.Phil.Soc. 23 937 (1927)
2) H.Langevin-Joliot - Ann.Phys. 2 16 (1957)
3) J.K.Knipp and G.E.Uhlenbeck - Physica 3 425 (1936)
4) F.Bloch - Phys.Rev. 50 275 (1936)
5) C.S.Wang Chang and D.L.Falkoff - Phys.Rev. 76 365 (1949)
6) S.B.Nilsson - Arkiv för Fysik 10 467 (1956)
7) E.J.Konopinski and G.E.Uhlenbeck - Phy.Rev. 47 202 (1935)
8) A.Michalowicz - Ann.Phys. 2 116 (1957)
9) H.Bethe and W.Heitler - Proc.Roy.Soc. 146A 83 (1934)
10) A.H.Compton and S.K.Allison - "X-Rays in Theory and Experiment" Page 90 (1935)
11) as 10) page 106
12) S.J.Wyard - Proc.Roy.Soc. A65 377 (1952)
13) J.v.d.Vate, O.Reifenschweiler and G.v.d.Ligt - Internal Report of the Philips Res.Lab.Versl.3710, 1961
14) D.P.Smith - "Hydrogen in Metals" v.of Chicago Press (1948)
15) O.Reifenschweiler - "A suitable Tritium Carrier for Gas Discharge Tubes" 2nd U.N.Geneva Conference 1958 Pergamon Press, London
16) V.D.Scott and L.W.Owen - British Journ.of App.Phy. 10 91 (1959)
17) O.Reifenschweiler - Phys.Verh. Mosbach, Nr.9, 181, 1961
18) O.Reifenschweiler - Nucleonics 18 69 1960 also O.Reifenschweiler - Philips Research Reports 16 no.5 1961

TABLE 1

Absorbtion of x-radiation of tritium in possible backings

Material	Count rate without absorbtion	count rate with absorbtion	reducing factor
Steel (16 /u)	28.000	4.400	6.37
Nickel (15/u)	28.000	6.300	4.45
Nickel (25/u)	28.000	1.680	16.7
Nickel (50/u)	28.000	362	77.3

TABLE 2

FOIL 1

Distance from evaporator 15 mm 100 mC tritium

E.B.G.	Z	Cpm with E.B.G.	Corrected for backing	
H	1 (o)	4899.1	2722.0	1.000
C	6	4944.3	2767.2	1.017
Al	13	5220.9	3043.8	1.118
Ti	22	6853.8	4676.7	1.718
Cr	24	7393.0	5215.9	1.916
Fe	26	6642.7	4465.6	1.640
Ni	28	5818.3	3641.2	1.338
Ge	32	5973.2	3796.1	1.395
Zr	40	5995.8	3818.7	1.403
Ag	47	6574.0	4396.9	1.615
25Ag-Au	66.1	7077.7	4890.6	1.796
W	74	7425.1	5248.0	1.928
Au	79	7119.3	4942.2	1.815
Pb	82	6502.2	4525.1	1.666
Backing		7076.2		
		4899.1		Error ± 6%
		2177.1		

TABLE 3

FOIL 2

Distance from evaporator 20 mm 100 mc tritium

E.B.G.	Z	CPM with EBG	Corrected for backing	$(\frac{CR_z}{CR_o})_{corr}$
H	1 (o)	3556.0	1351.9	1.000
C	6	3855.1	1651.0	1.221
Al	13	4152.7	1948.6	1.441
Ti	22	5655.4	3451.3	2.553
Cr	24	5886.1	3682.0	2.724
Fe	26	5803.2	3599.1	2.662
Ni	28	4780.5	2576.4	1.906
Ge	32	4766.9	2562.8	1.896
Zr	40	5068.4	2864.3	2.119
Ag	47	5283.3	3079.2	2.278
25Ag-Au	66.1	5666.4	3462.3	2.561
W	74	5867.1	3663.0	2.710
Au	79	5631.5	3427.4	2.535
Pb	82	5291.0	3096.9	2.291
Steel backing		5760.1		
		3556.0		Error ± 6%
		2204.1		

TABLE 4

FOIL 3

Distance from evaporator 30 mm 100 mc tritium

E.B.G.	Z	CPM with EBG	Corrected for backing	
H	1 (o)	2273.5	776.7	1.000
C	6	2361.1	864.3	1.113
Al	13	2682.4	1183.6	1.524
Ti	22	3608.0	2111.2	2.718
Cr	24	3965.4	2468.6	3.178
Fe	26	3609.7	2112.9	2.720
Ni	28	3044.5	1547.7	1.993
Ge	32	3129.8	1633.0	2.103
Zr	40	3182.4	1685.6	2.170
Ag	47	3403.3	1906.5	2.455
25Ag-Au	66.1	3865.0	2368.2	3.049
W	74	3963.4	2466.6	3.176
Au	79	3771.8	2275.0	2.929
Pb	82	3408.8	1912.0	2.460
Backing		3770.3		
		2273.5		Error ± 6%
		1496.8		

TABLE 5

FOIL 4

Distance from evaporator 40 mm 100 mc tritium

E.B.G.	Z	CPM with EBG	Corrected for backing	
H	1 (o)	1034.0	287.1	1.000
C	6	1143.0	396.1	1.380
Al	13	1249.1	502.2	1.749
Ti	22	1744.0	997.1	3.473
Cr	24	1836.3	1089.4	3.795
Fe	26	1745.5	998.6	3.478
Ni	28	1508.8	761.9	2.654
Ge	32	1411.7	664.8	2.316
Zr	40	1481.4	734.5	2.558
Ag	47	1583.0	836.1	2.912
25Ag-Au	66.1	1812.8	1065.9	3.718
W	74	1887.9	1141.0	3.974
Au	79	1821.4	1074.5	3.743
Backing		1780.9		
		1034.0		Error
		746.9		± 6%

TABLE 6

FOIL 5

Distance from evaporator 50 mm 100 mc tritium

E.B.G.	Z	CPM with EBG	Corrected for backing	
H	1 (o)	801.3	329.1	1.000
C	6	882.6	410.4	1.246
Al	10	957.9	485.7	1.478
Ti	22	1243.6	771.4	2.343
Cr	24	1353.6	881.4	2.678
Fe	26	1263.0	790.8	2.400
Ni	28	1111.1	638.9	1.940
Ge	32	1087.0	614.8	1.868
Zr	40	1132.6	660.4	2.002
Ag	47	1224.1	751.9	2.283
25Ag-Au	66.1	1310.1	837.9	2.543
W	74	1428.2	956.0	2.907
Au	79	1379.2	907.0	2.754
Pb	82	1171.8	699.6	2.125
Backing		1273.5		
		801.3		Error
		472.2		± 6%

TABLE 7

FOIL 11

Distance from evaporator 15 mm 1 C tritium

E.B.G.	Z	CPM with EBG	Corrected for backing	
H	1 (o)	22948	10932	1.000
Be	4	24518	12502	1.144
C	6	24354	12338	1.129
Qu	10	25783	13767	1.259
Al	13	26486	14470	1.324
Si	14	26342	14326	1.310
S	16	26632	14616	1.337
Ti	22	35558	23542	2.154
Cr	24	37458	25442	2.327
Fe	26	34860	22844	2.090
Ni	28	30698	18682	1.709
Cu	29	30394	18378	1.581
Zn	30	30118	18102	1.656
Ge	32	28696	16680	1.526
Se	34	29277	17261	1.579
Zr	40	31072	19056	1.743
50Ag-Cu	40.4	31454	19438	1.778
Mo	42	32351	20335	1.860
Ag	47	33553	21537	1.970
75Ag-Au	53.6	33906	21890	1.970
50Ag-Au	58.1	35842	23826	2.179
25Ag-Au	66.1	36821	24805	2.269
W	74	37467	25451	2.328
Au	79	36784	24768	2.266
Pb	82	34612	22596	2.067
Bi	83	36256	24240	2.217
A	18	23437	11421	1.004
Backing		34964 22948 12016		Error ± 2.74%

TABLE 8

FOIL 12

Distance from evaporator 20 mm 1 C tritium

E.B.G.	Z	Cpm with EBG	Corrected for backing	
H	1 (o)	19151	9183	1.000
Be	4	20327	10359	1.128
C	6	20269	10301	1.111
Qu	10	21570	11602	1.263
Al	13	21977	12009	1.308
Si	14	21626	11658	1.270
S	16	22103	12135	1.321
Ti	22	29448	19480	2.121
Cr	24	31438	21470	2.338
Fe	26	28671	18704	2.037
Ni	28	25394	15426	1.680
Cu	29	25369	15401	1.677
Zn	30	24725	14757	1.607
Ge	32	24205	14237	1.550
Se	34	24226	14258	1.553
Zr	40	26036	16068	1.750
50Ag-Cu	40.5	26135	16168	1.761
Mo	42	26827	16859	1.836
Ag	47	27987	18019	1.962
75Ag-Au	53.6	28798	18830	2.051
50Ag-Au	58.1	30035	20067	2.185
25Ag-Au	66.1	30187	20219	2.202
W	74	31190	21222	2.311
Au	79	30765	20797	2.265
Pb	82	28890	18922	2.061
Bi	83	30421	20453	2.231
Backing		29119		
		19151		Error
		9968		± 2.74%

TABLE 9

FOIL 13

Distance from evaporator 30 mm 1C tritium

E.B.G.	Z	Cpm with EBG	Corrected for backing	
H	1 (o)	6207.7	2749.2	1.000
Be	4	6617.6	3159.1	1.149
C	6	6572.5	3114.0	1.133
Qu	10	6906.2	3447.7	1.254
Al	13	7210.3	3751.8	1.365
Si	14	7116.3	3657.8	1.331
S	16	7143.9	3685.4	1.340
Ti	22	9634.3	6175.8	2.247
Cr	24	10368.0	6909.5	2.513
Fe	26	9464.7	6006.2	2.185
Ni	28	8301.3	4842.8	1.762
Cu	29	8338.4	4879.9	1.775
Zn	30	8169.0	4710.5	1.713
Ge	32	8072.2	4613.7	1.678
Se	34	8005.0	4546.5	1.654
Zr	40	8581.7	5123.2	1.864
50Ag-Cu	40.4	8800.0	5341.5	1.943
Mo	42	8754.9	5296.4	1.927
Ag	47	9028.1	5569.6	2.026
75Ag-Au	53.6	9336.0	5877.5	2.138
50Ag-Au	58.1	9605.8	6147.3	2.236
25Ag-Au	66.1	10000.0	6541.5	2.380
W	74	10146.0	6687.5	2.433
Au	79	10075.0	6616.5	2.407
Pb	82			
Bi	83	9898.0	6439.5	2.341
Backing		9666.2 6207.7		Error ± 3.34%
		3458.5		

TABLE 10

FOIL 14
Distance from evaporator 40 mm 1C tritium

E.B.G.	Z	Cpm with EBG	Corrected for backing	
H	1 (o)	5803.6	2685.8	1.000
Be	4	6170.5	3052.7	1.137
C	6	6143.0	3025.2	1.126
Qu	10	6470.5	3352.7	1.248
Al	13	6601.0	3483.2	1.297
S	16	6675.6	3557.8	1.325
Ti	22	9014.5	5896.7	2.195
Cr	24	9471.9	6354.1	2.366
Fe	26	8803.0	5685.2	2.117
Ni	28	7759.0	4641.2	1.728
Cu	29	7653.9	4536.1	1.689
Zr	40	7855.0	4737.2	1.764
Mo	42	8053.8	4936.0	1.838
Ag	47	8129.1	5011.3	1.866
75Ag-Au	53.6	8569.0	5451.2	2.030
50Ag-Au	58.1	8911.6	5793.8	2.157
25Ag-Au	66.1	9116.7	5958.9	2.233
W	74	9316.2	6198.4	2.308
Au	79	9157.0	6039.2	2.249
Pb	82	8714.2	5596.4	2.084
Backing		8921.4		Error
		5803.6		± 4.40%
		3117.8		

TABLE 11

FOIL 15

Distance from evaporator 50 mm 1C tritium

E.B.G.	Z	Cpm with EBG	Corrected for backing	
H	1 (o)	3004.1	1632.1	1.000
Be	4	3222.4	1850.4	1.134
C	6	3227.1	1855.1	1.137
Qu	10	3399.1	2027.1	1.242
Al	13	3405.8	2033.8	1.246
Si	14	3430.2	2058.2	1.260
S	16	3480.0	2108.0	1.292
Ti	22	4449.6	3077.6	1.886
Cr	24	4625.4	3253.4	1.993
Fe	26	4418.6	3046.6	1.867
Ni	28	3936.1	2564.1	1.571
Cu	29	3965.8	2593.8	1.589
Ge	32	3864.1	2492.1	1.527
Zr	40	3927.7	2555.7	1.566
Mo	42	4111.3	2739.3	1.678
Ag	47	4233.7	2861.7	1.753
75Ag-Au	53.6	4319.4	2947.4	1.806
50Ag-Au	58.1	4565.9	3193.9	1.957
25Ag-Au	66.1	4545.7	3173.7	1.945
W	74	4624.3	3252.3	1.993
Au	79	4556.2	3184.2	1.952
Pb	82	4229.6	2857.6	1.751
Backing		4376.1		
		3004.1		Error
		1372.0		± 4.40%

TABLE 12

FOIL 16

Distance from evaporator 60 mm 1C tritium

E.B.G.	Z	Cpm with EBG	Corrected for backing	
H	1 (o)	2181.2	1593.6	1.000
Be	4	2308.3	1720.7	1.080
C	6	2270.7	1683.1	1.056
Qu	10	2355.6	1768.0	1.109
Al	13	2388.5	1800.9	1.130
Si	14	2388.9	1801.3	1.130
S	16	2367.6	1780.0	1.117
Ti	22	2773.5	2185.9	1.372
Cr	24	2827.9	2240.3	1.406
Fe	26	2805.1	2217.5	1.392
Ni	28	2528.2	1940.6	1.218
Cu	29	2513.3	1925.7	1.208
Ge	32	2536.5	1948.9	1.223
Se	34	2506.6	1919.0	1.204
Zr	40	2579.8	1992.2	1.250
Mo	42	2609.3	2021.7	1.269
Ag	47	2619.1	2031.5	1.275
75Ag-Au	53.6	2666.0	2078.4	1.304
50Ag-Au	58.1	2732.5	2144.9	1.346
25Ag-Au	66.1	2781.3	2193.7	1.377
W	74	2824.5	2236.9	1.404
Au	79	2815.2	2227.6	1.398
Pb	82	2652.0	2064.4	1.295
Backing		2768.8		
		2181.2		Error
		587.6		± 4.40%

TABLE 13

EXPERIMENTAL VALUES OF α AND β

a) Foils 1-5

Foil	$\frac{1}{\alpha^2} \times 10^{-2}\ cm^{-2}$	$\alpha_{exp} \times 10^{-2}$	$\beta_{exp} \times 10^{-6}$	$\frac{\beta}{\alpha} \times 10^{-5}$
1	44.5	4.02	1.22	3.08
2	25.0	7.12	2.16	3.06
3	11.1	9.02	2.74	3.03
4	6.3	12.12	3.68	3.06
5	4.0	7.72	2.28	2.96

b) Foils 11-16

Foil	$\frac{1}{\alpha^2} \times 10^{-2}\ cm^{-2}$	$\alpha_{exp} \times 10^{-2}$	$\beta_{exp} \times 10^{-6}$	$\frac{\beta}{\alpha} \times 10^{-5}$
11	44.5	5.38	1.64	3.04
12	25.0	5.22	1.59	3.05
13	11.1	6.04	1.88	3.12
14	6.3	4.98	1.54	3.09
15	4.0	3.98	1.21	3.05
16	2.8	1.54	0.49	3.18

c) Foil 11 with absorbers

Absorber	$\alpha_{exp} \times 10^{-2}$
Al (50/u)	7.44
Al (100/u)	6.96
Ti (50/u)	2.72
Fe (50/u)	5.37
Ni (50/u)	6.02
Sn (10/u)	5.53

theory	0.4640
v.d.Vate	0.0264

TABLE 14

X-Ray Critical Absorption Energies in Kev *

Element	Z	K	L_1	L_{11}	L_{111}
Be	4	0.112			
C	6	0.284			
O	8	0.532			
Al	13	1.559	0.087	0.072	
Si	14	1.838	0.118	0.098	
S	16	2.469	0.193	0.163	0.163
Ti	22	4.966	0.530	0.462	0.456
Cr	24	5.988	0.679	0.584	0.574
Fe	26	7.113	0.849	0.722	0.709
Ni	28	8.337	1.015	0.877	0.858
Cu	29	8.982	1.100	0.954	0.935
Zn	30	9.662	1.200	1.047	1.024
Ge	32	11.100	1.42	1.244	1.212
Se	34	12.653	1.66	1.472	1.431
Zr	40	17.998	2.534	2.308	2.224
Mo	42	20.003	2.869	2.630	2.525
Ag	47	25.535	3.828	3.547	3.375
Sn	50	29.182	4.445	4.139	3.911
W	74	69.51	12.094	11.538	10.200
Au	79	80.713	14.351	13.731	11.916
Pb	82	88.001	15.861	15.200	13.033
Bi	83	90.521	16.380	15.709	13.417

* From E.Segrè "Experimental Nuclear Physics" Vol.III (J.Wiley 1959)

TABLE 15

FOIL 11 Absorber Aluminium (50/u)

E.B.G.	Z	Cpm with EBG	Corrected for backing	
H	1 (o)	3724.5	1376.5	1.000
Be	4	3855.9	1507.9	1.096
C	6	3910.7	1562.7	1.136
Qu	10	4076.1	1728.1	1.255
Al	13	4224.6	1876.6	1.363
Si	14	4168.0	1820.0	1.322
S	16	4215.2	1867.2	1.356
Ti	22	4675.6	2327.6	1.691
Cr	24	5645.2	3297.2	2.395
Fe	26	6251.5	3903.5	2.836
Ni	28	5030.0	2682.0	1.948
Cu	29	4944.7	2596.7	1.843
Ge	32	4820.8	2472.8	1.796
Se	34	4768.1	2420.1	1.758
Zr	40	5010.8	2662.8	1.934
Mo	42	5129.3	2781.3	2.021
Ag	47	5329.6	2981.6	2.166
75Ag-Au	53.6	5511.8	3163.8	2.298
50Ag-Au	58.1	5873.3	3525.3	2.561
25Ag-Au	66.1	5959.6	3611.6	2.624
W	74	6255.1	3907.1	2.838
Au	79	6123.3	3775.3	2.743
Pb	82	5575.2	3227.2	2.345
Backing		6072.5		
		3724.5		Error
		2348.0		± 6%

TABLE 16

FOIL 11 Absorber Aluminium 100 /u

E.B.G.	Z	Cpm with EBG	Corrected for backing	
H	1 (o)	1025.7	431.7	1.000
Be	4	1091.0	497.0	1.151
Qu	10	1123.9	529.9	1.227
Al	13	1143.2	549.2	1.272
S	16	1174.4	580.4	1.344
Ti	22	1220.5	626.5	1.452
Cr	24	1344.0	750.0	1.737
Fe	26	1678.8	1084.8	2.514
Ni	28	1354.7	760.7	1.762
Cu	29	1302.8	708.8	1.642
Zn	30	1351.8	757.8	1.755
Ge	32	1355.6	761.6	1.764
Zr	40	1377.4	783.4	1.815
Ag	47	1420.0	826.0	1.914
50Ag-Au	58.1	1658.4	1064.4	2.466
W	74	1787.6	1193.6	2.719
Au	79	1718.3	1124.3	2.604
Backing		1619.7		Error
		1025.7		± 6%
		594.0		

TABLE 17

FOIL 11 Absorber Titanium 50/u

E.B.G.	Z	Cpm with EBG	Corrected for backing	
H	1 (o)	725.9	586.9	1.000
Be	4	726.4	587.4	1.001
C	6	747.2	608.2	1.036
Qu	10	811.8	672.8	1.146
Al	13	793.5	654.5	1.115
Si	14	798.9	659.9	1.124
S	16	789.5	650.5	1.108
Ti	22	1569.1	1430.1	2.437
Cr	24	879.9	740.9	1.262
Fe	26	915.0	776.0	1.323
Ni	28	907.8	768.8	1.310
Cu	29	912.9	773.9	1.319
Zn	30	949.2	810.2	1.380
Ge	32	915.3	776.3	1.324
Zr	40	955.9	816.9	1.393
Ag	47	985.7	846.7	1.443
50Ag-Au	58.1	1045.6	906.6	1.545
W	74	1109.1	980.1	1.670
Au	79	1066.7	927.7	1.581

Backing 864.9

725.9

139.0

Error ± 6%

TABLE 18

FOIL 11 Absorber Iron 50/u

E.B.G.	Z	Cpm with EBG	Corrected for backing	
H	1 (o)	600.8	227.8	1.000
Be	4	603.1	230.1	1.012
Qu	10	620.7	247.7	1.088
Al	13	638.2	265.2	1.165
Ti	22	666.7	293.7	1.289
Cr	24	775.4	402.4	1.764
Fe	26	1041.7	668.7	2.937
Ni	28	709.8	336.8	1.480
Cu	29	737.0	364.0	1.593
Ge	32	710.2	337.2	1.481
Se	34	696.5	323.5	1.420
Zr	40	748.5	375.5	1.651
Ag	47	763.2	390.2	1.716
50Ag-Au	58.1	852.3	479.3	2.107
W	74	904.0	531.0	2.323
Au	79	870.1	497.1	2.184
Backing		973.8 600.8 373.0		Error ± 6%

TABLE 19

FOIL 11 Absorber Nickel 50/u

E.B.G.	Z	Cpm with EBG	Corrected for backing	
H	1 (o)	900.0	338.6	1.000
Be	4	906.0	344.6	1.018
Qu	10	946.7	385.3	1.138
Al	13	986.7	425.3	1.256
S	16	985.2	423.8	1.252
Ti	22	1079.9	518.4	1.531
Cr	24	1190.3	628.9	1.857
Fe	26	1601.2	1039.8	3.071
Ni	28	1212.1	650.7	1.923
Cu	29	1187.6	626.2	1.849
Zn	30	1120.6	559.2	1.651
Ge	32	1155.4	594.0	1.754
Se	34	1083.7	522.3	1.543
Zr	40	1144.2	582.8	1.722
Ag	47	1222.3	660.9	1.954
50Ag-Au	58.1	1352.9	791.5	2.338
W	74	1405.4	844.0	2.494
Au	79	1411.1	849.7	2.510
Backing		1461.4		
		900.0		Error
		561.4		± 6%

TABLE 20

FOIL 11 Absorber Tin 10/u

E.B.G.	Z	Cpm with EBG	Corrected for backing	
H	1 (o)	717.3	374.4	1.000
Be	4	718.4	375.5	1.003
Qu	10	727.5	384.6	1.028
Al	13	768.9	426.0	1.138
Ti	22	811.9	469.0	1.252
Cr	24	881.7	538.8	1.438
Fe	26	1086.3	743.4	1.985
Ni	28	918.9	576.0	1.539
Cu	29	902.7	559.8	1.496
Ge	32	912.1	569.2	1.521
Ag	47	1001.5	658.6	1.757
50Ag-Au	58.1	1121.6	778.7	2.078
W	74	1228.0	885.1	2.363
Au	79	1145.1	792.2	2.114
Bi	83	1191.5	858.6	2.295
Backing		1060.2		Error
		717.3		± 6%
		342.9		

NAT.LAB.
VERSLAG Nr.3701
D.K. Wickenden
Dr. O. Reifenschweiler

A,B and C staineless steel
D nickel

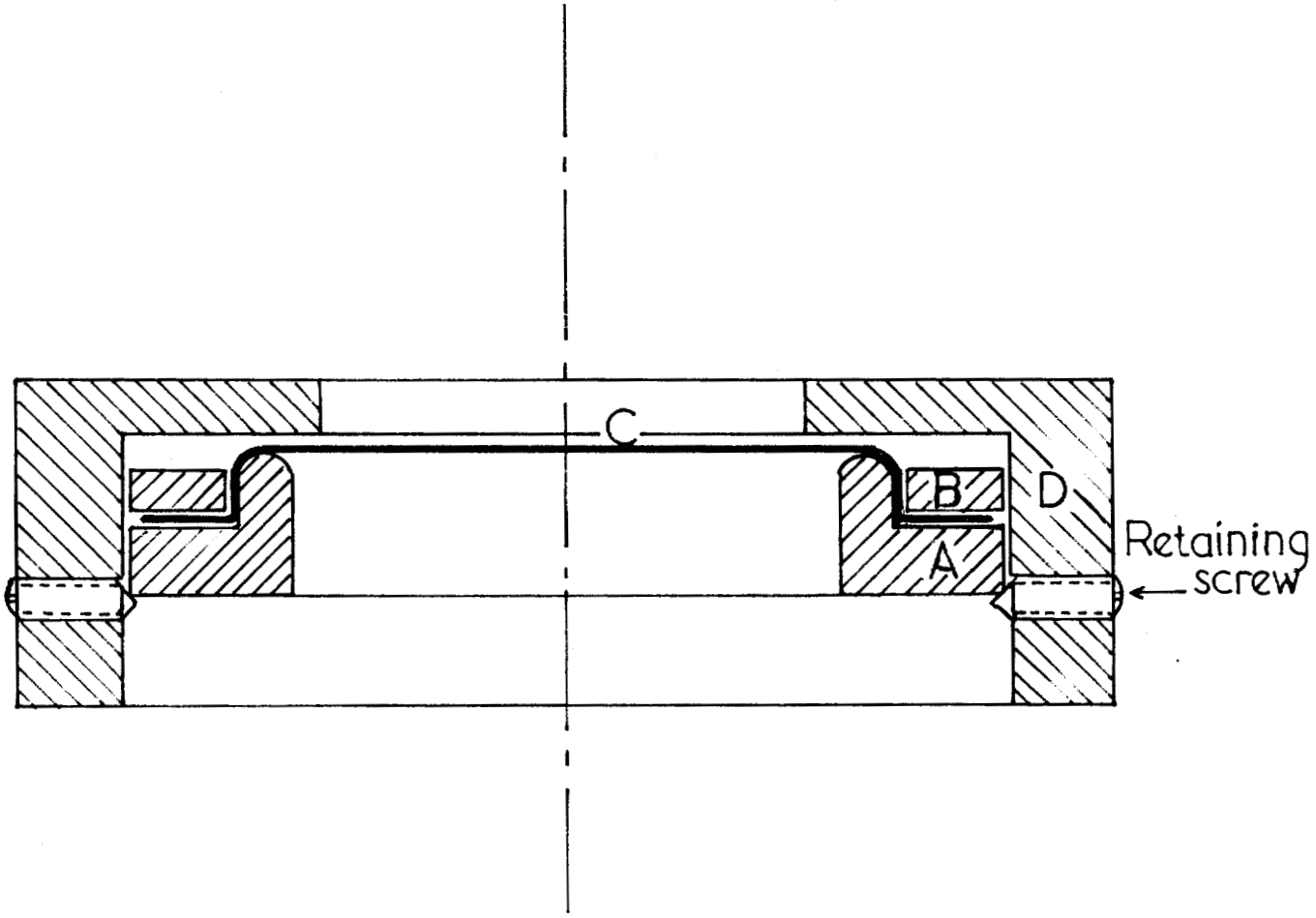

Fig.1

Foil construction and holder

$V_1 - V_5$ Valves

$B_1 - B_2$ Breaking seals

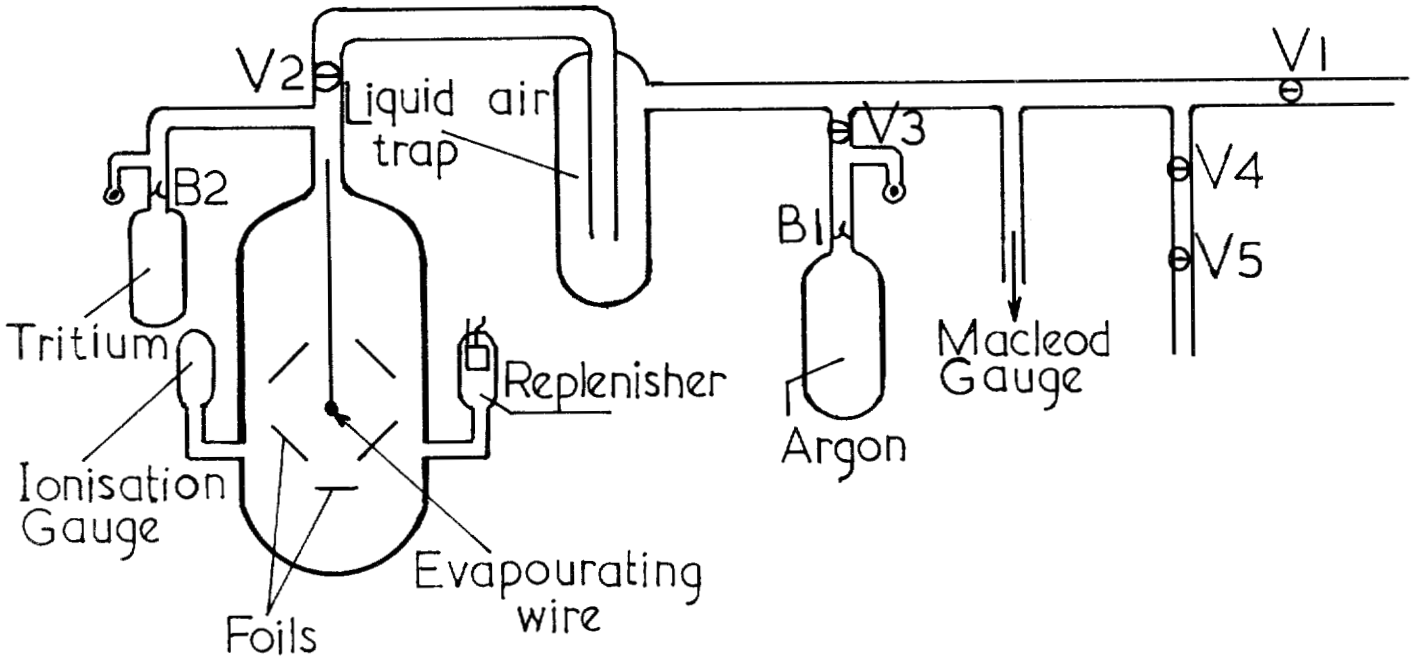

Fig. 2

Vacuum system

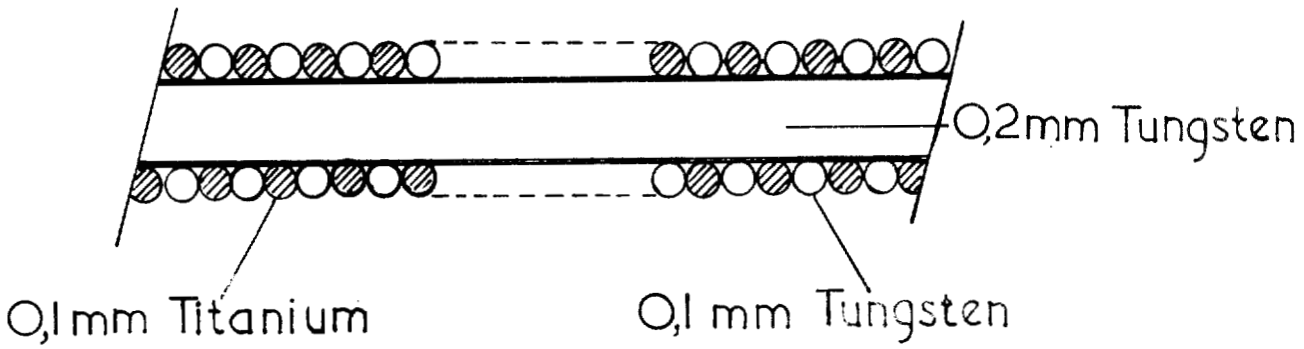

Fig. 2a

Evapouratour wire

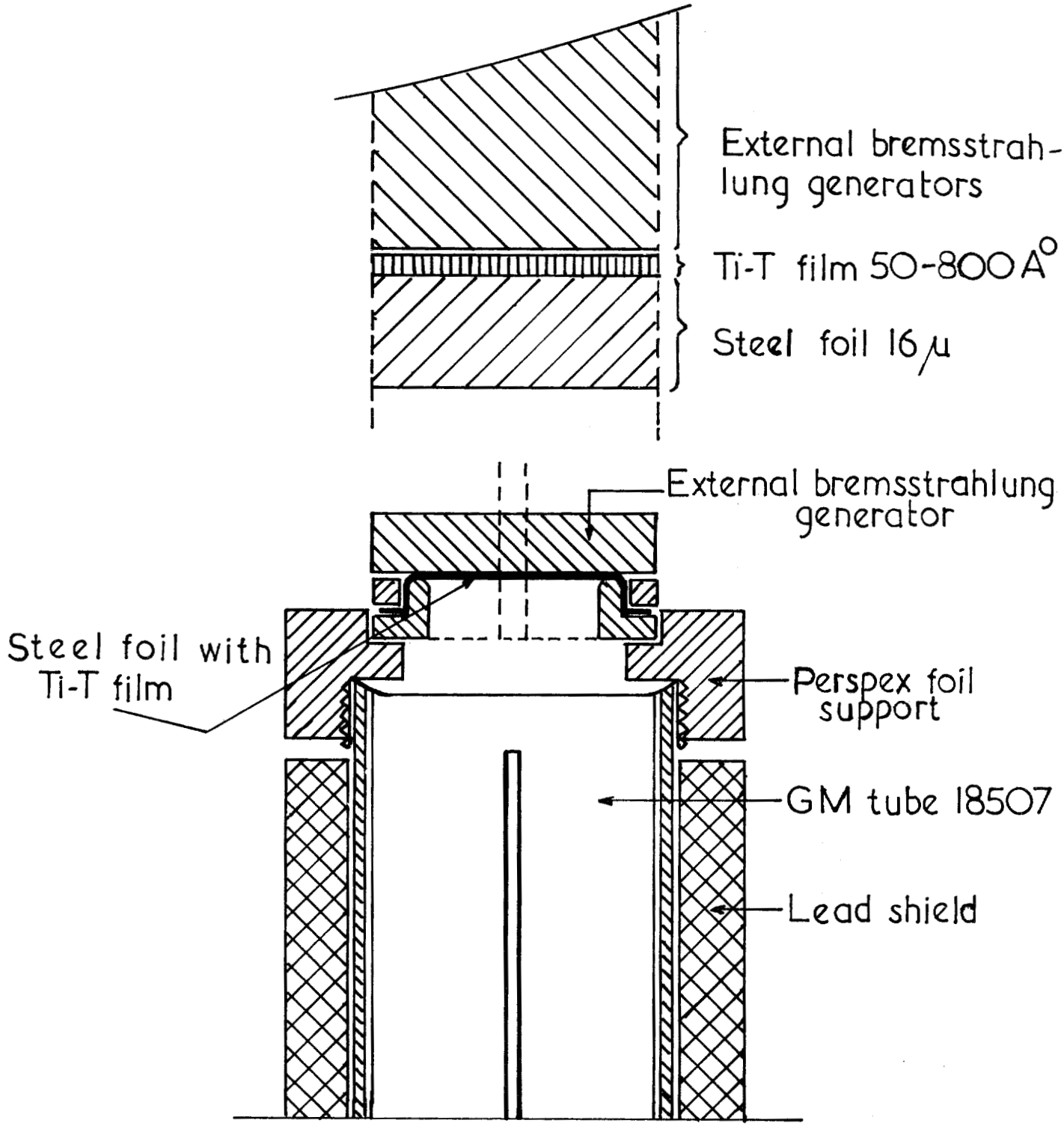

Fig. 3

Experimental arrangement for solid bremsstrahlung generators

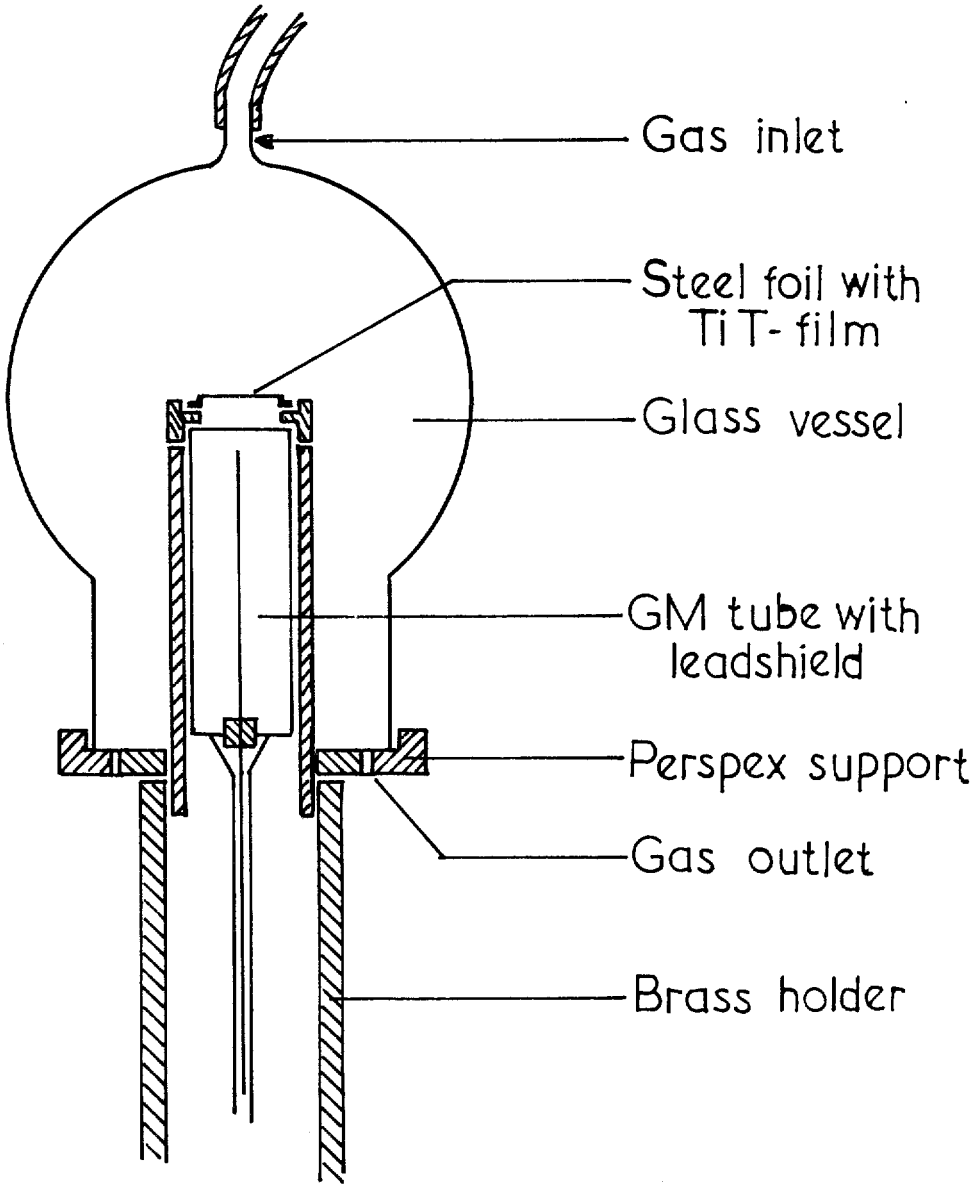

Fig. 4

Experimental arrangement for gaseous bremsstrahlung generators

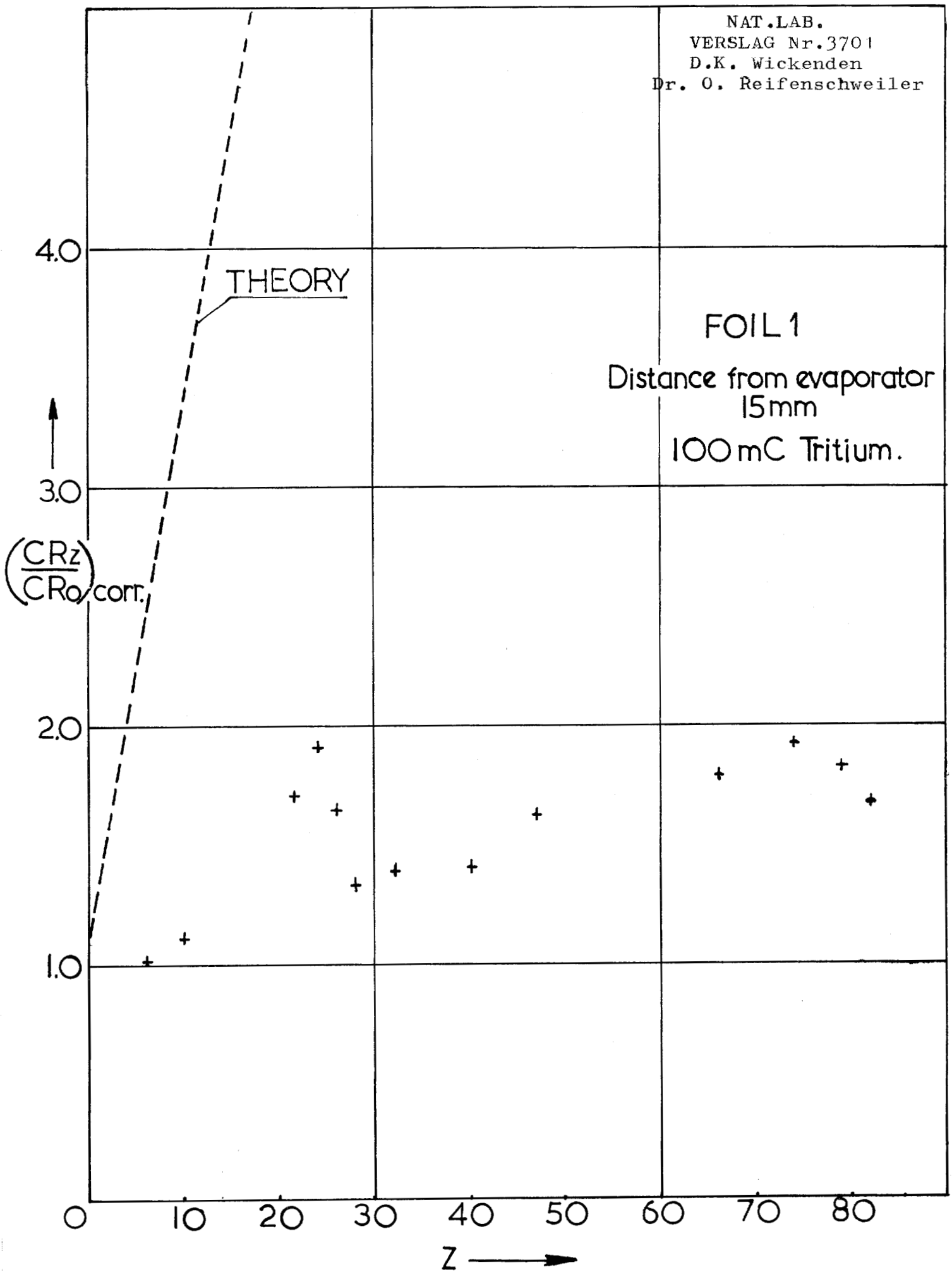
NAT.LAB.
VERSLAG Nr.3701
D.K. Wickenden
Dr. O. Reifenschweiler
THEORY
FOIL 1
Distance from evaporator
15mm
100mC Tritium.
4.0
3.0
2.0
1.0
0
10
20
30
40
50
60
70
80
Z
(CRz/CRo)corr.

Fig.5

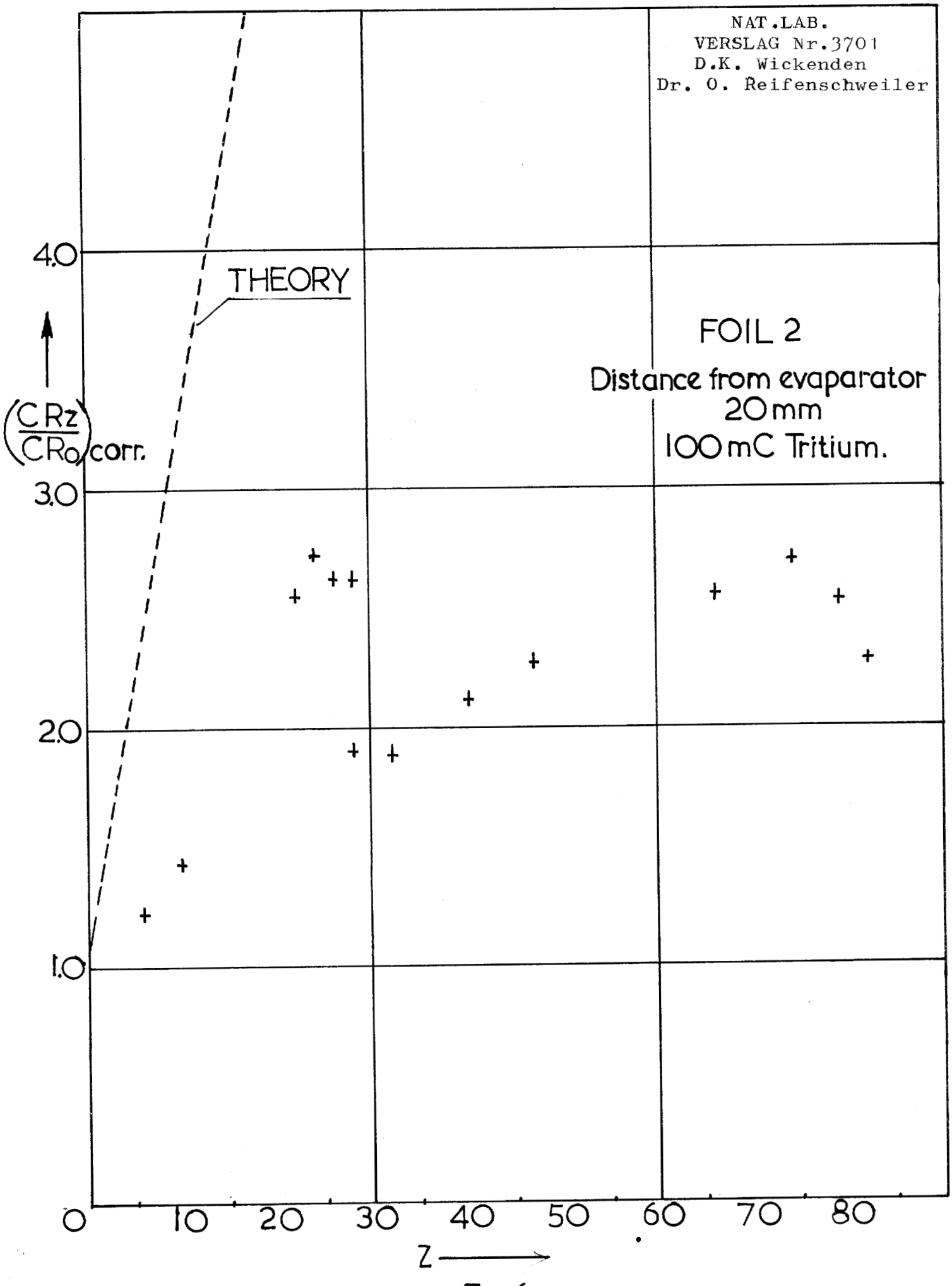
NAT.LAB.
VERSLAG Nr.3701
D.K. Wickenden
Dr. O. Reifenschweiler
THEORY
FOIL 2
Distance from evaporator
20 mm
100 mC Tritium.
(CRz/CRo) corr.
4.0
3.0
2.0
1.0
0
10
20
30
40
50
60
70
80
Z

Fig.6

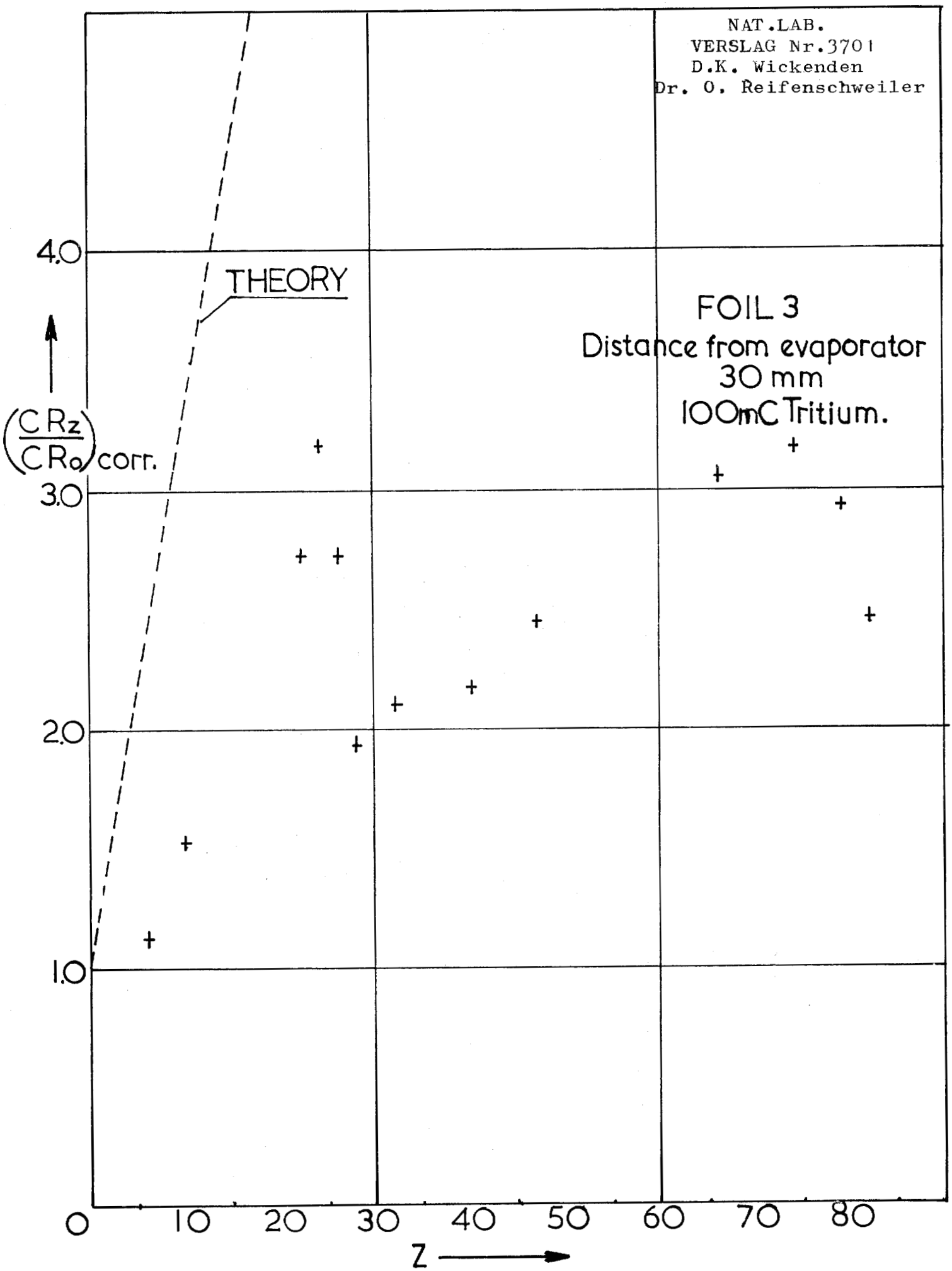
NAT.LAB.
VERSLAG Nr.3701
D.K. Wickenden
Dr. O. Reifenschweiler
THEORY
FOIL 3
Distance from evaporator
30 mm
100mC Tritium.
(CRz/CRo)corr.
4.0
3.0
2.0
1.0
0
10
20
30
40
50
60
70
80
Z

Fig. 7

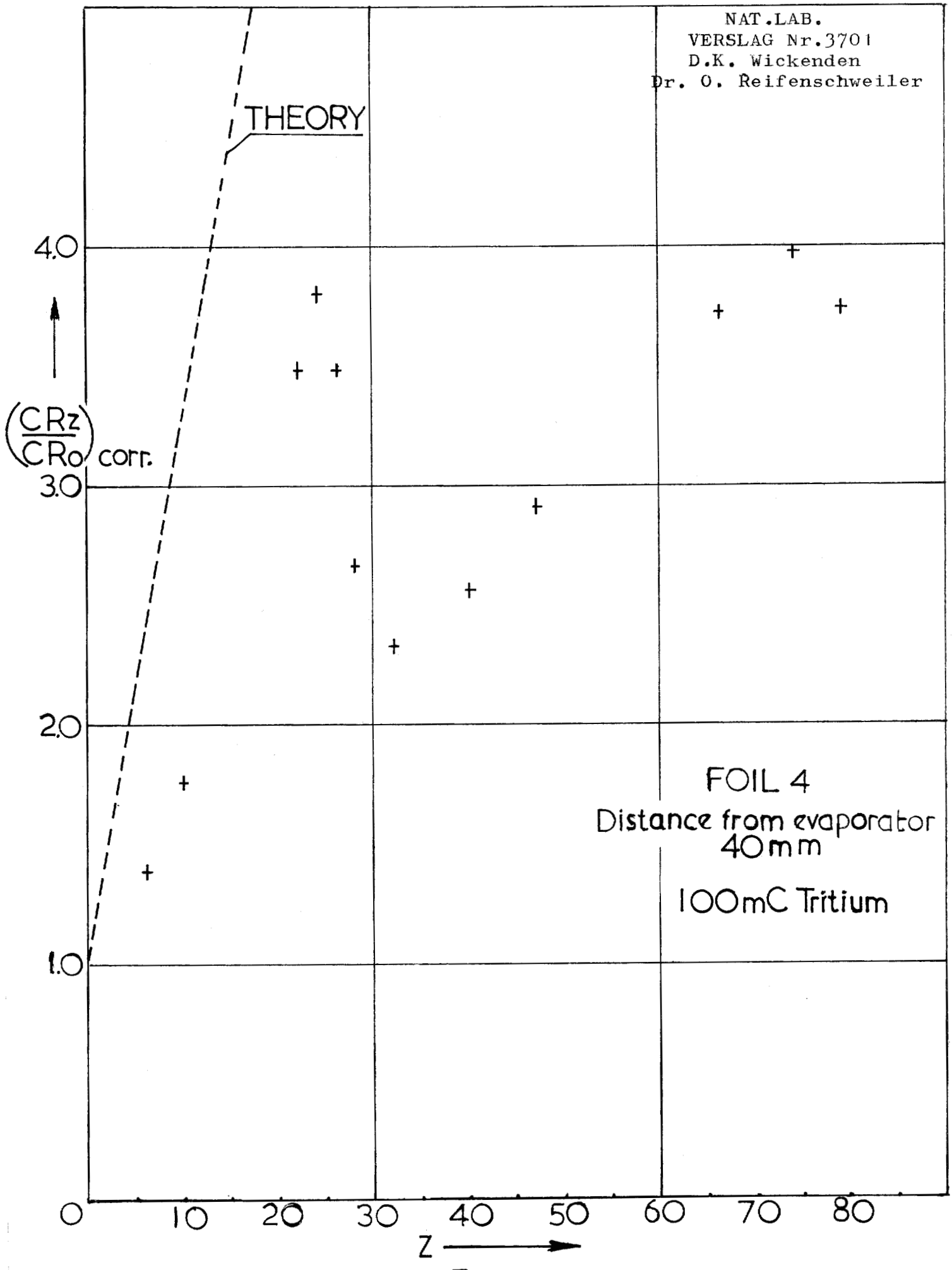
NAT.LAB.
VERSLAG Nr.3701
D.K. Wickenden
Dr. O. Reifenschweiler
THEORY
4.0
3.0
2.0
1.0
(CRz/CRo) corr.
FOIL 4
Distance from evaporator
40mm
100mC Tritium
0
10
20
30
40
50
60
70
80
Z

Fig. 8

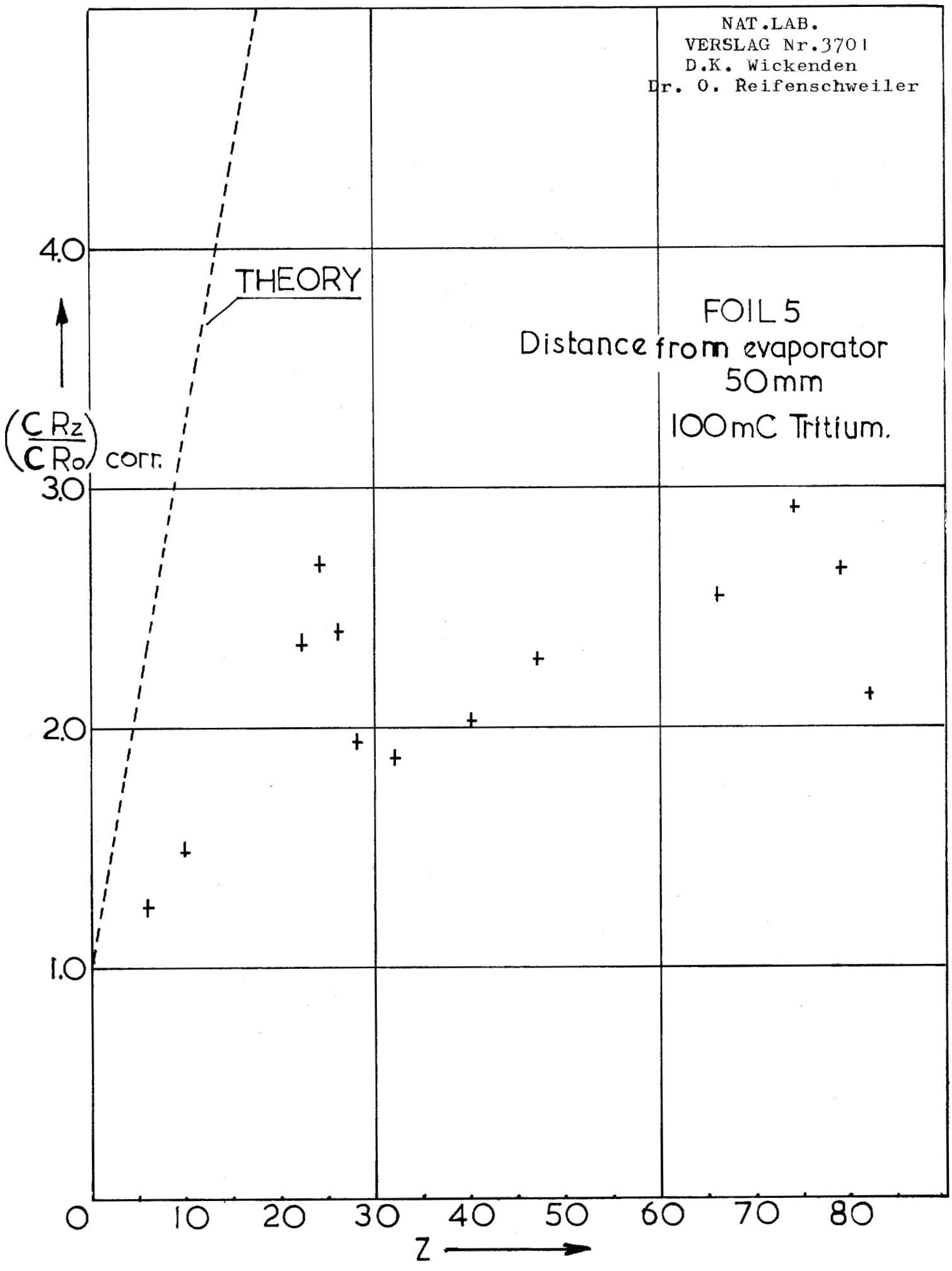
NAT.LAB.
VERSLAG Nr.3701
D.K. Wickenden
Dr. O. Reifenschweiler
THEORY
FOIL 5
Distance from evaporator
50 mm
100 mC Tritium.
(C Rz / C Ro) corr.
4.0
3.0
2.0
1.0
0
10
20
30
40
50
60
70
80
Z

Fig. 9

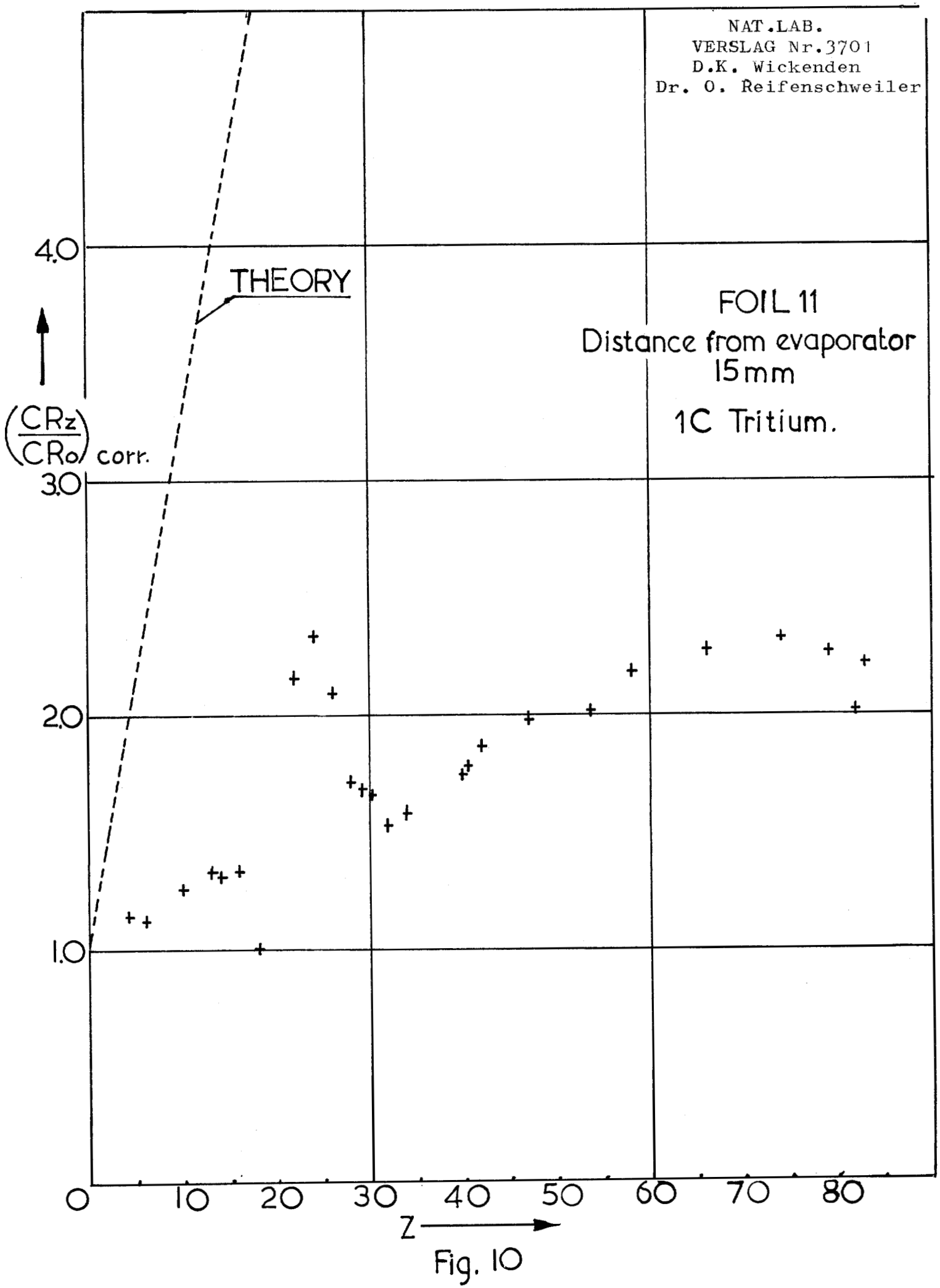
NAT.LAB.
VERSLAG Nr.3701
D.K. Wickenden
Dr. O. Reifenschweiler
THEORY
FOIL 11
Distance from evaporator
15mm
1C Tritium.
(CRz/CRo) corr.
4.0
3.0
2.0
1.0
0
10
20
30
40
50
60
70
80
Z

Fig. 10

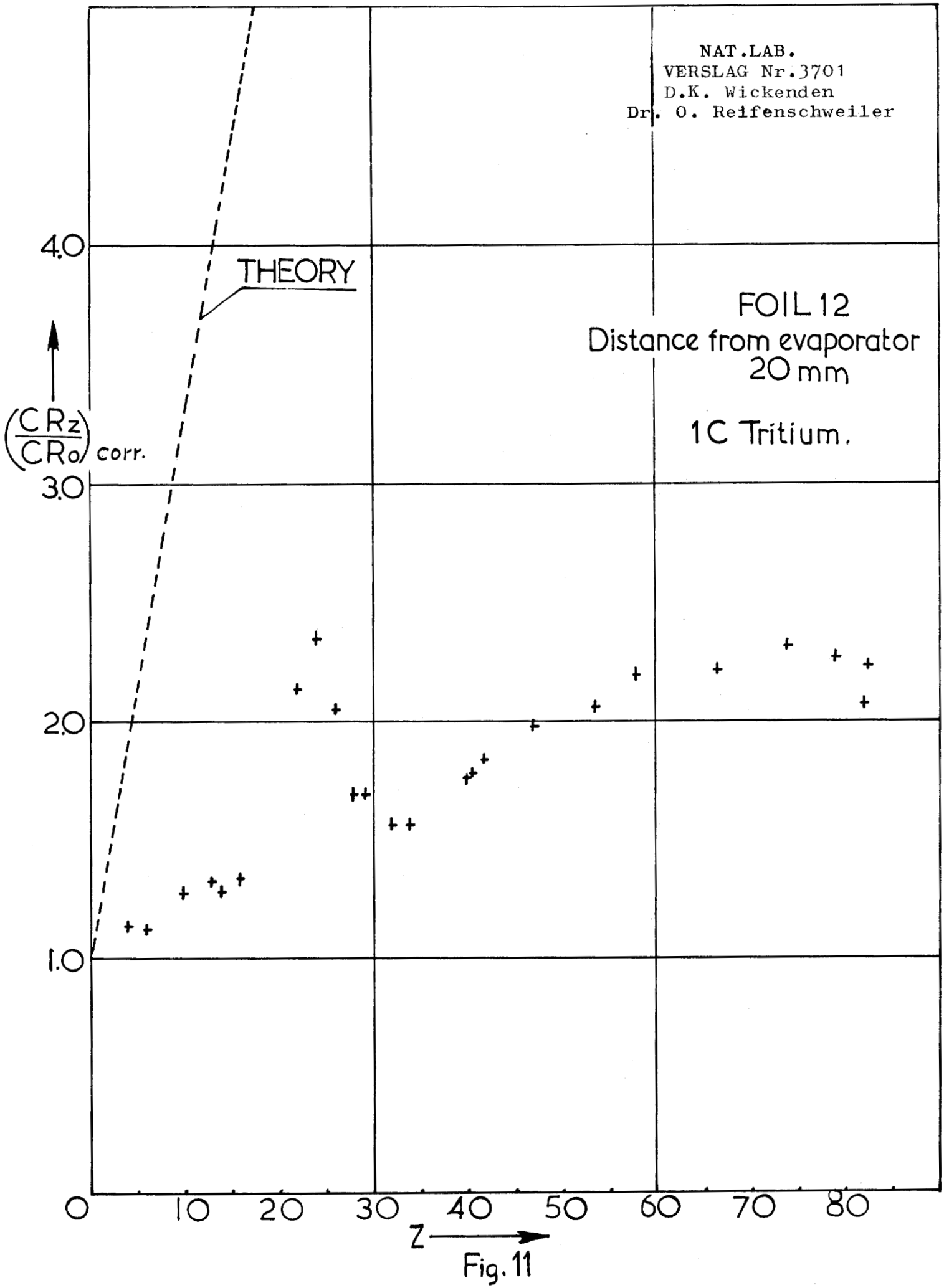
NAT.LAB.
VERSLAG Nr.3701
D.K. Wickenden
Dr. O. Reifenschweiler
THEORY
FOIL 12
Distance from evaporator
20 mm
1C Tritium.
(CRz/CRo) corr.
4.0
3.0
2.0
1.0
0
10
20
30
40
50
60
70
80
Z

Fig. 11

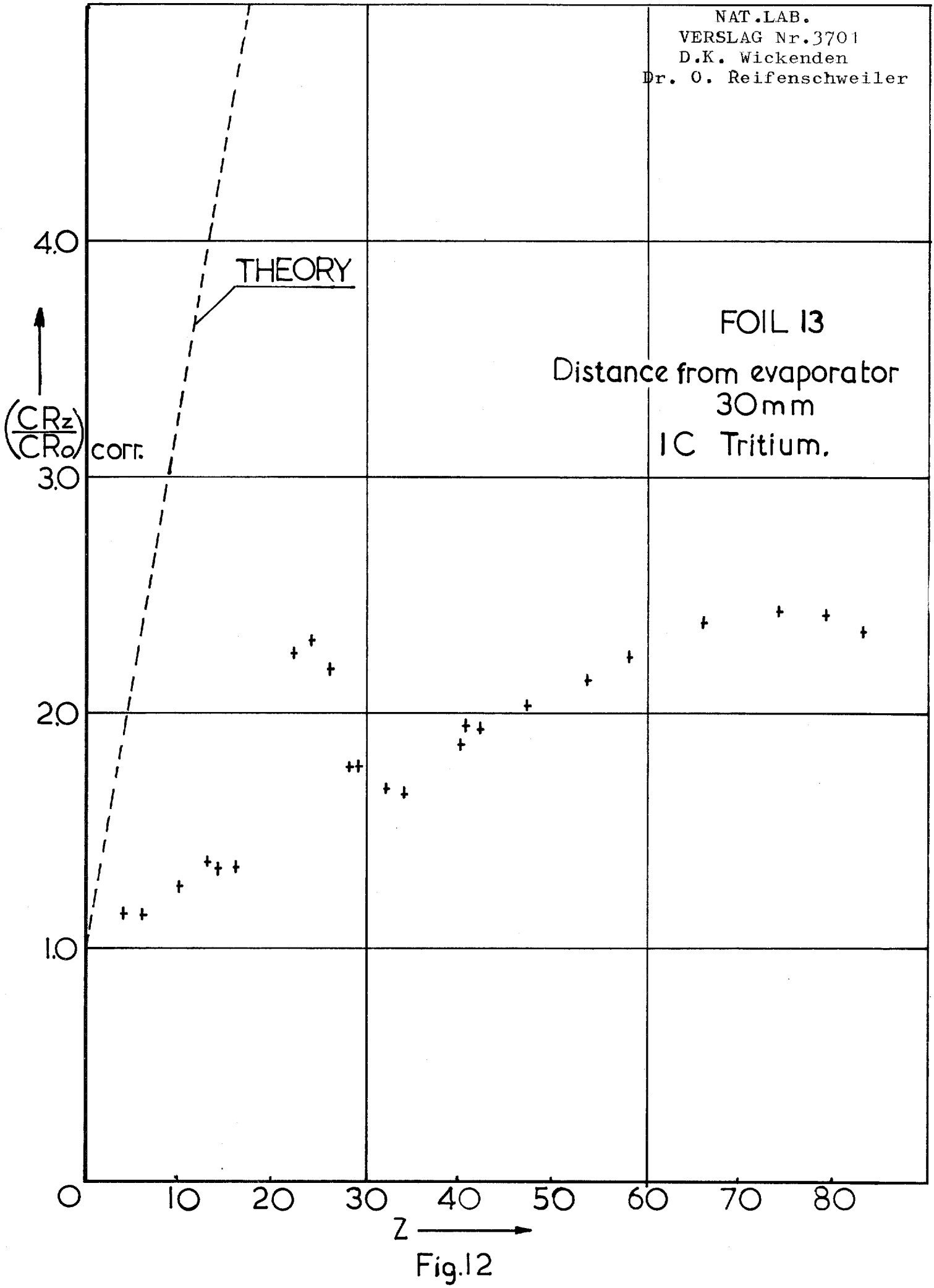
NAT.LAB.
VERSLAG Nr.3701
D.K. Wickenden
Dr. O. Reifenschweiler
THEORY
FOIL 13
Distance from evaporator
30mm
1C Tritium.
(CRz/CRo) corr.
4.0
3.0
2.0
1.0
0
10
20
30
40
50
60
70
80
Z

Fig.12

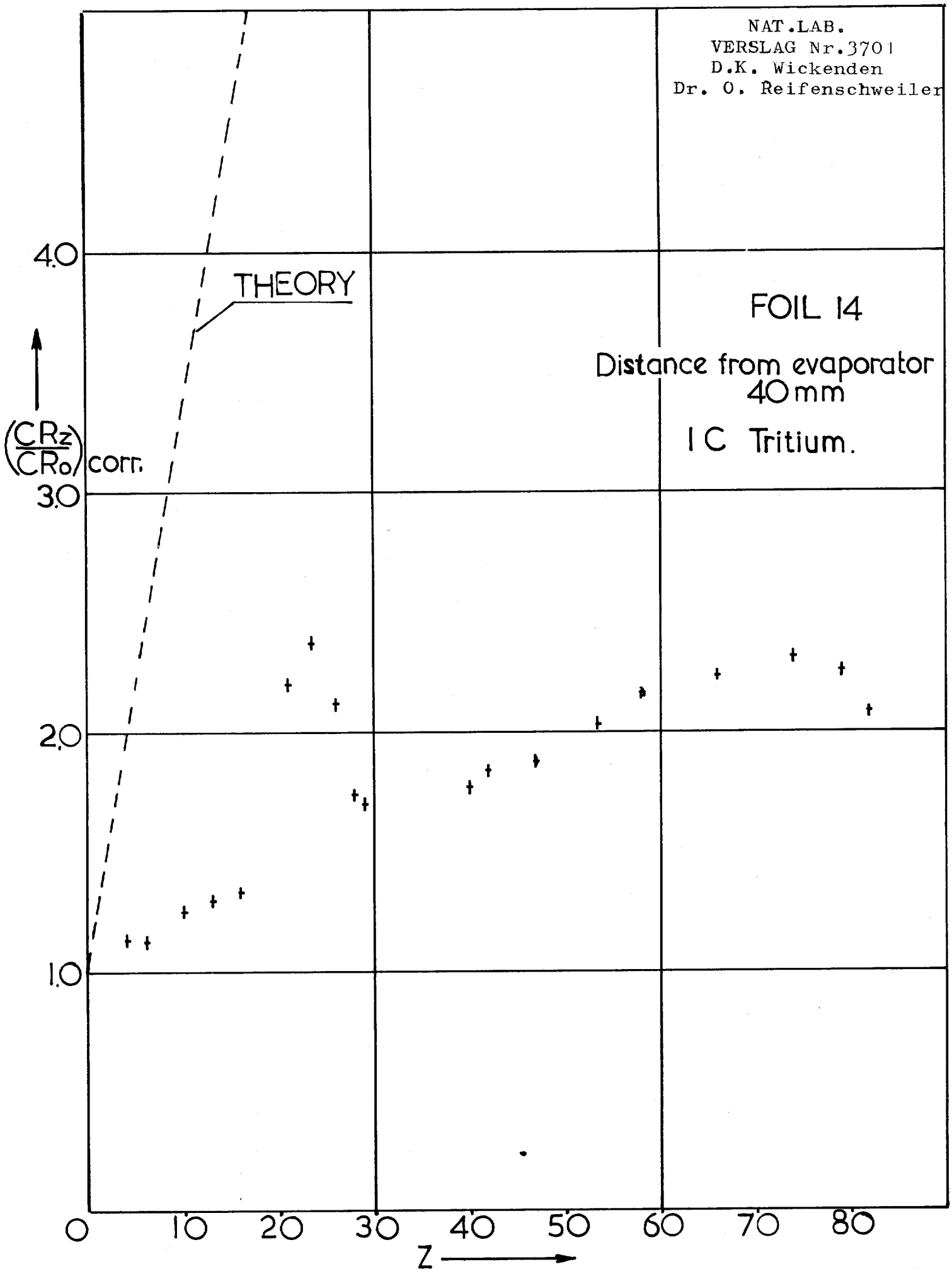
NAT.LAB.
VERSLAG Nr.3701
D.K. Wickenden
Dr. O. Reifenschweiler
THEORY
FOIL 14
Distance from evaporator
40 mm
1 C Tritium.
(CRz/CRo) corr.
4.0
3.0
2.0
1.0
0
10
20
30
40
50
60
70
80
Z

Fig. 13

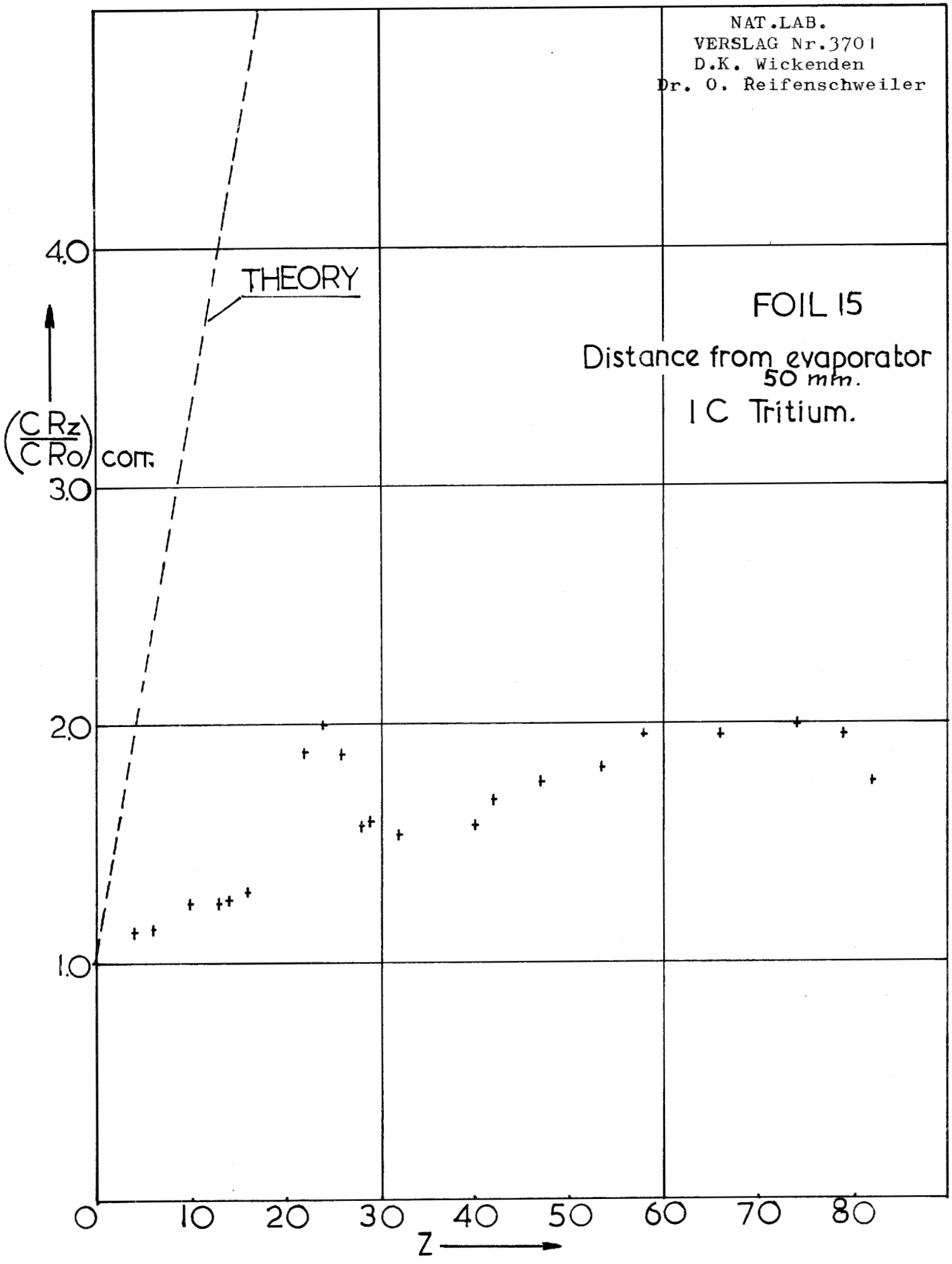
NAT.LAB.
VERSLAG Nr.3701
D.K. Wickenden
Dr. O. Reifenschweiler
THEORY
FOIL 15
Distance from evaporator
50 mm.
1 C Tritium.
(CRz/CRo) corr.
4.0
3.0
2.0
1.0
0
10
20
30
40
50
60
70
80
Z

Fig. 14

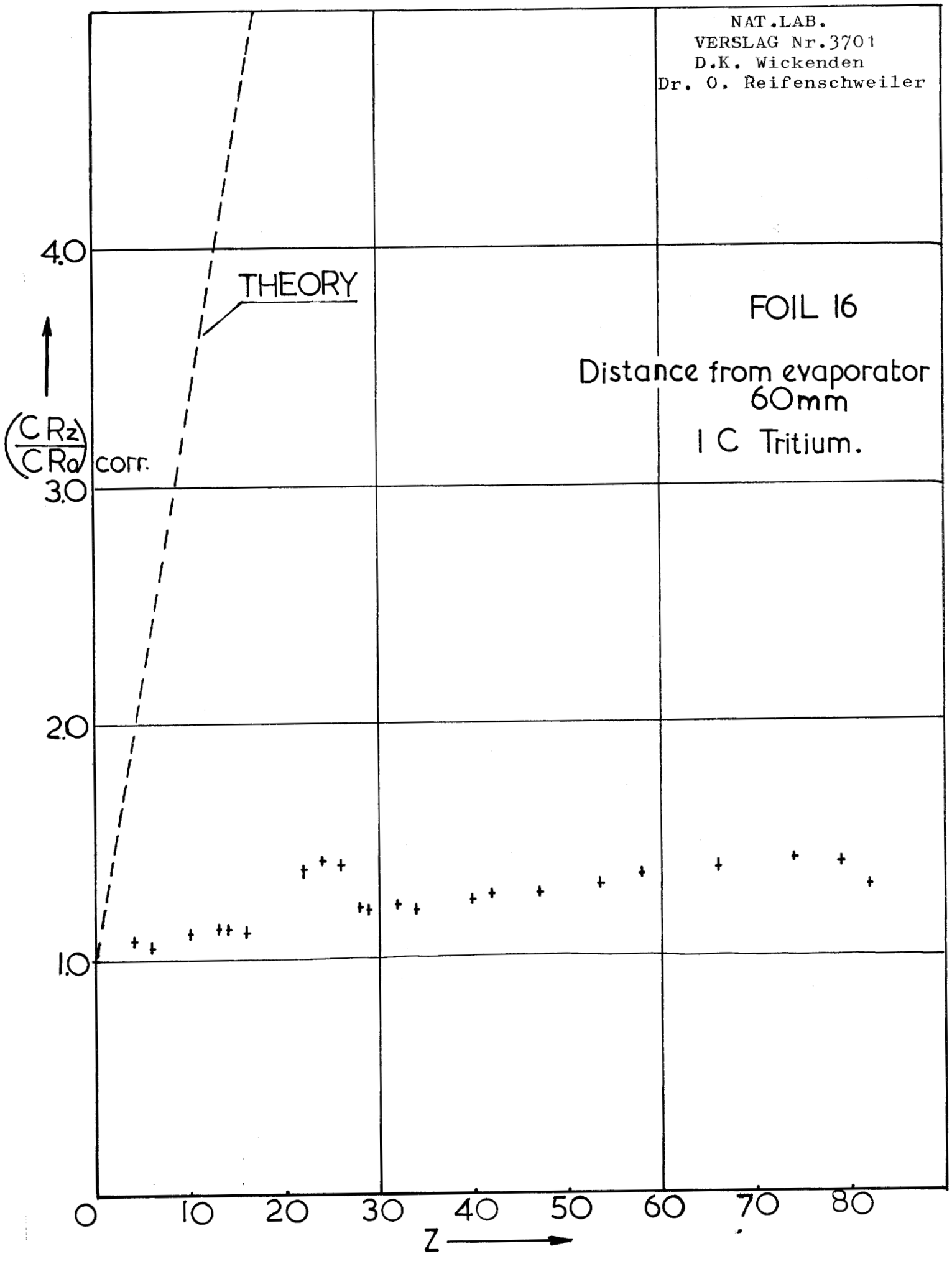
NAT.LAB.
VERSLAG Nr.3701
D.K. Wickenden
Dr. O. Reifenschweiler
THEORY
FOIL 16
Distance from evaporator
60mm
1 C Tritium.
(CRz/CRo) corr.
4.0
3.0
2.0
1.0
0
10
20
30
40
50
60
70
80
Z

Fig 15

NAT.LAB.
VERSLAG Nr.3701
D.K. Wickenden
Dr. O. Reifenschweiler

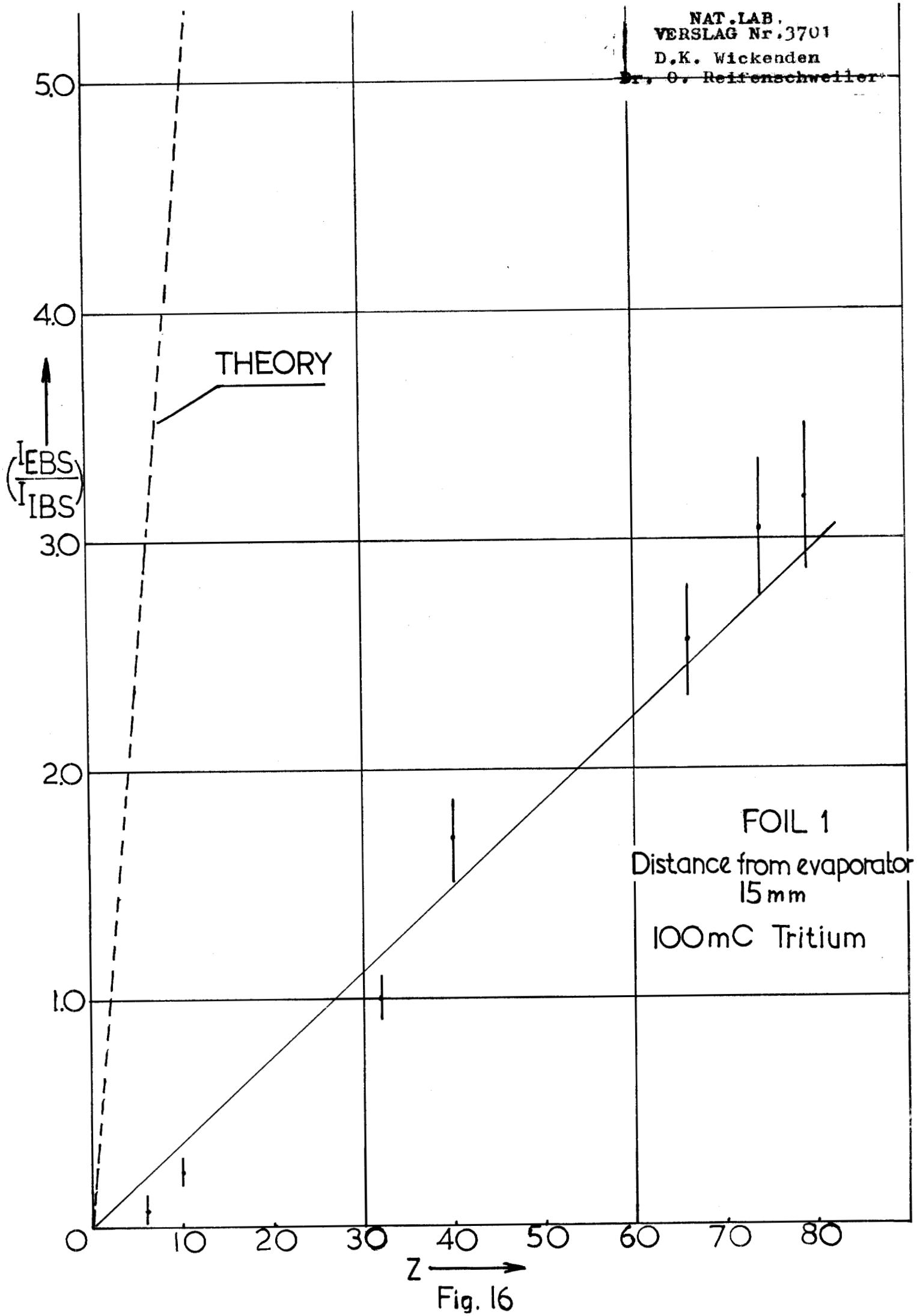

Fig. 16

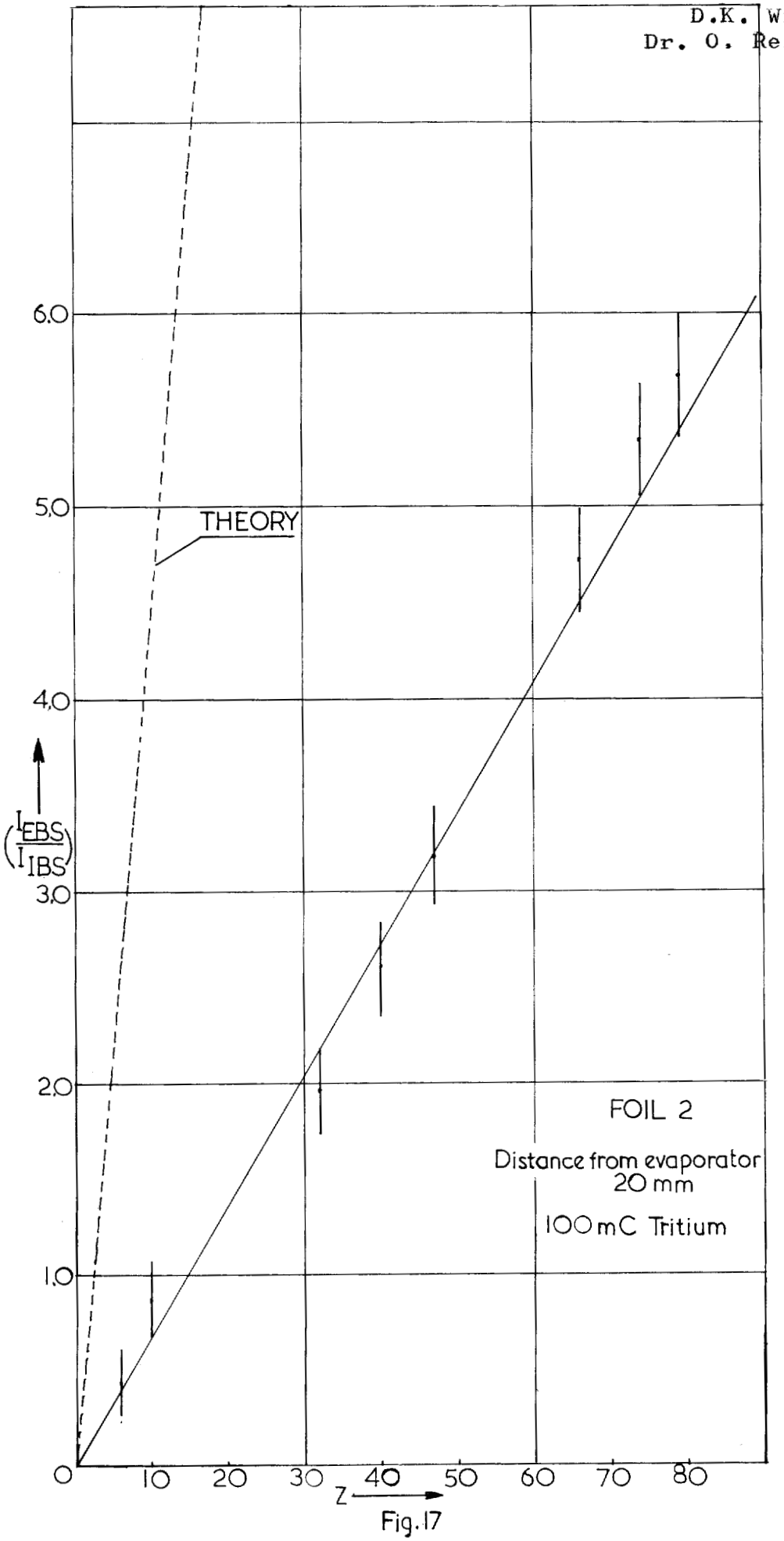
6.0
5.0
4.0
3.0
2.0
1.0
0
THEORY
$\left(\frac{I_{EBS}}{I_{IBS}}\right)$
10
20
30
40
50
60
70
80
Z
FOIL 2
Distance from evaporator
20 mm
100 mC Tritium

Fig. 17

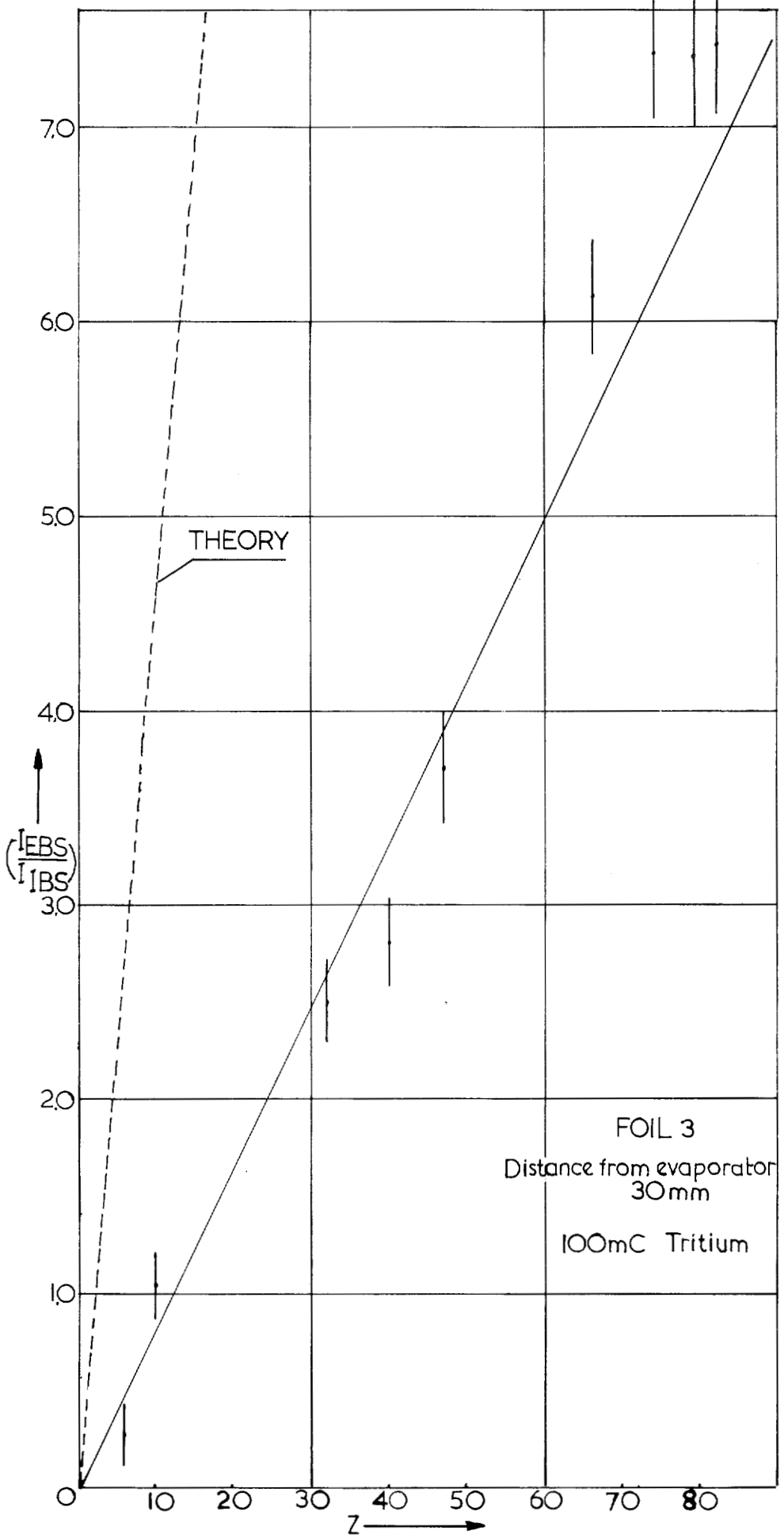
7.0
6.0
5.0
4.0
3.0
2.0
1.0
0
THEORY
$\left(\frac{I_{EBS}}{I_{IBS}}\right)$
10
20
30
40
50
60
70
80
Z
FOIL 3
Distance from evaporator
30mm
100mC Tritium

Fig. 18

NAT.LAB.
VERSLAG Nr.3701
D.K. Wickenden
Dr. O. Reifenschweiler

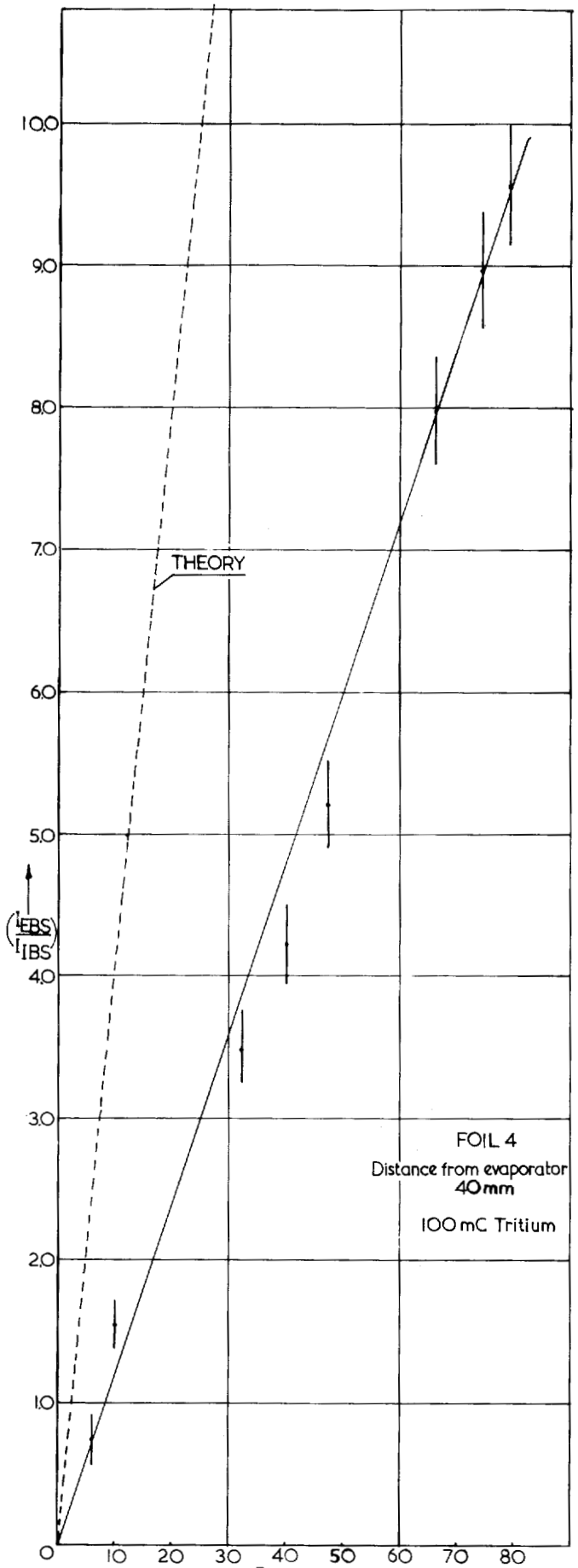

Fig. 19

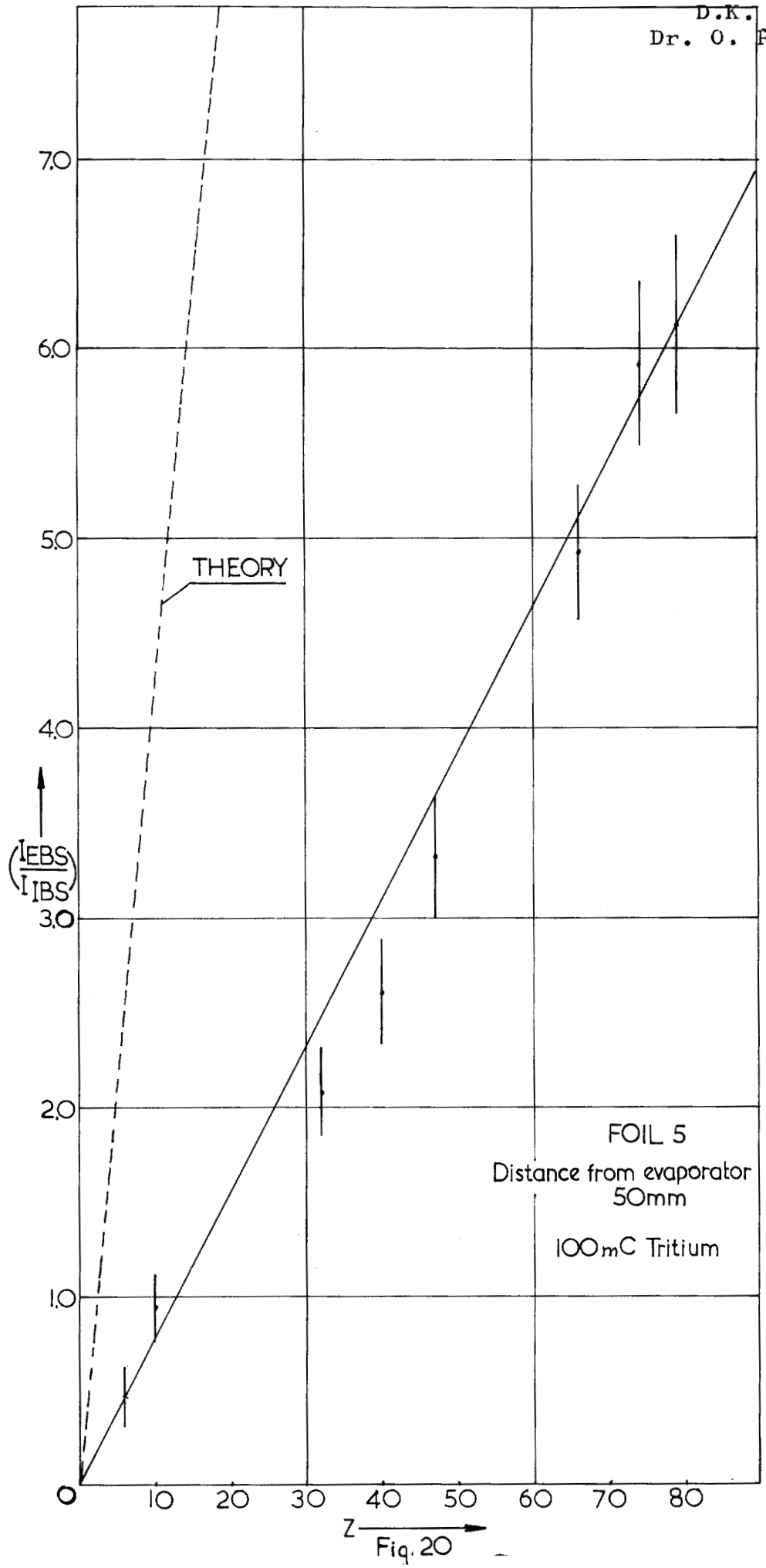
7.0
6.0
5.0
4.0
3.0
2.0
1.0
0
THEORY
$\left(\frac{I_{EBS}}{I_{IBS}}\right)$
10
20
30
40
50
60
70
80
Z
FOIL 5
Distance from evaporator
50mm
100mC Tritium

Fig. 20

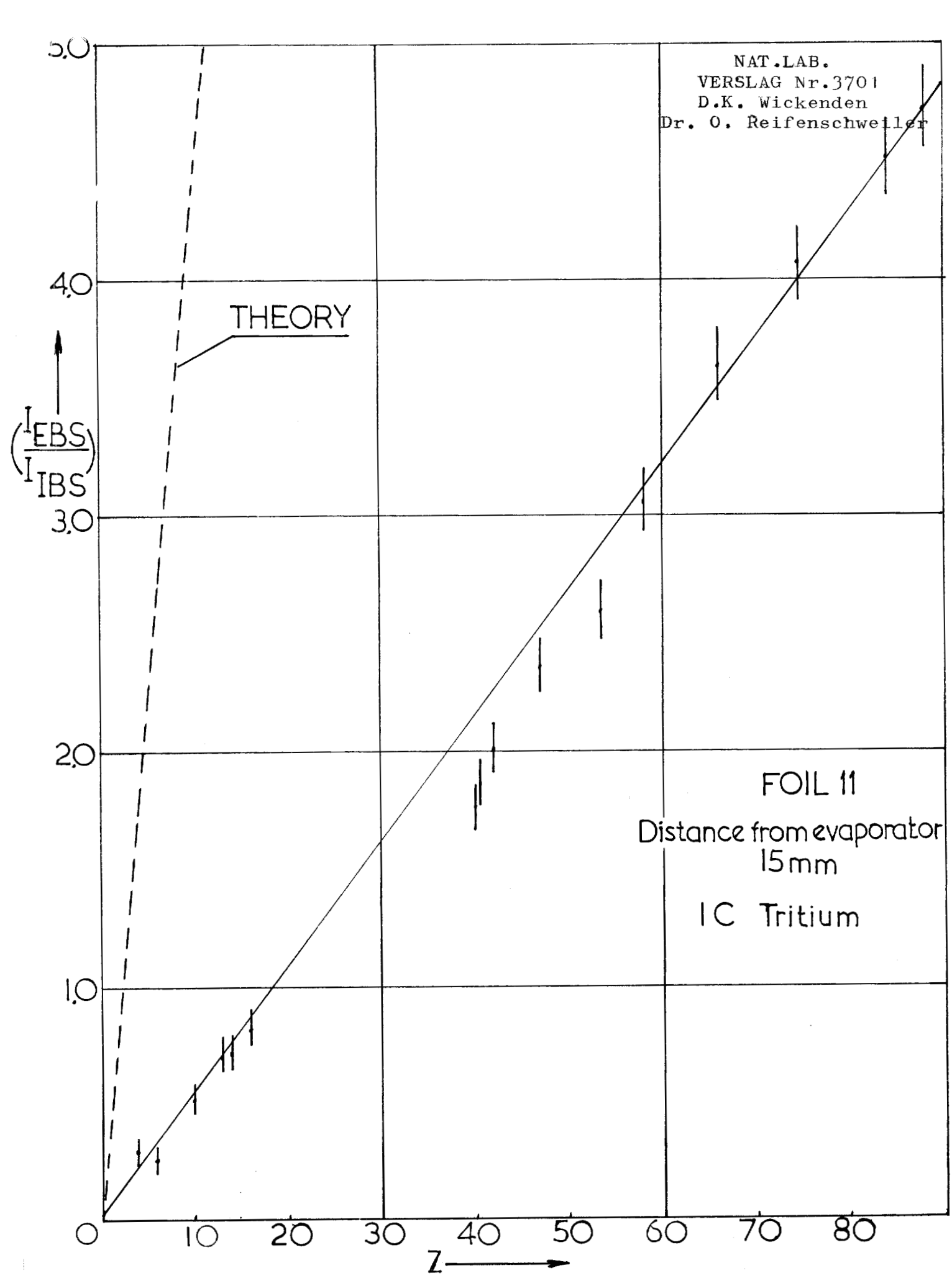
NAT.LAB.
VERSLAG Nr.3701
D.K. Wickenden
Dr. O. Reifenschweiler
5.0
4.0
3.0
2.0
1.0
0
THEORY
$\left(\frac{I_{EBS}}{I_{IBS}}\right)$
FOIL 11
Distance from evaporator
15 mm
1 C Tritium
10
20
30
40
50
60
70
80
Z

Fig. 21

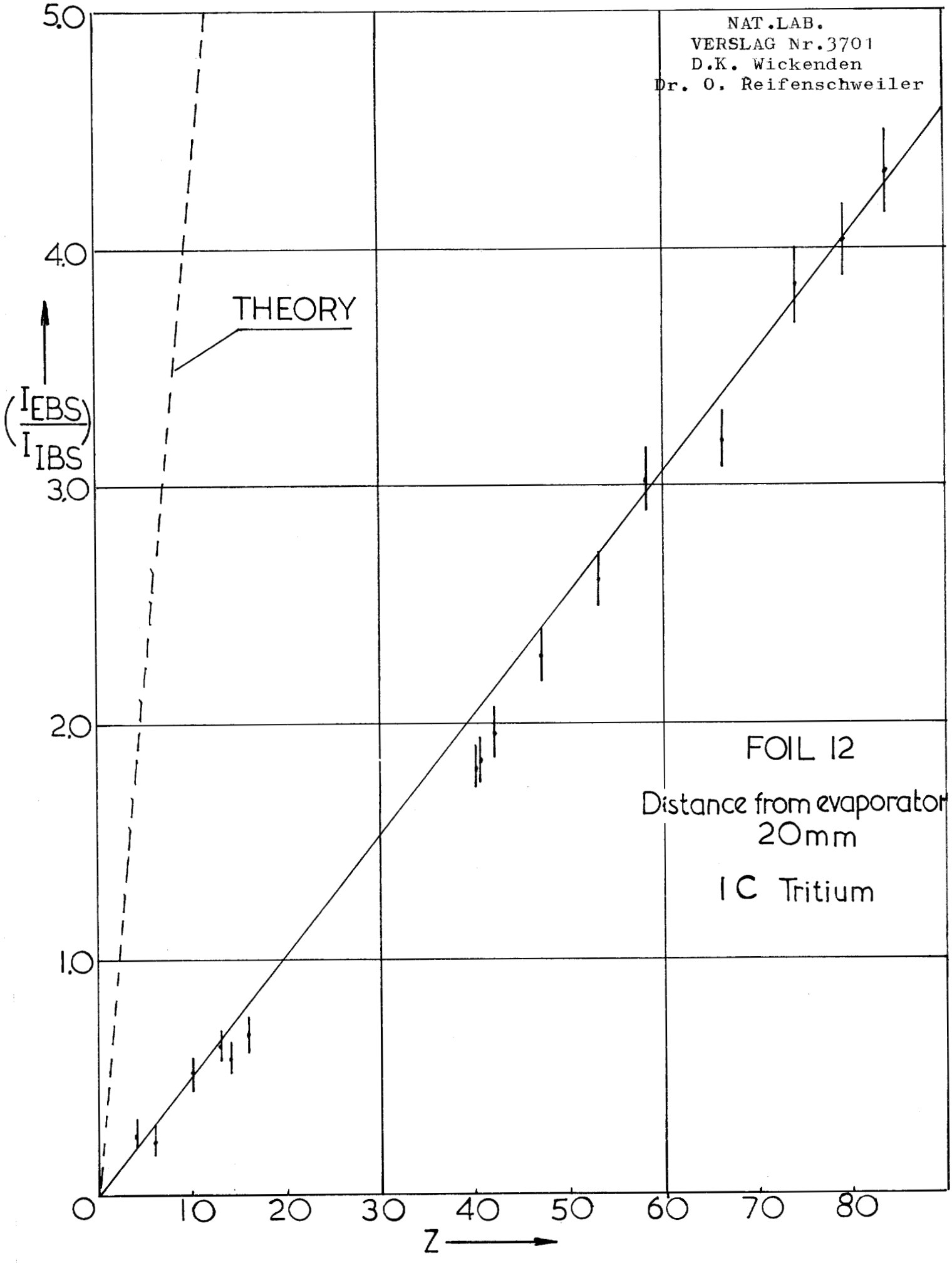
NAT.LAB.
VERSLAG Nr.3701
D.K. Wickenden
Dr. O. Reifenschweiler
THEORY
$\left(\frac{I_{EBS}}{I_{IBS}}\right)$
FOIL 12
Distance from evaporator
20mm
1C Tritium
Z
0
10
20
30
40
50
60
70
80
1.0
2.0
3.0
4.0
5.0

Fig. 22

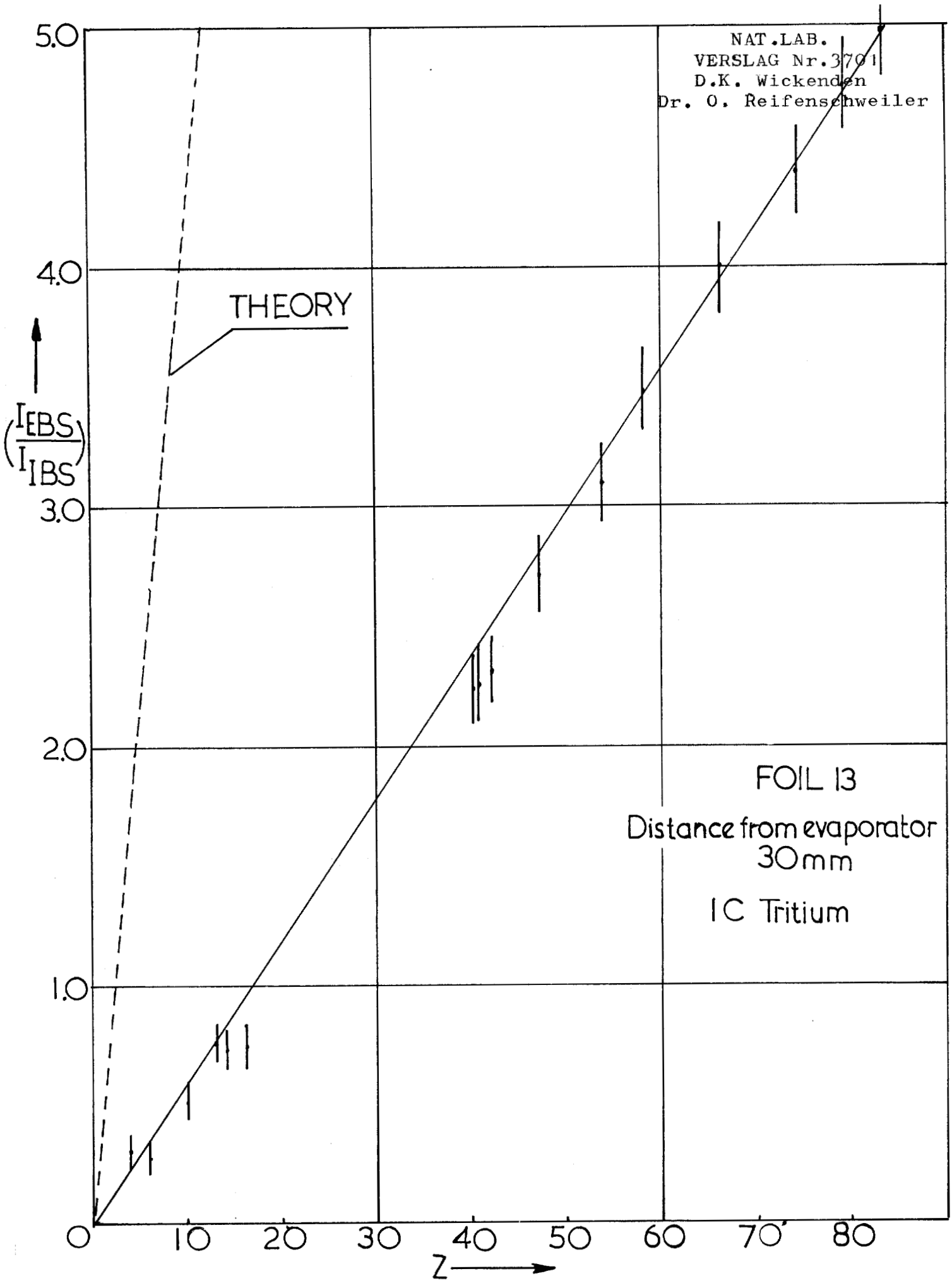
NAT.LAB.
VERSLAG Nr.3701
D.K. Wickenden
Dr. O. Reifenschweiler
THEORY
$\left(\frac{I_{EBS}}{I_{IBS}}\right)$
5.0
4.0
3.0
2.0
1.0
0
10
20
30
40
50
60
70
80
Z
FOIL 13
Distance from evaporator
30mm
1C Tritium

Fig. 23

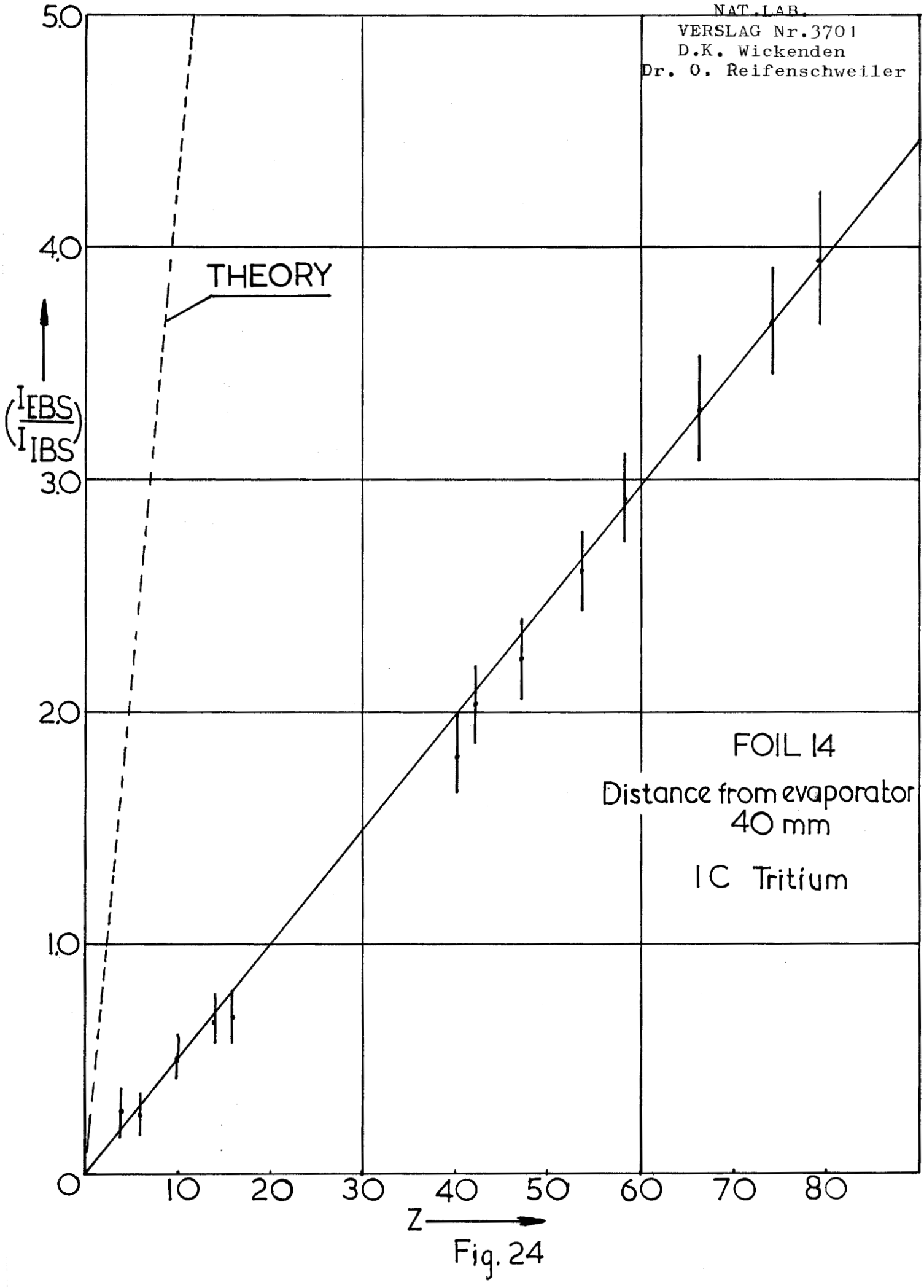
NAT.LAB.
VERSLAG Nr.3701
D.K. Wickenden
Dr. O. Reifenschweiler
5.0
4.0
3.0
2.0
1.0
0
THEORY
$\left(\frac{I_{EBS}}{I_{IBS}}\right)$
FOIL 14
Distance from evaporator
40 mm
1 C Tritium
10
20
30
40
50
60
70
80
Z

Fig. 24

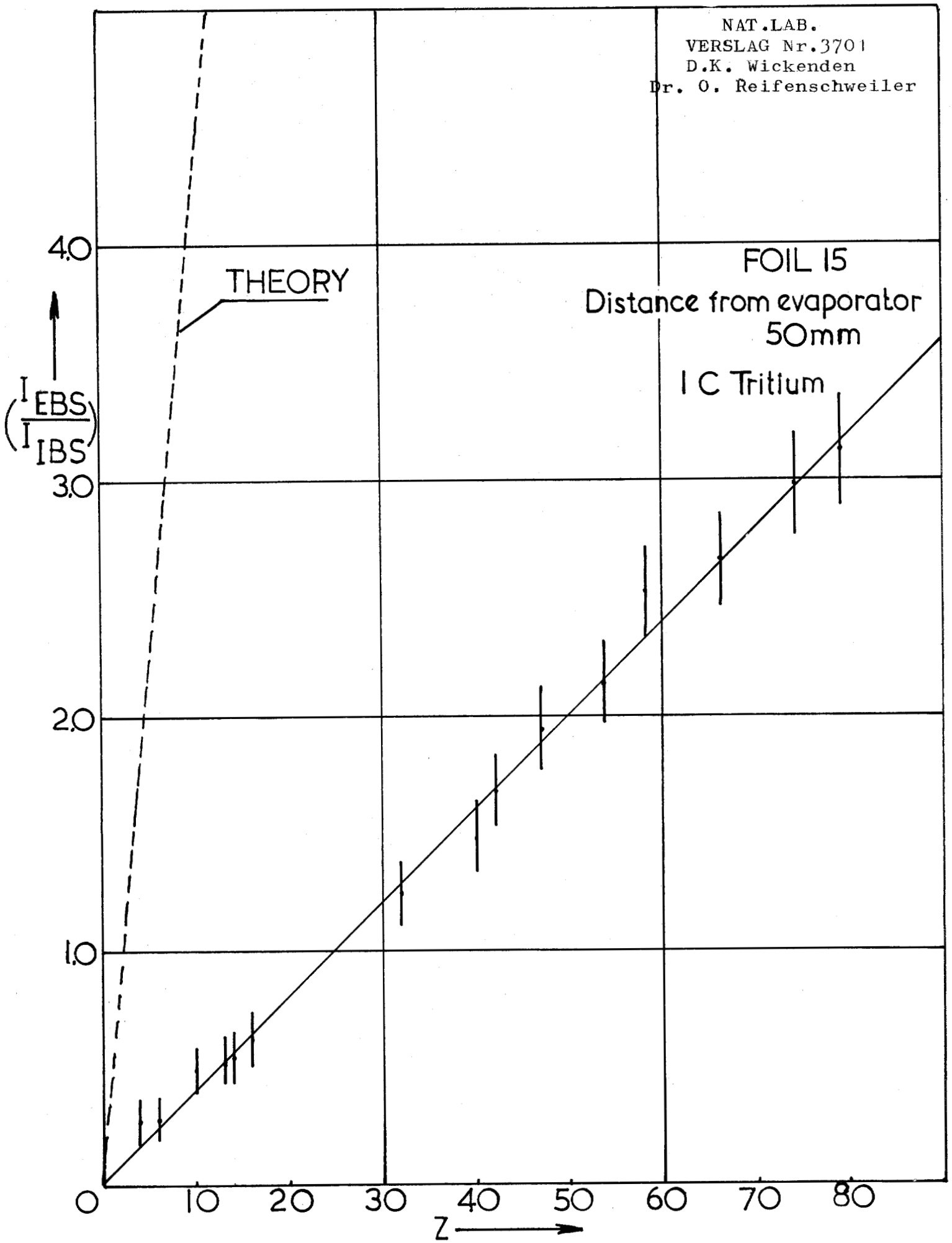
NAT.LAB.
VERSLAG Nr.3701
D.K. Wickenden
Dr. O. Reifenschweiler
THEORY
FOIL 15
Distance from evaporator
50mm
1 C Tritium
$\left(\frac{I_{EBS}}{I_{IBS}}\right)$
4.0
3.0
2.0
1.0
0
10
20
30
40
50
60
70
80
Z

Fig. 25

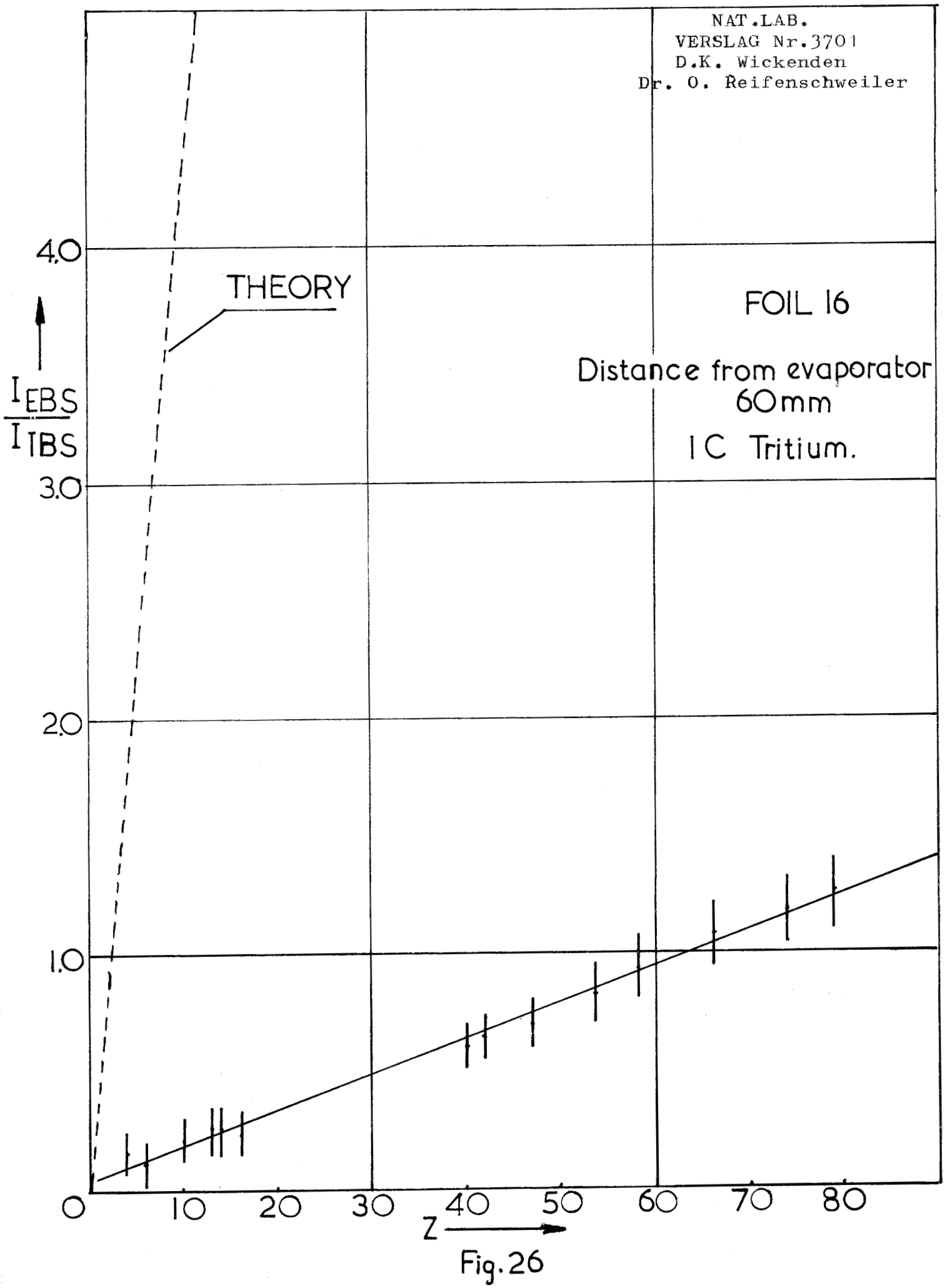
NAT.LAB.
VERSLAG Nr.3701
D.K. Wickenden
Dr. O. Reifenschweiler
THEORY
FOIL 16
Distance from evaporator
60mm
1 C Tritium.
$\frac{I_{EBS}}{I_{IBS}}$
4.0
3.0
2.0
1.0
0
10
20
30
40
50
60
70
80
Z

Fig. 26

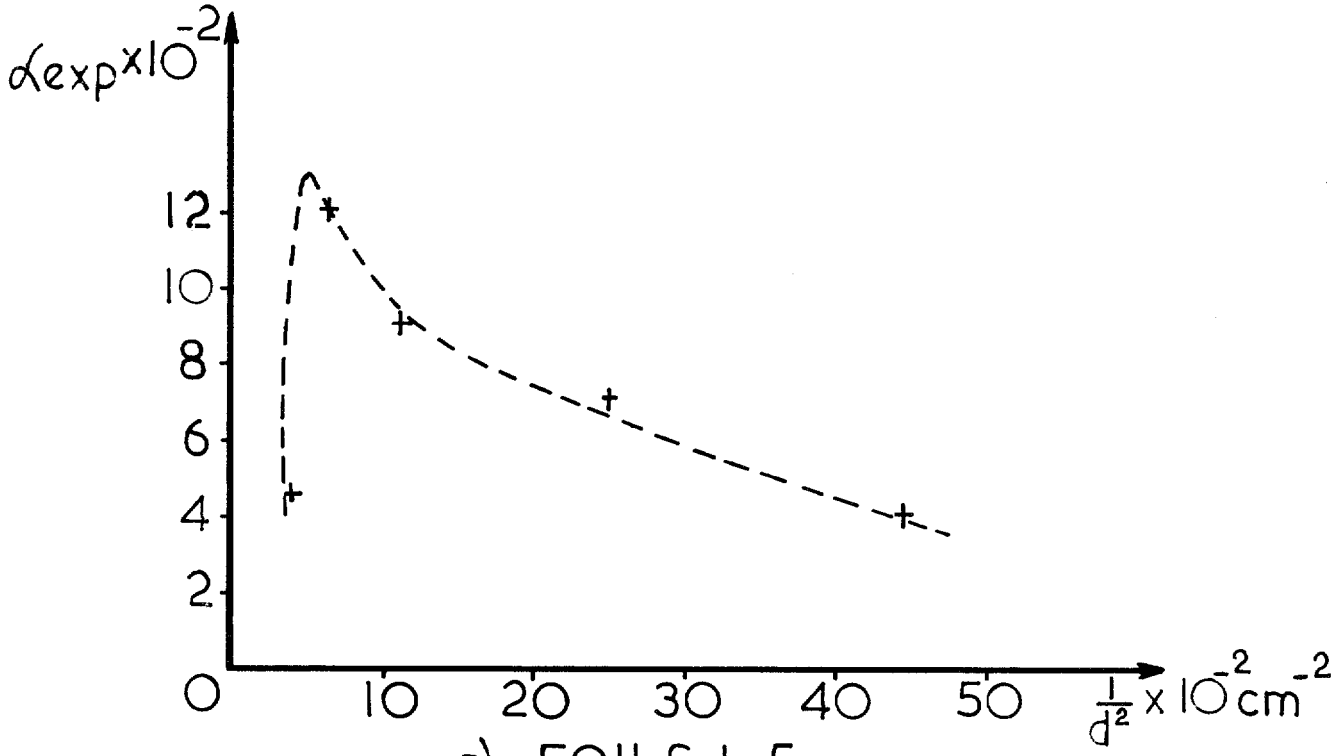

a) FOILS 1-5

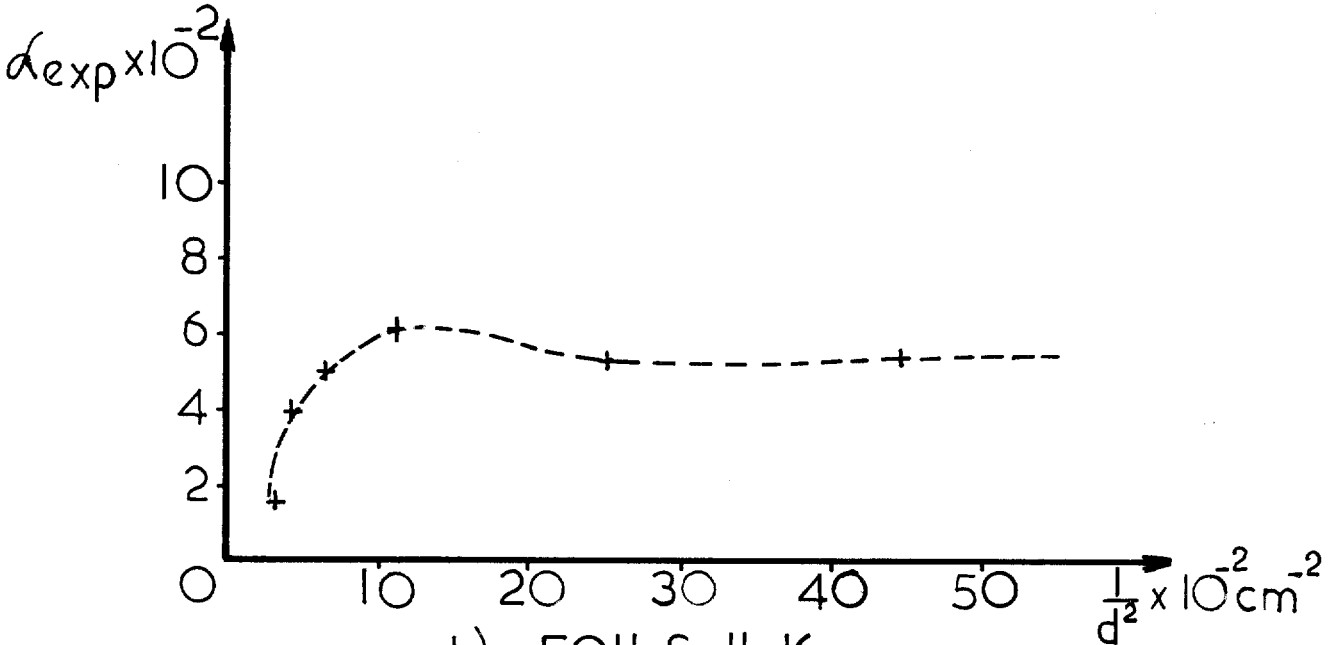

b) FOILS 11-16

Fig. 27 a) and b)

α_{exp} As a Function of $\frac{1}{d^2}$

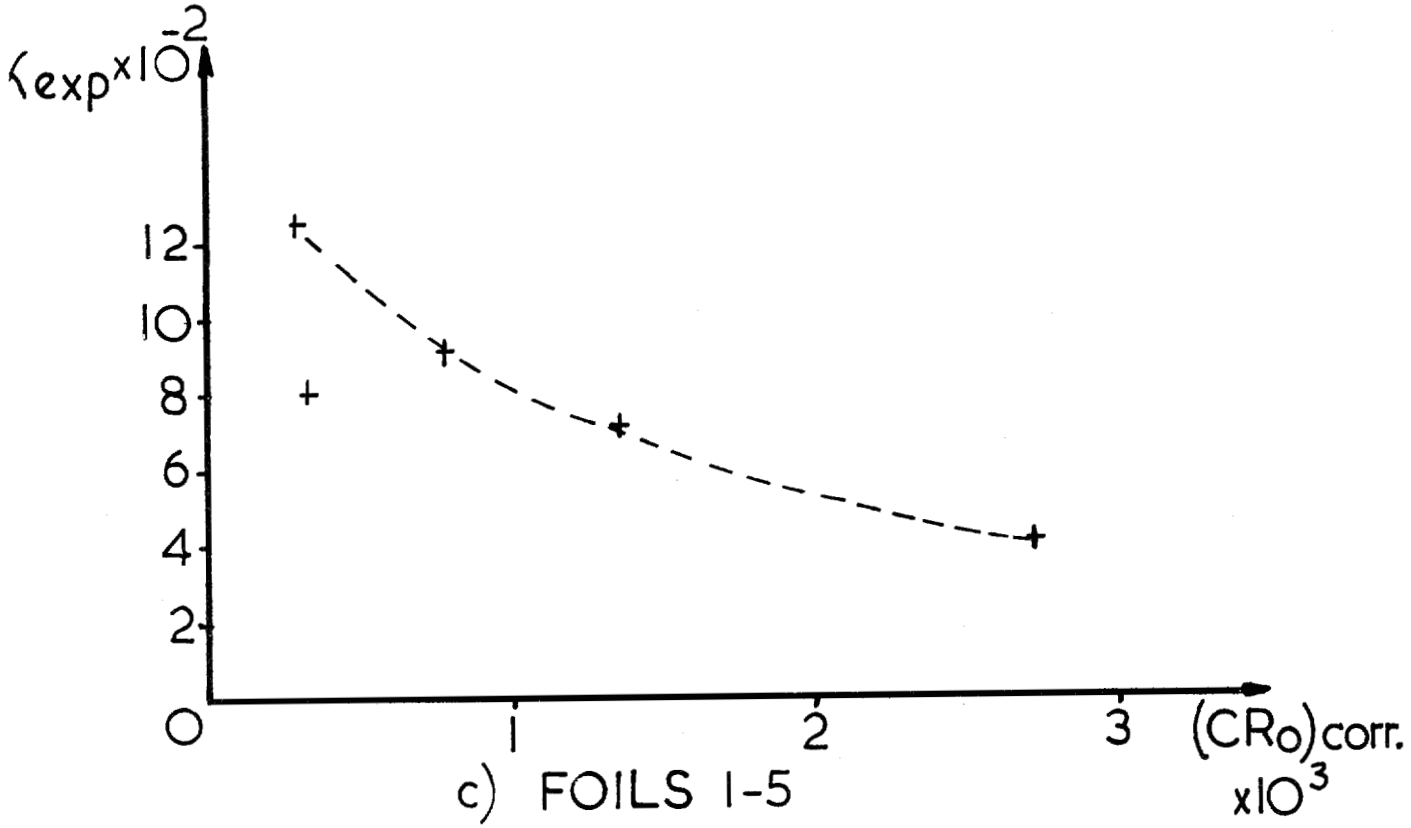

c) FOILS 1-5

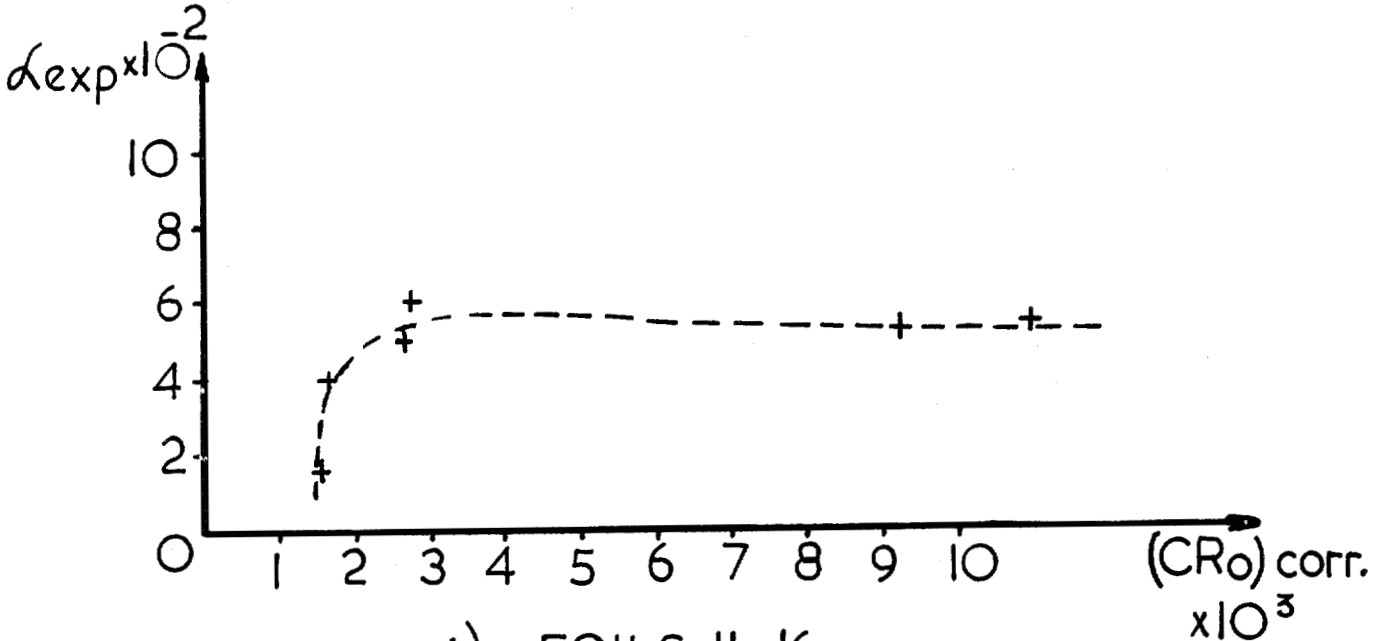

d) FOILS 11-16

Fig. 27 c) and d)

α_{exp} As a Function of $(CR_o)_{corr.}$

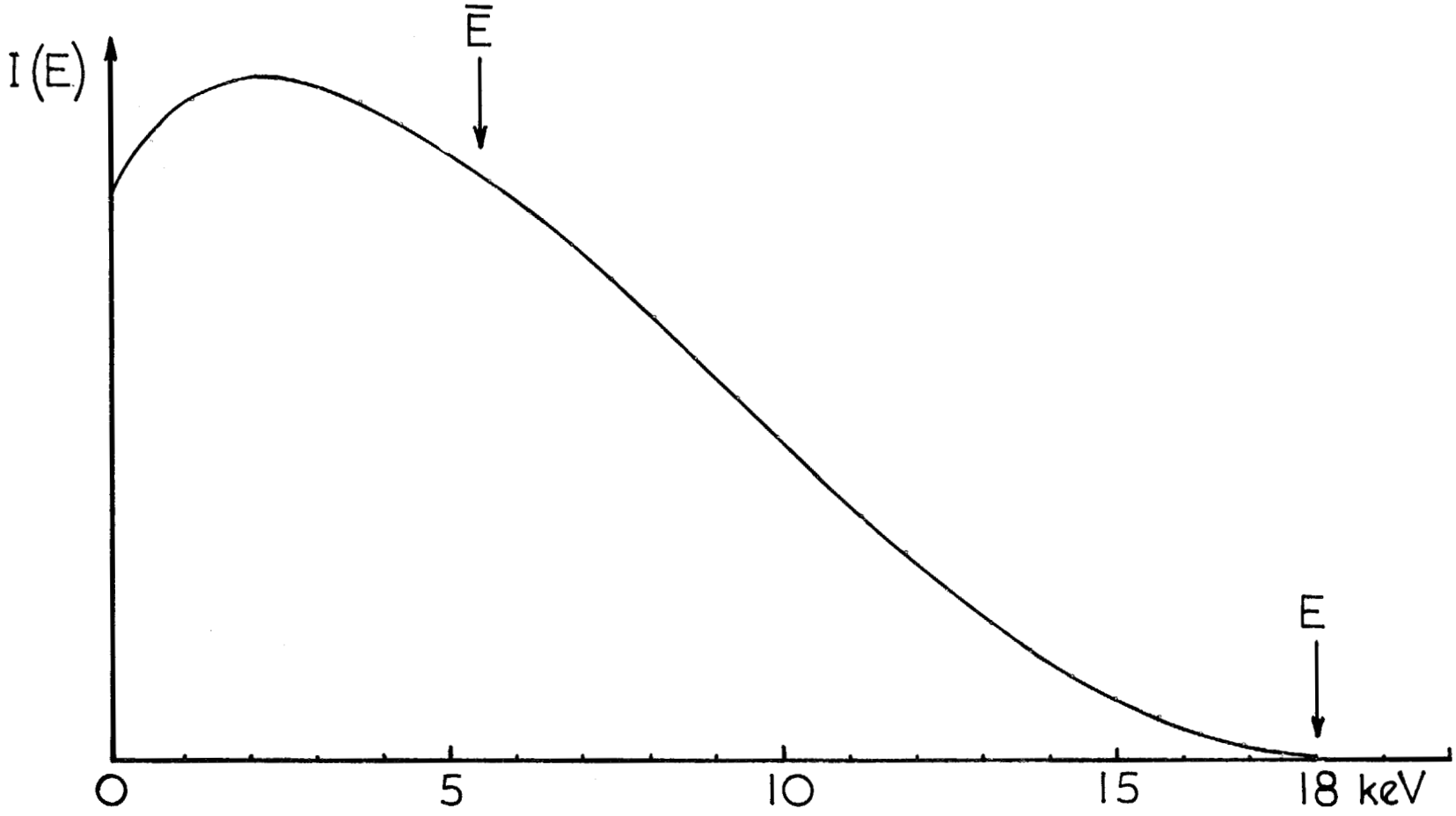

Fig. 28

Energy spectum of tritium.

NAT.LAB.
VERSLAG Nr.3701
D.K. Wickenden
Dr. O. Reifenschweiler

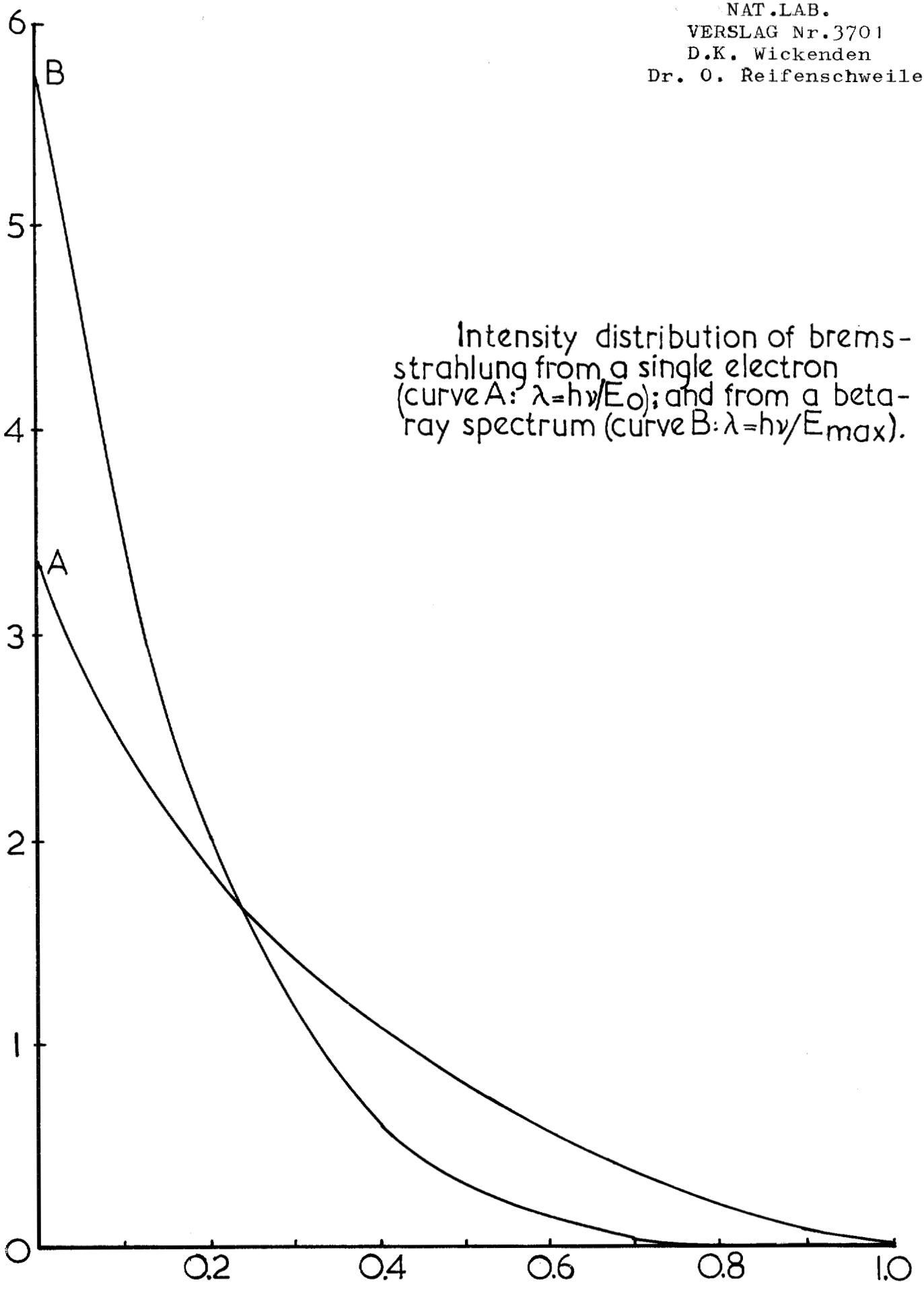

Intensity distribution of bremsstrahlung from a single electron (curve A: $\lambda = h\nu/E_0$); and from a beta-ray spectrum (curve B: $\lambda = h\nu/E_{max}$).

Fig. 29

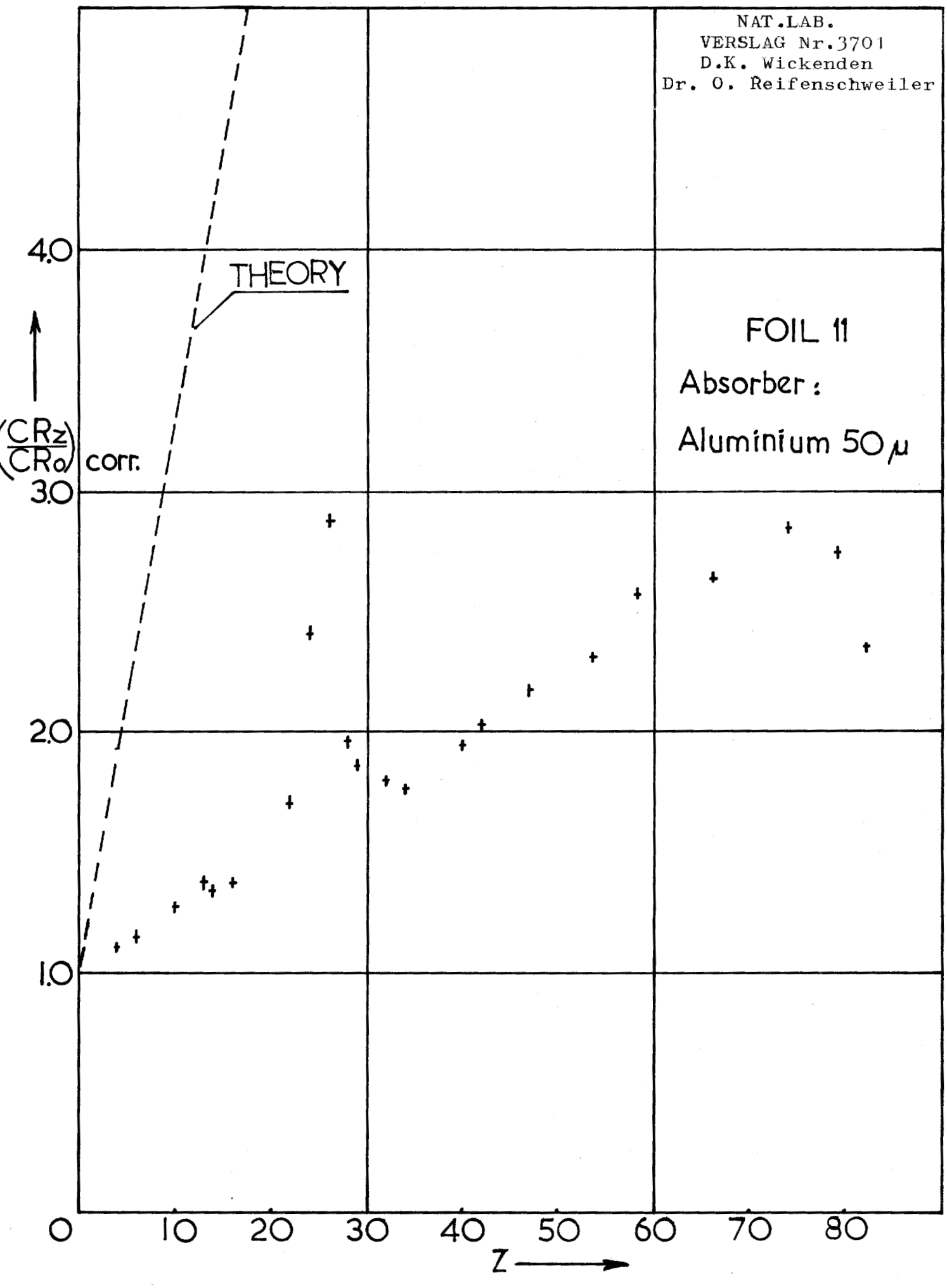
NAT.LAB.
VERSLAG Nr.3701
D.K. Wickenden
Dr. O. Reifenschweiler
THEORY
FOIL 11
Absorber :
Aluminium 50 μ
(CRz/CRo) corr.
4.0
3.0
2.0
1.0
0
10
20
30
40
50
60
70
80
Z

Fig. 30

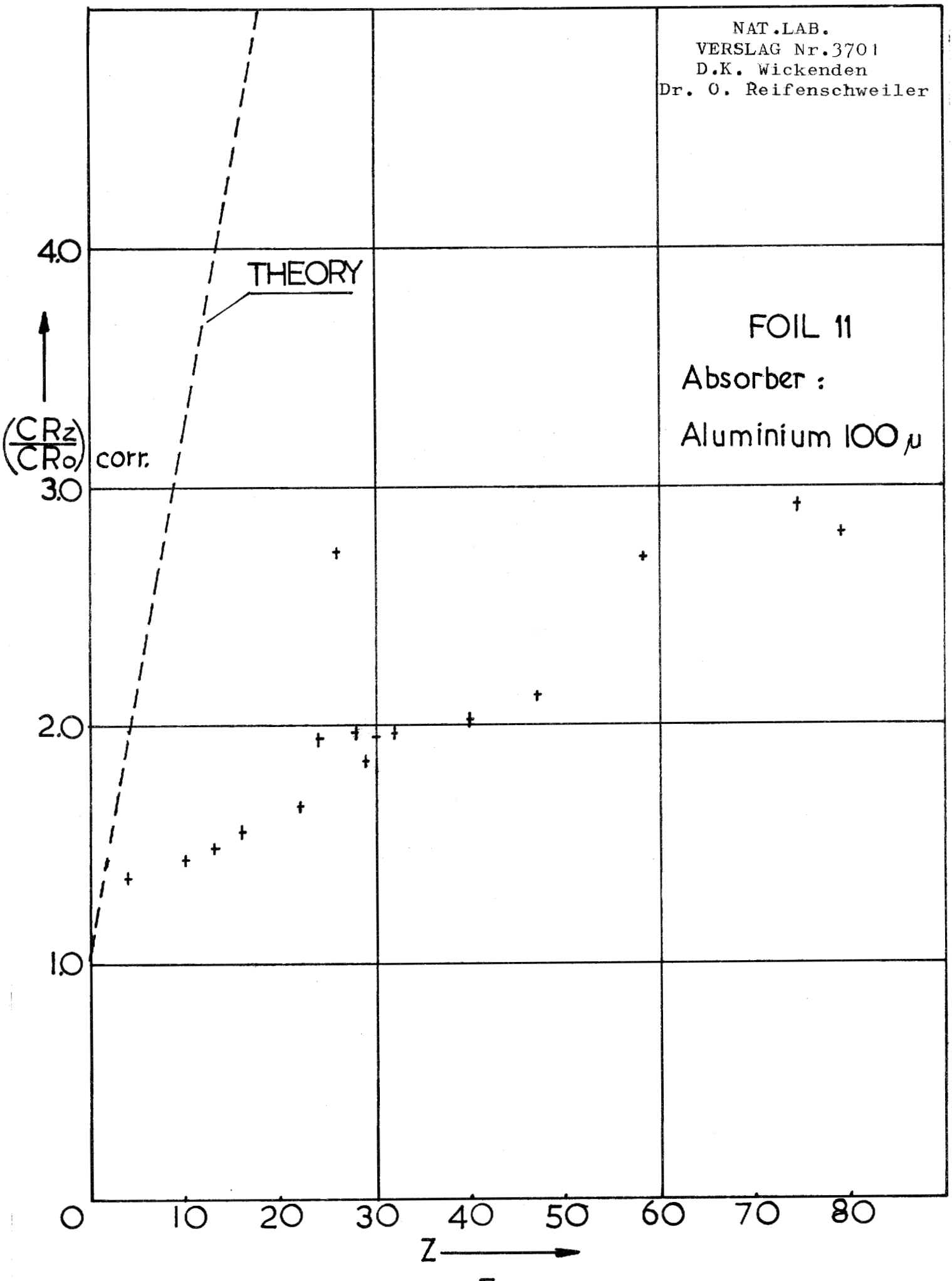
NAT.LAB.
VERSLAG Nr.3701
D.K. Wickenden
Dr. O. Reifenschweiler
THEORY
FOIL 11
Absorber :
Aluminium 100 μ
(CRz/CRo) corr.
4.0
3.0
2.0
1.0
0
10
20
30
40
50
60
70
80
Z

Fig. 31

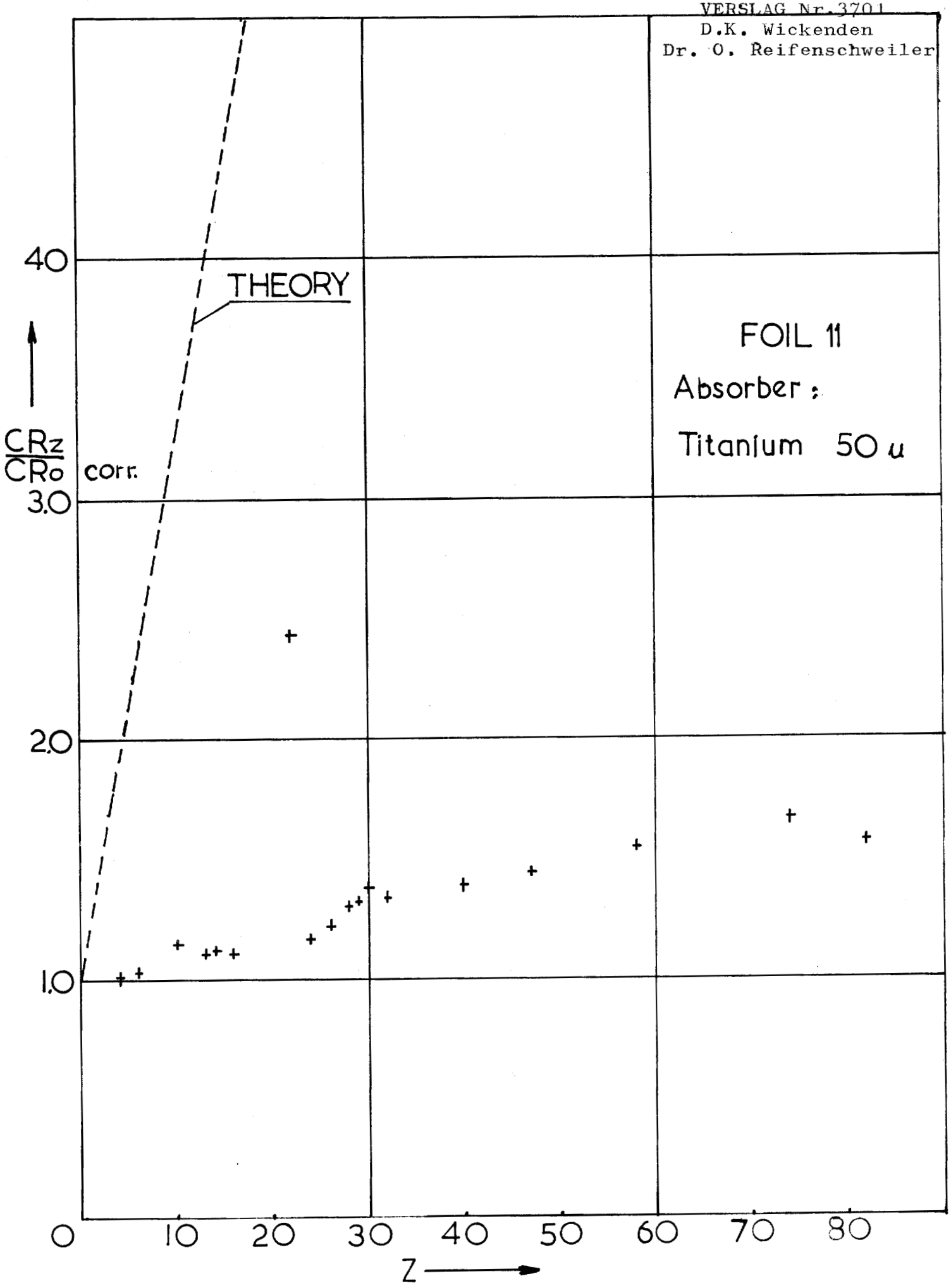
THEORY
FOIL 11
Absorber :
Titanium 50 u
CRz/CRo corr.
40
3.0
2.0
1.0
0
10
20
30
40
50
60
70
80
Z

Fig. 32

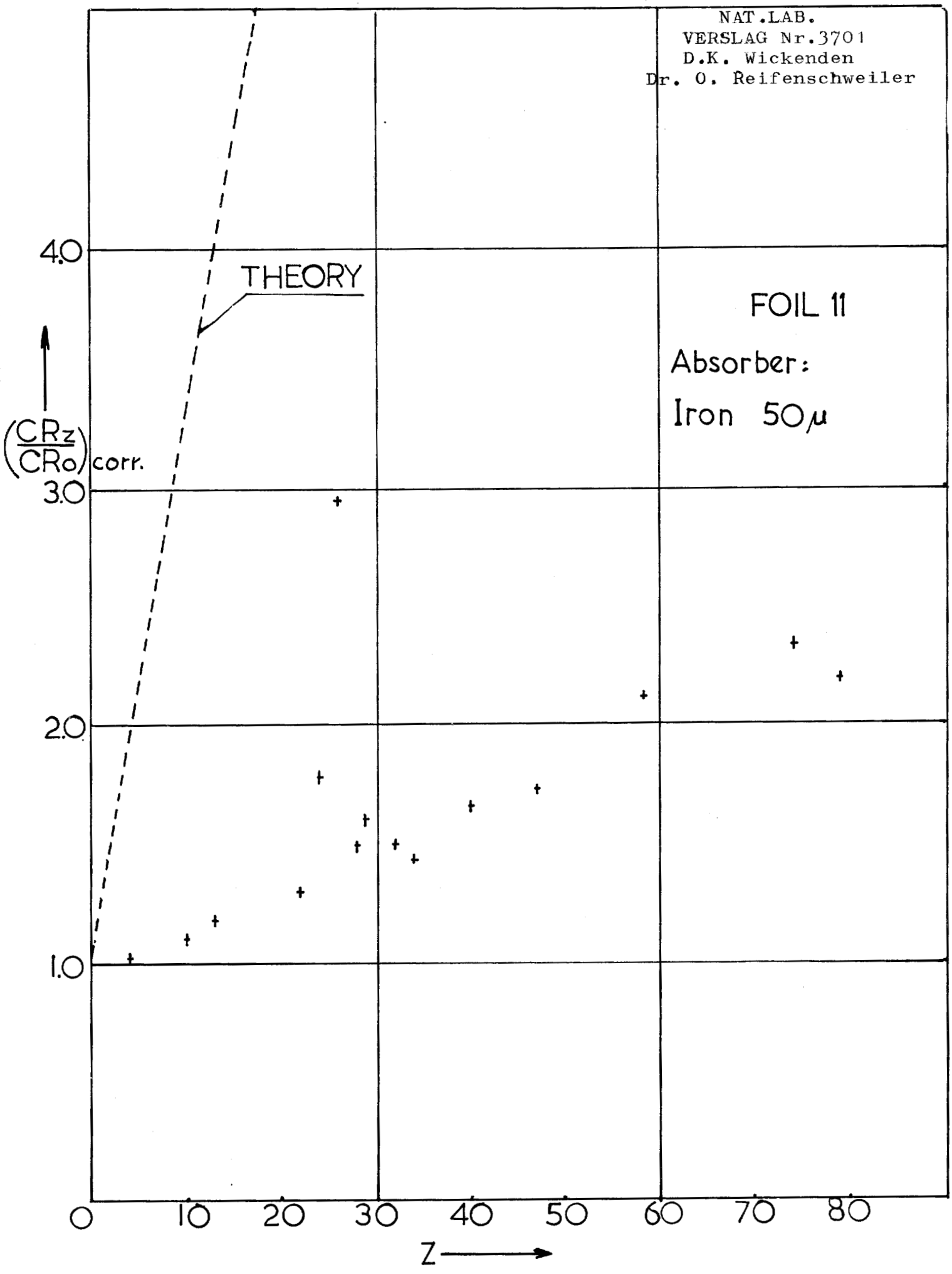
NAT.LAB.
VERSLAG Nr.3701
D.K. Wickenden
Dr. O. Reifenschweiler
THEORY
FOIL 11
Absorber:
Iron 50μ
(CRz/CRo) corr.
4.0
3.0
2.0
1.0
0
10
20
30
40
50
60
70
80
Z

Fig.33

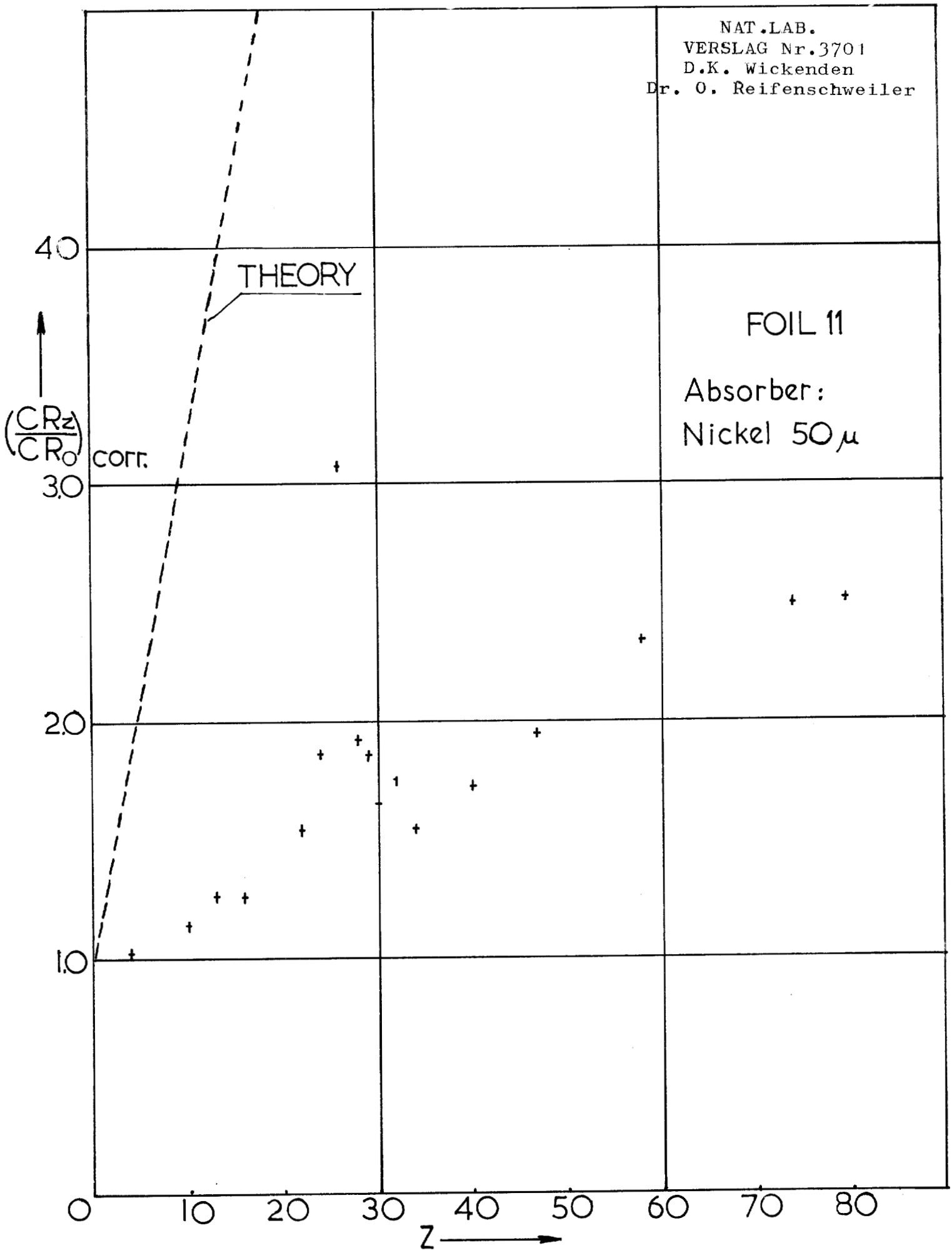
NAT.LAB.
VERSLAG Nr.3701
D.K. Wickenden
Dr. O. Reifenschweiler
THEORY
FOIL 11
Absorber:
Nickel 50 μ
(CRz/CRo) corr.
4.0
3.0
2.0
1.0
0
10
20
30
40
50
60
70
80
Z

Fig. 34

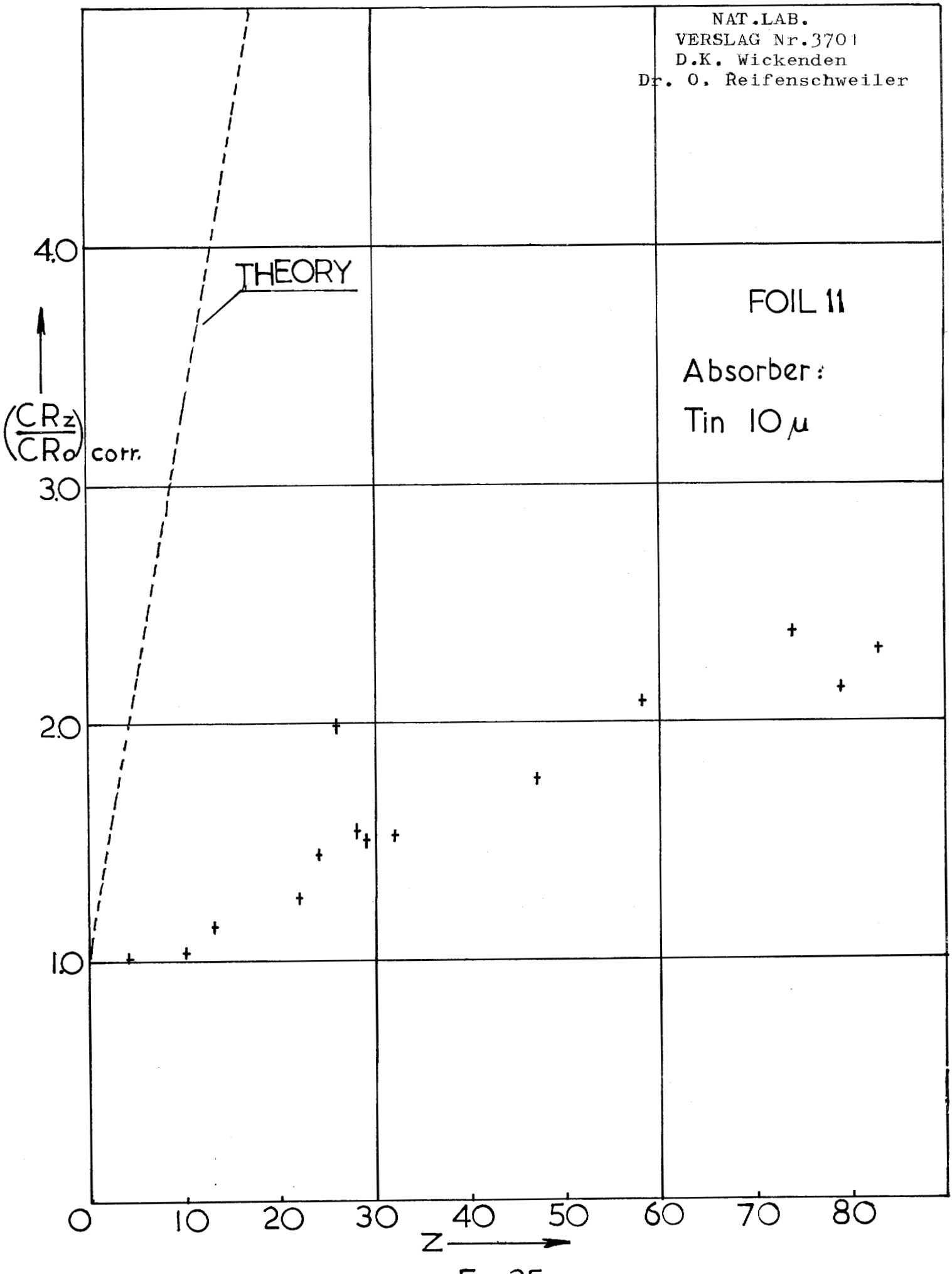
NAT.LAB.
VERSLAG Nr.3701
D.K. Wickenden
Dr. O. Reifenschweiler
THEORY
FOIL 11
Absorber:
Tin 10 μ
(CRz/CRo) corr.
4.0
3.0
2.0
1.0
0
10
20
30
40
50
60
70
80
Z

Fig. 35

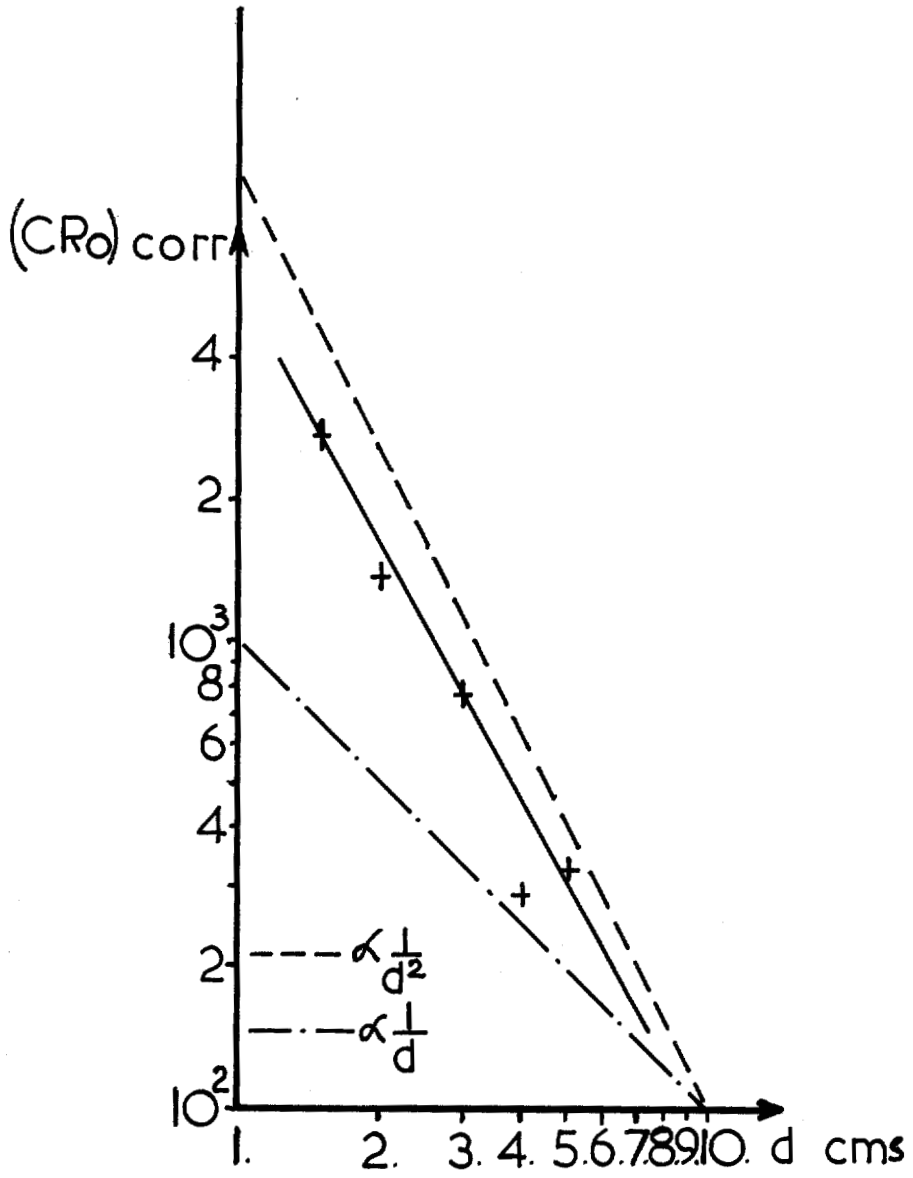

Fig. 36 FOILS 1-5

(CRo) corr. As a function of d

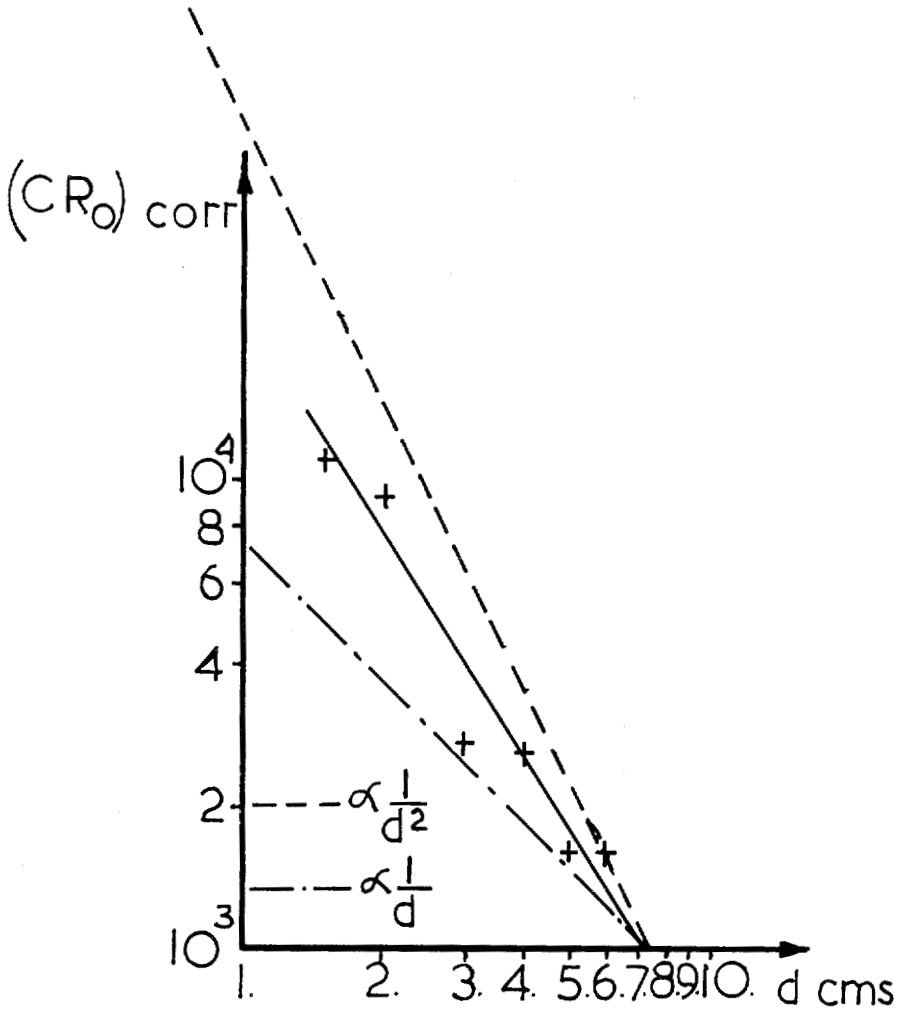

Fig. 37 FOILS 11-16

(CR0) corr. As a function of d

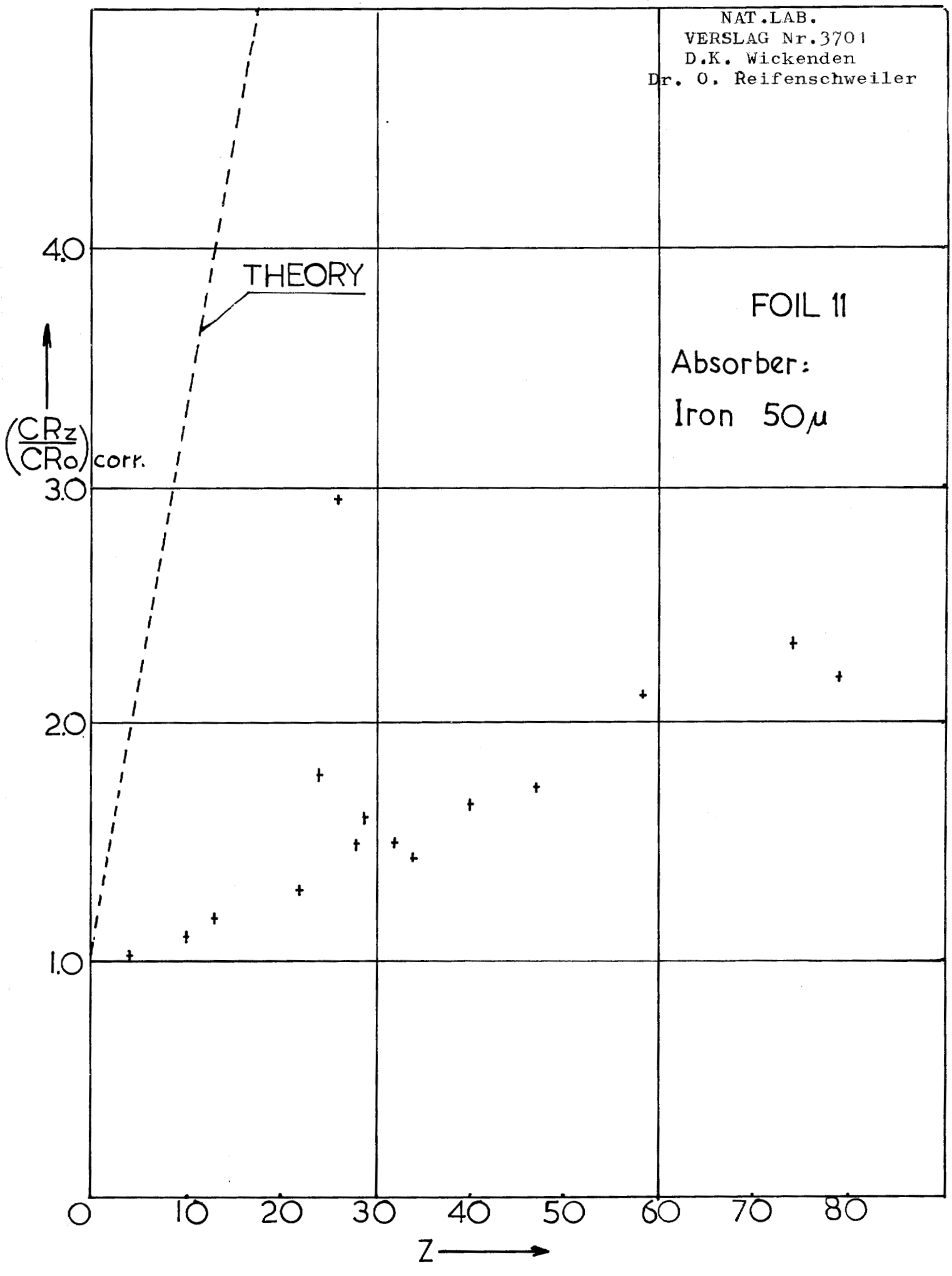
NAT.LAB.
VERSLAG Nr.3701
D.K. Wickenden
Dr. O. Reifenschweiler
THEORY
FOIL 11
Absorber:
Iron 50μ
(CRz/CRo)corr.
4.0
3.0
2.0
1.0
0
10
20
30
40
50
60
70
80
Z

Fig.33